UNIVERSITY OF CALIFORNIA,
IRVINE

Elucidating the role of cholesterol during Chlamydia infection using the novel anti-chlamydial inhibitor, H89

DISSERTATION

submitted in partial satisfaction of the requirements
for the degree of

DOCTOR OF PHILOSOPHY

in Developmental and Cell Biology

by

Karissa Jade Muñoz

Thesis Committee:
Professor Christine Suetterlin, Co-Chair
Professor Ming Tan, Co-Chair
Professor Melissa Lodoen
Professor Lee Bardwell
Professor Aimee Edinger (2020-2022)
Professor Zeba Wunderlich (2018-2020)

2022

DEDICATION

To

My parents, Lorena and Robert Muñoz
My siblings, Kristen, Bobby, Danny, and TJ
My incredible partner in crime, Camille
My hard-working undergrad, Priscilla
My amazing friends and family
And a special thank you to my forever fan, Tata Oscar.

<u>We did it!</u>

The years have been long
And the struggle a plenty.
Many phone calls and tears
For most of my twenties.

You were there for them all,
The moments, good and bad.
Thank you for the love and support
Because now…
I'm a Ph.D. grad!

<u>Forever a student</u>

A student of 24 years.
School is my place to grow and explore.
Collecting degrees because
I've always desired something…more.

Although to the classroom I do not return,
Still, there are things I wish to learn.
And I *will* keep learning.

I am a student of the world
A forever student, I shall be.
Motivated by unknown experiences
The world is full of opportunity.

- Karissa Jade Muñoz

TABLE OF CONTENTS

FIGURES

TABLES

ABBREVIATIONS

ABCA1	ABC transporter A1
ACAT	Acyl-CoA: cholesterol acyltransferase
AMPK	AMP-activated protein kinase
ADRP	Adipocyte differentiation related protein
BFA	Brefeldin A
C_6-NBD-Cer	Fluorescent ceramide analog
CompC	Compound C
CRISPRi	Clustered regularly interspaced short palindromic repeats interference
CD	Cyclodextrin
EB	Elementary body
EGF	Epidermal growth factor
EGFR	Epidermal growth factor receptor
EM	Electron microscopy
ER	Endoplasmic reticulum
ESCRT	Endosomal sorting complexes required for transport
FBS	Fetal Bovine Serum
HeLa	Henrietta Lacks cells
HFFs	Human foreskin fibroblasts
IB	Intermediate body
KO	Knockout
LBPA	Lysobisphosphatidic acid
LD	Lipid droplet
LDL	Low-density lipoprotein
LE	Late endosome
LPDS	Lipoprotein deficient serum
LTP	Lipid transfer protein
LXR	Liver X receptor
LY	Lysosome
MEFs	Mouse embryonic fibroblasts
MOMP	Major outer membrane protein
MSK1	Mitogen- and stress-activated kinase 1
MTOC	Microtubule organizing center
MVB	Multi-vesicular body
PKA	Protein kinase A
PKC	Protein kinase C
PID	Pelvic inflammatory disease
PM	Plasma membrane
PS	Phosphatidylserine
qPCR	Quantitative polymerase chain reaction
Rab GTPase	Rab guanine triphosphatase
ROCK	Rho-associated protein kinase

RB	Reticulate body
RPEs	Retinal pigmented epithelial cells
S6K1	Ribosomal protein S6 kinase 1
SNARE	Soluble N-ethylmaleimide-sensitive factor attachment protein receptor
TS	Temperature sensitive
T3SS	Type III secretion system
WT	Wild-type

ACKNOWLEDGEMENTS

“For a research worker, the unforgotten moments of [their] life are those rare ones which come after years of plodding work, when the veil over nature’s secret seems suddenly to lift and when what was dark and chaotic appears in a clear & beautiful light and pattern.” – Gerty Cori, M.D.

There have been many people who have contributed to my success as a graduate student. First, I want to thank my co-advisors, Dr. Christine Suetterlin and Dr. Ming Tan, for the numerous helpful lab meetings and discussions. Over the years, you have both helped me grow so much as an independent scientist. Also, thank you Christine for trusting me as your TA for D103. It was fun being able to dip my toes into the world of teaching and to work with other graduate students**.**

Thank you to my past and current lab mates, especially Kevin Wang, who has been my rock and lab sibling throughout grad school. Our friendship is something I will always cherish. I also want to thank my undergrad, future Dr. Priscilla Nguyen, who was a fast learner and a pleasure to teach. We were able to accomplish so much together, and I appreciate your patience with me as we navigated my thesis project.

I would like to thank my committee members, Dr. Melissa Lodoen and Dr. Lee Bardwell for providing me with guidance and support during my early stages as a scientist. Also, a big thank you to Dr. Zeba Wunderlich and Dr. Aimee Edinger who worked as a tag-team duo to serve as my fifth committee members. I appreciate the flexibility and generosity with your time.

Thank you to Dr. Harinder Singh and Dr. David Fruman for providing the wonderful resources through the GPS-STEM program to help me grow as a scientific writer and communicator. I had a ton of fun and because of the amazing experience, I decided to pursue medical writing.

Thank you to Dr. Hans Keirstead who gave me my first opportunity as a medical writer while I was still a Ph.D. candidate at UC Irvine. You are an inspiring mentor and I look forward to working with you as Dr. Muñoz after graduation.

A huge thank you to the National Science Foundation for believing in me as a scientist and funding my Ph.D. with the Graduate Student Research Fellowship (ID: 2018262334).

Lastly, I thank the University of California, Irvine for giving me the permission to include copyrighted data as part of my dissertation and for providing a beautiful environment to live in for 6 years.

VITA

Karissa Jade Muñoz

As an NSF fellow and recent PhD graduate from the University of California, Irvine, I have the skills and motivation to become a successful science communicator. My work experiences as a medical writer for AVITA Biomedical and a podcast writer for the Loh Down on Science have trained me to work efficiently in teams to distill complex science for any audience. My passion for science communication is highlighted by my participation in numerous professional development courses. My career goal is to collaborate with scientists to inform the public on the latest medical advancements.

EDUCATION

2016-present University of California, Irvine (UCI) – Irvine, CA
Ph.D. in Developmental and Cell Biology, School of Biology, GPA 3.9

2012-2016 Claremont McKenna College – Claremont, CA
B.A., Dual major in Biology and Spanish, *Cum laude*, GPA 3.7

2014 Studied abroad at La Universidad Pontificia de Salamanca – Salamanca, Spain. Coursework was completed in Spanish, GPA 4.0

HONORS AND AWARDS

2021 Rose Hills Foundation Science & Engineering Scholarship
2021 2nd Place at UCI's Science Policy Pitch Competition through the Graduate Professional Success (GPS-STEM) program
2021 1st Place Scientific Writing Award in Developmental and Cell Biology
2021 Joseph H. Stephens Memorial Fellowship Award
2021 Selected to design the cover for the July issue of *Infection and Immunity,* the same issue that includes my first, first-author publication.
2021 Phi Beta Kappa Honor Society
2020 Rose Hills Science & Engineering Scholarship
2019 1st Place at UCI's Business Pitch Competition through GPS-STEM
2018 National Science Foundation Graduate Research Fellowship (NSF-GRFP)
2016 Francisco J. Ayala Graduate Fellowship
2016 UC Irvine Diversity Recruitment Fellowship
2016 Graduated *Cum laude* from Claremont McKenna College
2013-2016 Rose Hills Foundation of Science and Engineering Academic Scholarship

2015 Society for the Advancement of Chicanos and Native Americans in Science (SACNAS) Conference Outstanding Poster Presentation Award

2015 Annual Biomedical Research Conference for Minority Students (ABRCMS) Travel Scholarship
2015 Summer Research Opportunities Program (SROP) Conference Outstanding Scientific Writing Award
2015 SROP Conference Outstanding Poster Presentation Award
2015 Claremont McKenna College Dean's List (top 15%)
2012-2015 Chicano Latino Student Affairs Dean's List (top 15%)
2015 Sigma Xi International Scientific Honor Society
2015 Sigma Delta Pi National Spanish Honor Society
2013-2015 Dolores Huerta Leadership Award
2014 Medal of Leadership as a Chicano Latino Sponsor
2014 Rose Hills Science and Engineering Summer Research Scholarship

RESEARCH EXPERIENCE

2018-present Ph.D. thesis in the Department of Developmental and Cell Biology at the University of California, Irvine (UCI)
- Provided a comprehensive approach for studying inhibitors of the chlamydial infection.
- Defined the mechanisms by which the novel anti-chlamydial inhibitor, H89, slows *Chlamydia* inclusion growth and production of infectious progeny.

Co-research advisors: Dr. Christine Suetterlin and Dr. Ming Tan

2017-2018 Ph.D. student in the Department of Physiology and Biophysics at UCI
- Investigated the role of Regulatory T cells (Tregs) in a mouse model of Duchenne Muscular Dystrophy.

Research Advisor: Dr. Armando Villalta

2014-2016 Senior Thesis Research, Keck Science Department at the Claremont Colleges
- Thesis title "Regulation of Histone H3 tail clipping in *Tetrahymena thermophila*"
- Engineered H3 mutants to identify sequence requirements for histone H3 tail "clipping" in *Tetrahymena thermophila*.

Research Advisor: Dr. Emily Wiley

2015 Summer Research, Department of Molecular and Cellular Biology at the University of Illinois at Urbana-Champaign
- Collected sewage samples from the Urbana Sewage Department and isolated phages.
- Calculated efficiency of plating for *E. coli* with/without nine cryptic prophages that were infected with known laboratory phages or unidentified sewage phages.

Research Advisor: Dr. Cari Vanderpool

2014 Summer Research, Keck Science Department of the Claremont Colleges
- Designed histone H3 mutants to identify sequence requirements for histone H3 tail "clipping" in *Tetrahymena thermophila.*

Research Advisor: Dr. Emily Wiley

SKILLS/TRAINING

Medical Writing Internship at AIVITA Biomedical

Jun-Aug 2020 **Medical Writer**

Worked in collaboration with Dr. Hans Keirstead and Dr. Alexa Poole to analyze and summarize data for various projects at AIVITA Biomedical. Projects ranged from the development of a COVID-19 vaccine to production of anti-aging, stem cell-based serums. Pieces will be used in grants and future publications. Active member of weekly project and marketing meetings, that provided training on how to take bench science to the market.

Graduate Professional Success (GPS-Biomed/STEM) Program at UCI:

2021-present **Podcast Writer for "The Loh Down on Science"**

Hired as a science writer by Dr. Sandra Loh for her daily radio science podcast aired on KPCC 89.3 FM/NPR. These 90-second episodes are intended for a general audience. Read scientific literature and wrote scripts on a range of current topics.

2021 **Science Policy & Advocacy for STEM Scientists**

Offered in collaboration between several programs: UC Irvine, Journal of Science Policy & Governance, Union of Concerned Scientists, UCI's Ridge-2-Reef, and Stempeers. Students learned to: identify a science policy topic, discuss the current data for that topic, write a report of the data, summarize an action plan to address the issue, and create a 2-minute pitch of the significance of said issue.

2020-2021 **GPS-Biomed Trainee Council Member**

One of three members in charge of the Scientific Communications branch of GPS-Biomed/STEM. Collected, compiled, and contributed written articles for an online Science Café. Edited GPS-Biomed podcasts ranging in content from promoting mental health awareness, discussing ways to improve the graduate and postdoctoral experience, as well as sharing professional development advice for a variety of scientific careers.

2019 **"Business Concepts for STEM Scientists" Course**

Course was instructed by Dr. Matthew Hanson of the UC Irvine Beall

Applied Innovation Center. Participated in a 10-week training program to develop a fundamental understanding of business terminology and communication skills as a scientific businessperson. Member of First Place winning team who showcased its business pitch to a panel of professional businesspeople.

2019 **"How to Communicate Your Science to Any Audience" Course**
Course was instructed by a communications coach, Mark Bayer. Engaged in a 6-week training program to develop effective skills of conveying scientific topics to policymakers and the public.

2018 **"Effective Communication for Scientists" Course**
Worked in groups and individually with speech coach Bri McWhorter. Became certified in techniques for effective communication of scientific research for a range of audiences.

TEACHING EXPERIENCE

2021-2022 **Mentor for undergraduate student researcher**
Trained an undergraduate student to develop a basic understanding of experimental design and analysis. Helped improve their scientific communication skills for their presentation at the UC Irvine undergraduate research symposium.

2019-2021 **Teaching Assistant (TA)**
TA for the Undergraduate Cell Biology Course D103 at UCI (3 quarters). Attended lectures to address students' questions. Graded assignments and created a weekly problem set in collaboration with other TAs. Lead and conducted weekly student discussion sections with the goal of helping students understand the course concepts to apply them in experimental scenarios.

2015 **Undergraduate Mentor for student researchers**
Mentored students who were starting research projects in Dr. Wiley's lab. Instructed in basic Molecular Biological techniques.

2013 **Teacher of the "Chemistry of Cookie Baking Course"**
Worked with EXPLO summer program in Southborough, Massachusetts to design lesson plans and teach a food science course for students aged 9-11.

RESEARCH TECHNIQUES

Very Familiar
Chlamydia infections in tissue culture
Optimization of inhibitors for *in vitro* studies
qPCR
Bacterial and *Tetrahymena* transformations
Genomic DNA and Plasmid isolation
Restriction Digest Analysis
Western blot analysis
Mouse Breeding
Isolating immune cells from muscle
Fluorescence microscopy

Familiar
Site-directed mutagenesis
Flow Cytometry
ELISA
Phage isolation
Immunohistochemistry
Isolating cells from muscle
RNA isolation, cDNA synthesis
PCR, primer design
Site-directed mutagenesis
Isolating PBMCs from blood

PUBLICATIONS

Muñoz, Karissa J., Ming Tan, and Christine Sütterlin. "Differential effects of small molecule inhibitors on the intracellular *Chlamydia* infection." *mBio*, 2022. https://doi.org/10.1128/IAI.00729-20.

Wang, Kevin, **Karissa J. Muñoz**, Ming Tan, and Christine Sütterlin. "Chlamydia and HPV Induce Centrosome Amplification in the Host Cell through Additive Mechanisms." *Cellular Microbiology*, October 30, 2021, e13397. https://doi.org/10.1111/cmi.13397.

Muñoz, Karissa J., Kevin Wang, Lauren M. Sheehan, Ming Tan, and Christine Sütterlin. "The Small Molecule H89 Inhibits *Chlamydia* Inclusion Growth and Production of Infectious Progeny." *Infection and Immunity*, April 5, 2021. https://doi.org/10.1128/IAI.00729-20.

Kastenschmidt, Jenna M., Ali H. Mannaa, **Karissa J. Muñoz**, and S. Armando Villalta. "Immune System Regulation of Muscle Injury and Disease." In *Muscle Gene Therapy*, edited by Dongsheng Duan and Jerry R. Mendell, 121–39. Cham: Springer International Publishing, 2019. https://doi.org/10.1007/978-3-030-03095-7_7.

Vaccari, Monica, Slim Fourati, Shari N. Gordon, [and 30 others, including **Munoz, KJ**]. "HIV Vaccine Candidate Activation of Hypoxia and the Inflammasome in CD14+ Monocytes Is Associated with a Decreased Risk of SIVmac251 Acquisition." *Nature Medicine*, 2018 Jun;24(6):847-856. https://doi.org/10.1038/s41591-018-0025-7.

CONFERENCE PRESENTATIONS

Talks:

Muñoz, Karissa, “Inhibitors cause discordant effects on the *Chlamydia* infection,” for the “Chlam Talks” hosted by the International Chlamydia Basic Research Society (January, 2022)

Muñoz, Karissa, “H89 as a novel small molecule inhibitor of *Chlamydia* infection,” for the Associated Graduate Students Symposium at UC Irvine (April, 2021)

Muñoz, Karissa, “Regulation of Histone H3 tail clipping in *Tetrahymena thermophila,*” for the ABRCMS National Conference in Seattle, Washington (November 2015)

Muñoz, Karissa, “Role of *E. coli* cryptic prophages in providing resistance to the bacterial host against future phage infection,” for the SROP Conference in Urbana, Illinois (July 2015)

Muñoz, Karissa, “Regulation of Histone H3 tail clipping in *Tetrahymena thermophila,*” for the Ciliate Molecular Biology Conference in Camerino, Italy (July 2015)

Muñoz, Karissa, “Regulation of Histone H3 tail clipping in *Tetrahymena thermophila,*” for the Keck Science Summer Symposium (July 2014)

Posters:

Muñoz, Karissa, “A potential role for Tregs in suppressing muscle inflammation and promoting regeneration,” presentation at the La Jolla Immunology Conference (October 2017)

Muñoz, Karissa, “A potential role for Tregs in suppressing muscle inflammation and promoting regeneration,” presentation for the School of Medicine Grad Day at the University of California, Irvine (September 2017)

Muñoz, Karissa, “Regulation of Histone H3 tail clipping in *Tetrahymena thermophila,*” poster presentation for the Society for the Advancement of Chicanos and Native Americans in Science (SACNAS) National Conference in Washington D.C. (October 2015)

Muñoz, Karissa, “Role of *E. coli* cryptic prophages in providing resistance to the bacterial host against future phage infection,” for the SROP Conference in Urbana, Illinois (July 2015)

Muñoz, Karissa, “Regulation of Histone H3 tail clipping in *Tetrahymena thermophila,*” poster presentation for the National Science Foundation Camp Symposium at the University of California Irvine (February 2013)

OTHER SKILLS

Language: Spanish

DISSERTATION ABSTRACT

Elucidating the role of cholesterol during *Chlamydia* infection using the novel anti-chlamydial inhibitor, H89

By
Karissa Jade Muñoz

Ph.D. in Developmental and Cell Biology
University of California, Irvine, 2022
Professor Christine Suetterlin, Co-chair
Professor Ming Tan, Co-chair

Two unanswered questions in the field of *Chlamydia* are 1) How does the inclusion grow over time? and 2) What promotes RB-to-EB conversion? Small molecule compounds have been widely used to manipulate infection conditions to determine specific targets required for these stages of chlamydial development. Although there are many publications describing the effects of anti-chlamydial inhibitors, the lack of a standard approach makes it challenging to compare these effects across studies.

In chapter 3, our manuscript (submitted) defines the weaknesses in the current methodologies that the *Chlamydia* field implements to study inhibitor treatments during the infection. We additionally demonstrate approaches to yield more information from inhibitor studies to more accurately describe the ways different conditions alter the infection. Using published and novel *chlamydial* inhibitors, we found that analysis with one assay at one or two time points in the infection is insufficient because inhibitors can change the length of the infection. Furthermore, we showed that phenotypes can vary depending on the time of analysis and the assay used. To circumvent these issues, we propose a novel measurement, $Progeny_{max}$, which takes changes in the length of the

developmental cycle into consideration and can easily be used to compare differences in progeny, regardless of the condition.

In chapter 4, we describe a novel inhibitor of the chlamydial infection, H89, which slowed inclusion growth and caused a block in RB-to-EB conversion. We tested several known kinases and pathways that were previously reported to be blocked by H89, but none were inhibited by our H89 treatment conditions. In chapter 5, we continued to explore the mechanisms targeted by H89 to elucidate why the inhibitor was such a strong anti-chlamydial inhibitor. We found that H89 causes lysosomal accumulation of cholesterol, which correlated with a defect in lysosomal acidification. These studies suggest that H89 prevents lysosomal acidification, resulting in cholesterol accumulation. Previous studies suggest that cholesterol may be necessary for the chlamydial infection, meaning these H89-mediated defects on inclusion growth and progeny production are likely due to a decrease in cholesterol transport out of the lysosome and reduced cholesterol accessibility by chlamydiae.

CHAPTER 1: INTRODUCTION

"A disease does not exist until we have agreed that it does, by perceiving, naming, and responding to it." – Charles Rosenberg, Ph.D. in Science History

1.1 The (short) history of *Chlamydia* infection

For the past three decades, *Chlamydia* has been the number one reported sexually transmitted infection (STI) in both the United States and Europe (Centers for Disease Control and Prevention CDC – Chlamydia Statistics, 2019). The term "*Chlamydia"* refers to the disease-causing bacterial agent, *Chlamydia trachomatis,* and "chlamydia" refers to the disease itself. However, *Chlamydia* was not officially recognized as an STI until the 1970s and patient records of the infection did not start until the late 1980s (Worboys, 2019). Today, in the U.S. about 1.8 million people are diagnosed with *Chlamydia* infection each year.

Chlamydia infection is highly transmissible through vaginal, anal, or oral sex with an infected individual (Centers for Disease Control and Prevention CDC – Chlamydia Statistics, 2019). In the United States, women are more likely to be diagnosed with infection compared to men, which is likely because women are screened more routinely (United Health Foundation, 2021). Moreover, those who are pregnant can spread the infection to their baby during childbirth, making the disease especially tragic.

1.2 Symptoms of disease

Some clinicians refer to *Chlamydia* as the "silent" infection because about 70% of

women and 90% of men who are diagnosed are asymptomatic (*Centers for Disease Control and Prevention CDC – Chlamydia Statistics*, 2019). This poses a serious health threat because infected individuals can unknowingly spread the disease, and if left untreated, the infection can result in fertility issues (Farley et al., 2003). Unfortunately, the infection causes disproportionately greater health consequences for women. Undiagnosed chlamydial infections can spread to the uterus and fallopian tubes, resulting in pelvic inflammatory disease (PID) and hydrosalpinx, both which can contribute to infertility (*Centers for Disease Control and Prevention CDC – Chlamydia Statistics*, 2019; Hoenderboom et al., 2020; Tang et al., 2020). There is conflicting evidence regarding the effects of *Chlamydia* infection on male fertility (Goulart et al., 2020). Some reports suggest decreased sperm count (Ahmadi et al., 2018) and motility (Sonnenberg et al., 2013), while other publications report no defects (Günyeli et al., 2011; Hosseinzadeh et al., 2004).

Chlamydia trachomatis is also the leading cause of preventable blindness called trachoma (Center for Disease Control and Prevention, 2021). Infections under these circumstances are due to inadequate access to clean water and sanitation. The infection can cause severe scarring of the inner eyelid, which slowly damages the cornea and eventually results in irreversible vision loss.

1.3 Treatments and prevention

Chlamydia infections are effectively treated with antibiotics such as doxycycline and azithromycin (*CDC – Chlamydia Treatment*, 2021). However, there are currently no

vaccines to prevent the spread of disease. The lack of a *Chlamydia* vaccine coupled with the fact that most infected individuals are asymptomatic is what contributes to the high incidence of infection each year. As Dr. Sheldon Jacobson and Dr. Janet Jokela from the University of Illinois Urbana-Champaign put it, “precautions taken to avoid and prevent sexually transmitted diseases are similar to those for avoiding and preventing COVID-19, with condoms replaced by face masks.”

1.4 Chlamydial species

The *Chlamydiaceae* family is comprised of 16 *Chlamydia* species which have adapted to infect a variety of organisms including humans, mice, guinea pigs, birds, pigs, cats, livestock, marsupials, snakes, and turtles (Phillips et al., 2019). Two species that specifically infect humans are *C. pneumoniae,* which causes respiratory infection, and *C. trachomatis*, which causes urogenital and ocular infections (Phillips et al., 2019). There are three biovars of *C. trachomatis*, which are subdivided into 15 main serovars based on genetic variations of the chlamydial major outer membrane protein (MOMP) (Bugalhão & Mota, 2019). The trachoma biovar includes serovars A-C, which cause non-congenital blindness in people living in developing countries (C. Elwell et al., 2016). The genital biovar includes serovars D-K, which are the most prevalent sexually transmitted chlamydiae. Lastly, the lymphogranuloma venereum (LGV) biovar includes serovars L1-L3, which cause anorectal or urogenital infections (C. Elwell et al., 2016).

1.5 The *Chlamydia* developmental cycle

Chlamydia are Gram-negative, obligate intracellular bacteria that undergo a unique, dimorphic developmental cycle within eukaryotic host cells (Fig. 1.1). The bacteria convert between two distinct forms, the infectious elementary body (EB) and a metabolically active, non-infectious reticulate body (RB). The infection begins with the endocytic uptake of an EB into the eukaryotic host cell, where it is maintained within a membrane bound inclusion vacuole derived from the host cell membrane. For *C. trachomatis* infections, after about 6-8 hours, the EB converts into an RB (Belland et al., 2003). Starting around 12-16 hours post infection (hpi), the RB will undergo several rounds of replication and division, expanding the RB population (Belland et al., 2003). Starting at 24 hpi, the RBs will asynchronously convert into intermediate bodies (IBs) and then back into EBs. IBs represent the transition state between RBs and EBs, but do not have a clearly defined function or markers. Roughly 1,000 infectious EBs are produced per infected host cell by the end of the chlamydial infection (J. K. Lee et al., 2018).

After 48-72 hpi, depending on the species, the inclusion either lyses to release the bacteria or is extruded from an intact host cell (Hybiske & Stephens, 2007). In the case of lysis, both the inclusion and host cell membranes rupture over the span of minutes (Hybiske & Stephens, 2007). Live cell imaging demonstrated that the inclusion membrane lyses prior to the host cell membrane, supporting that inclusion lysis is not a result of the host cell reaching its volumetric limits (Hybiske & Stephens, 2007). Also, about 95% of the inclusion is empty space, supporting that inclusion lysis is not caused

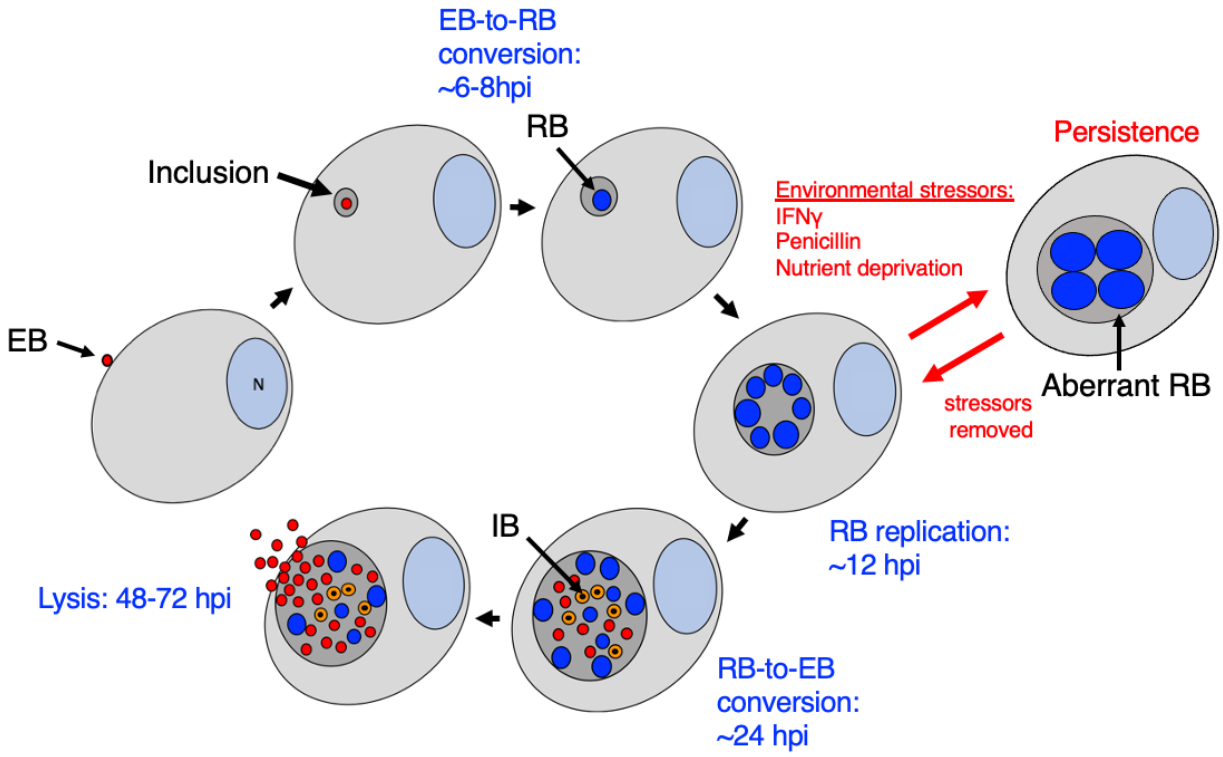

Figure 1.1. The developmental cycle of *C. trachomatis* within eukaryotes. Infection of eukaryotic host cells begins with internalization of EBs. Conversion of an EB to an RB occurs between 6-8 hours post infection (hpi), followed by RB replication starting at about 12 hpi. The RBs asynchronously undergo RB-to-EB conversion starting at 24 hpi, with the IB being the intermediate form. The developmental cycle is complete with the release of EBs between 48-72 hpi. If the infection is exposed to environmental stressors including IFNy, penicillin, and nutrient deprivation, chlamydiae will enter a state of persistence. Under persistence, RBs can continue replicating and they form large, aberrant RB bodies, but do not undergo RB-to-EB conversion. Once the environmental stressors are gone, the RBs can proceed with the developmental cycle.

by chlamydiae filling up the inclusion like a balloon (J. K. Lee et al., 2018). However, the mechanism and regulation for lysis is still not known. In the case of extrusion, which occurs in approximately 50% of infected cells, it is a slower process including pinching of the inclusion, protrusion of the inclusion out of the plasma membrane, and detachment from the host cell (Hybiske & Stephens, 2007). Several host cell proteins

and functions were shown to mediate extrusion including actin polymerization, neuronal Wiskott–Aldrich syndrome protein, myosin II, and Rho GTPase (Hybiske & Stephens, 2007). Thus, at the end of the infection, *Chlamydia* can implement two different methods of escaping its eukaryotic host.

Of note, conditions such as antibiotic treatment with penicillin, IFNγ, and nutrient deprivation disrupt the developmental cycle, causing the RBs to enter a state of persistence (Fig. 1.1) (Beatty et al., 1994; Panzetta et al., 2018). Persistence refers to a long-term association between chlamydiae and the host cell where the chlamydiae are viable, but cannot cause additional infection (Beatty et al., 1994). *In vitro*, persistence is referred to RBs that continue genome replication, but do not divide to produce more RBs. This replication results in enlarged, aberrant RBs that are clearly visible by either electron microscopy (EM) or immunofluorescence analyses. No infectious EBs are produced, and the inclusion does not lyse. In fact, the infection can remain dormant until conditions improve. *In vivo*, "persistence" does not always refer to the aberrant RB phenotype observed *in vitro* and understanding how chlamydiae persist *in vivo* is still an active area of research (Wyrick, 2010).

Each of the developmental forms of chlamydiae can be distinguished by electron microscopy (EM) imaging because of the differences in chromatin density (Fig. 1.2) (Matsumoto & Manire, 1970). EBs appear as small, black electron dense circles around 0.3 µm in diameter, whereas RBs are larger, gray circles about 1 µm in diameter (Becker, 1996; J. K. Lee et al., 2018; Matsumoto & Manire, 1970). IBs are about 0.4 µm in diameter and have a characteristic "bulls-eye" appearance, reflective of the transition

state between the metabolically active RB and “inactive” EB. Aberrant RBs are visibly larger than normal RBs, and there are only a few per inclusion (Skilton et al., 2009).

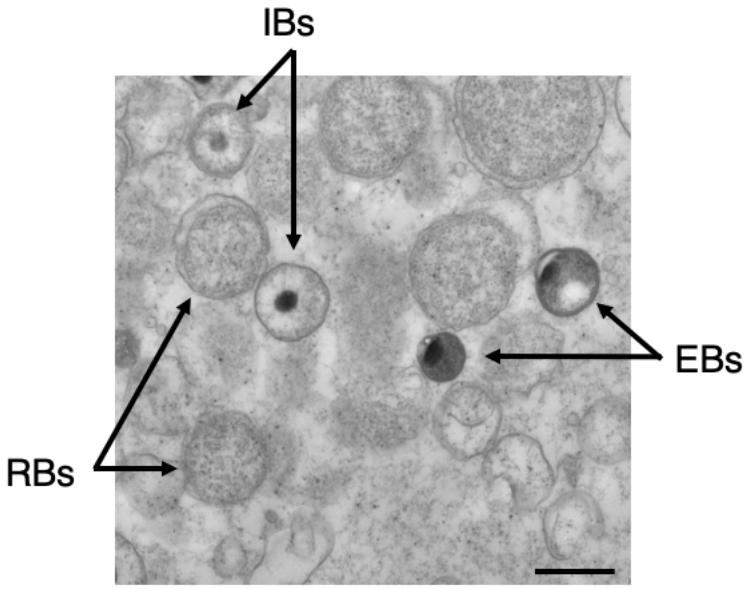

Figure 1.2. Developmental forms of *Chlamydia* by Electron Microscopy (EM). Zoomed in EM image of a *C. trachomatis*-infected HeLa cell at 36 hpi. The chlamydial developmental forms are indicated by black arrows: reticulate bodies (RBs), intermediate bodies (IBs), and elementary bodies (EBs). Scale bar = 500 nm.

Immunofluorescence microscopy is another method of identifying chlamydial forms based on the expression of certain genes. MOMP is a highly conserved chlamydial protein (Black et al., 1992). Thus, commercially available antibodies that recognize MOMP are widely used as a *Chlamydia* marker because they stain all developmental forms of chlamydiae. MOMP antibodies are commonly used in immunofluorescence analyses to visualize the chlamydiae that occupy the inclusion and are also used to indirectly measure inclusion size. There are also non-commercial antibodies that have been made against genes specific to EBs, which have been helpful in identifying EBs by immunofluorescence.

Recently, the lab of Isabelle Derré created a dual reporter system to distinguish between RBs and EBs by live cell imaging (Cortina et al., 2019). They transformed *C. trachomatis* to include plasmids that expressed mCherry driven under the RB-specific *groEL* promoter and GFP driven under the EB-specific *omcA* promoter (Cortina et al., 2019). Thus, an RB would initially appear red and then turn green as it converted into an EB. An advantage of this system is that the developmental forms can be monitored in real time, including the RB-to-EB conversion process. The downside is that there are no known markers of IBs, therefore IBs cannot be distinguished by any fluorescent method. Another drawback of this system is that both the red and green fluorescence channels are occupied by the reporters, limiting the visualization of other cell structures or chlamydial proteins. Nonetheless, these advances in detecting the chlamydial forms are beneficial in understanding the developmental cycle of *Chlamydia*.

1.6 The chlamydial inclusion

In addition to the growing chlamydial population, the chlamydial inclusion also grows 1000-fold in volume during the course of the infection (J. K. Lee et al., 2018). Interestingly, throughout this process, the inclusion compartment evades fusion with host endosomes and lysosomes, though this mechanism is still under investigation (Scidmore et al., 2003). To support the growth of the inclusion, *Chlamydia* hijacks membrane trafficking pathways of the host cell, which will be discussed further in the next section. The chlamydial inclusion also includes about 50 type III secreted effector proteins, Incs, which have a bi-lobed hydrophobic domain and are inserted into the

inclusion membrane (Bugalhão & Mota, 2019; Mital et al., 2013). The growth of the chlamydial inclusion is dependent on both the acquisition of host lipids as well as the functions of these Inc proteins.

The roles for most Incs are unknown, but several are shown to mediate host-pathogen interactions (Derré, 2015, 2017; C. A. Elwell et al., 2011; C. A. Elwell & Engel, 2012). For example, InaC interacts with host cell proteins 14-3-3β, ARF1/4, and VAMP7/8 to modify post-translational modifications of microtubules and facilitate Golgi-chlamydial membrane interactions (Delevoye et al., 2008; Kokes et al., 2015; Z. Li et al., 2008; Wesolowski et al., 2017). These interactions likely facilitate the acquisition of nutrients because post-Golgi vesicles are rerouted to transport host sphingolipids and cholesterol to both the inclusion and bacteria (Carabeo et al., 2003; Hackstadt et al., 1995, 1996). Another example includes IncV, which targets host proteins VAPA/B to form membrane contact sites between the chlamydial inclusion and the endoplasmic reticulum (Stanhope et al., 2017; X. Wang et al., 2018; Weber et al., 2015). These Incs likely bring the inclusion in close proximity to the ER because anterograde and retrograde transport between the ER and the Golgi was also shown to be important for the infection (Derré et al., 2007; Dickinson et al., 2019; Park et al., 2018). As these are only a few of the known functions of Incs, there are likely many other host-pathogen membrane interactions facilitated by these specialized chlamydial membrane proteins.

Additionally, Inc proteins are important for inclusion membrane interactions with other inclusions. IncA uses its SNARE-like properties to fuse inclusion membranes (Cingolani et al., 2019; Richards et al., 2013; Weber et al., 2016). In some cases,

multiple EBs are endocytosed into the same host cell, resulting in the formation of multiple membrane-bound inclusions. Microtubules traffic each inclusion to the microtubule organizing center (MTOC) and by 24 hpi, the inclusions have combined to form a single inclusion (Richards et al., 2013). Infections with chlamydial IncA mutants result in single cells with multiple inclusions that never fuse, also referred to as a non-fusogenic phenotype (Weber et al., 2016). Absence of other Incs such as IncC, CT229, and CT383 also prevents inclusion fusion, which may be due to decreased membrane stability (Weber et al., 2017). As previously mentioned, these chlamydial Incs promote the recruitment of host lipids to the inclusion membrane and thus, lacking certain Incs may limit the acquisition of lipids that maintain membrane structure and fluidity, making inclusion fusion more challenging. Strangely, IncA mutants produced the same amount of infectious EBs *in vitro* as their wild-type counterparts (Weber et al., 2016), meanwhile clinical isolates of non-fusogenic chlamydial strains produced a less severe infection with fewer chlamydiae (Geisler et al., 2001). Thus, these inclusion fusion membrane interactions appear to only be beneficial for *in vivo* infections.

1.7 *Chlamydia* manipulates host lipid trafficking

Lipids are important components of cell membranes for regulating structure and fluidity (Horn & Jaiswal, 2019). Both eukaryotic host cell and chlamydial membranes are constructed with lipids including sphingomyelin and cholesterol (Wylie et al., 1997). Chlamydiae have a reduced genome (~1,000 genes) and cannot synthesize most essential lipids, suggesting that this pathogen diverts host cell pathways to bring lipids

to the inclusion (Stephens et al., 1998). Types I/II fatty acid synthesis (FASII) are of the limited lipid production processes that chlamydiae are capable of (Henrichfreise et al., 2009), and they are essential for RB cell division (Yao et al., 2014). There have been challenges with studying the lipid content of the chlamydial inclusion because of the fragility of the organelle, but immunofluorescence analyses have supported the presence of lipids including sphingomyelin, ceramide, cholesterol, glycerophospholipids, phosphatidic acid, phosphatidylserine, phosphatidylinositol, phosphatidylcholine, and phosphatidylethanolamine (C. A. Elwell & Engel, 2012; Cox et al., 2016). Thus, to support the growing infection, *Chlamydia* takes advantage of several host lipid transport mechanisms to acquire these lipids for their membranes.

In uninfected eukaryotic cells, host lipids are trafficked using both vesicular and non-vesicular mechanisms. For vesicular transport, Rab GTPases help the Golgi complex move glycosphingolipids, sphingolipids, and nascent cholesterol along the endocytic and exocytic pathways and between organelles (C. A. Elwell & Engel, 2012). Meanwhile, lipid transfer proteins (LTPs) aid in non-vesicular lipid transport between organelles.

In *Chlamydia*-infected cells, chlamydiae use a multi-faceted approach for lipid acquisition. One approach is to hijack lipid rich vesicles transported from the Golgi and multi-vesicular bodies (MVBs) with the help of Rab GTPases (Beatty, 2006; Brumell & Scidmore, 2007; Homma et al., 2021; Rzomp et al., 2003). Another approach is to use non-vesicular means of lipid acquisition from lipid droplets (LDs) and LTPs. Rab GTPases are essential proteins of vesicular membrane trafficking that aid in the

transport, tethering, and fusion of membrane-bound organelles and vesicles (Homma et al., 2021). There are approximately 60 Rab GTPases and depending on the chlamydial species, a specific subset localizes to the inclusion membrane (Rzomp et al., 2003). Chlamydial Inc proteins aid in the recruitment of Rabs to the inclusion. For example, in *C. trachomatis*-infected cells, Rab4 interacts with CT229 (Rzomp et al., 2003) and in *C. pneumoniae*-infected cells Rabs 1, 10, and 11 interact with Cpn0585 (Cortes et al., 2007). These chlamydial and host protein interactions may be necessary for chlamydiae to fuse with host vesicles and have access to host lipids. CD59 and CD63 are the few host proteins reported inside the inclusion (Beatty, 2006; Hasegawa et al., 2009) and so fusion of host membranes with the inclusion is likely limited and tightly regulated. It is also possible that host materials are transported out of vesicles prior to integrating into the inclusion membrane, which is why host proteins are not typically found in the inclusion. That being said, sphingomyelin and cholesterol are the two most abundant host lipids found in chlamydial membranes (Carabeo et al., 2003; Hackstadt et al., 1995, 1996) and the ways in which the infection intercepts transport of these lipids will be discussed further.

1.8 Acquisition of sphingolipids by the chlamydial infection

Sphingomyelin is a lipid synthesized from ceramide that can be tracked by fluorescent imaging using the Golgi-specific ceramide analog, C_6-NBD-Cer (Hackstadt et al., 1995, 1996). Addition of C_6-NBD-Cer during *in vitro C. trachomatis* infection demonstrated that sphingolipids integrated into the inclusion and the membranes of

individual chlamydiae (Hackstadt et al., 1995). Surprisingly, about 40-50% of the sphingomyelin endogenously synthesized from C_6-NBD-ceramide was retained by the infection (Hackstadt et al., 1995, 1996, 1997). Treatment with Brefeldin A (BFA) inhibitor, which induces Golgi relocalization to the ER and blocks vesicular transport of host proteins from the Golgi, limited *Chlamydia* incorporation of sphingolipids, resulting in smaller inclusions (Hackstadt et al., 1995). Follow up studies showed that sphingomyelin is also essential for bacterial replication and reactivation from persistence (van Ooij et al., 2000; Robertson et al., 2009).

Under infection conditions, Rabs 6, 11, and 14 were all shown to promote sphingomyelin acquisition (Rejman Lipinski et al., 2009; Capmany & Damiani, 2010; Capmany et al., 2019). siRNA knockdown of Rabs 6 or 11 caused decreased sphingomyelin uptake and a defect in progeny production (Rejman Lipinski et al., 2009). Rab14-positive sphingolipid-containing vesicles were associated with the inclusion membrane as early as 10 hpi and the interaction was dependent on chlamydial protein synthesis (Capmany & Damiani, 2010). Infections in dominant negative Rab14 host cell mutants slowed inclusion growth and impaired progeny production (Capmany & Damiani, 2010). Thus, Rab GTPases are an important means by which chlamydiae intercept and acquire sphingolipids traveling by vesicular transport.

In addition to vesicular transport, chlamydiae take advantage of non-vesicular lipid transport pathways to bring ceramide and sphingomyelin to the inclusion. Specifically, chlamydial Incs interact with host cell lipid transfer proteins at membrane contact sites between the inclusion, Golgi, and ER membranes. In uninfected cells, the

ceramide transfer protein CERT transports ceramide from the ER to the Golgi, where it is converted into sphingomyelin by sphingomyelin synthases SMS1/2 (Hanada et al., 2003, 2009; Huitema et al., 2004). In *C. trachomatis*-infected cells, VAPA/B and IncD interactions help bring CERT to the vicinity of the chlamydial inclusion (Derré et al., 2011). This facilitates ceramide transfer to the inclusion where it can then be converted into sphingomyelin and incorporated into chlamydial membranes (Derré et al., 2011; C. A. Elwell et al., 2011). *C. caviae* is a chlamydial strain that lacks IncD and is incapable of recruiting CERT to the inclusion, highlighting the importance of IncD in the acquisition of non-vesicularly transported ceramide (Derré et al., 2011). However, **I hypothesize** that because there are several mechanisms chlamydiae can use to acquire sphingolipids, *C. caviae* infection conditions likely depend on vesicular trafficking of sphingomyelin to the inclusion. Additionally, SMS2 localized to the inclusion membrane and partially colocalized with CERT (C. A. Elwell et al., 2011). Deletion mutants for SMS1/2 and CERT significantly reduced infectious progeny, suggesting the infection acquires sphingolipids in two ways. One way is from ceramide that is transported directly from the ER to the inclusion before being converted into sphingomyelin by SMS1/2. The second way is from ceramide undergoing ER-to-Golgi vesicular trafficking, which is converted into sphingomyelin prior to association with the inclusion (Derré et al., 2011; C. A. Elwell et al., 2011). Thus, having multiple means of acquiring host cell lipids likely maximizes the survival of the developing chlamydial infection.

1.9 Acquisition of cholesterol by the chlamydial infection

Cholesterol is another lipid obtained by the chlamydial infection by intercepting vesicular trafficking. Visualization of cholesterol at the inclusion membrane has been made possible with the fluorescent binding molecule filipin (Carabeo et al., 2003). By immunofluorescence, cholesterol was clearly observed at both the inclusion and chlamydial membranes (Carabeo et al., 2003). Purification of EBs showed that at least 6% of their membranes are composed of cholesterol (Carabeo et al., 2003). Cholesterol transport to chlamydial membranes was partially blocked by BFA, which prevents vesicular transport to the Golgi (Carabeo et al., 2003). These data support that one of the methods that the *Chlamydia* infection acquires cholesterol is from cholesterol-containing vesicles trafficking from the Golgi.

Multivesicular bodies (MVBs) are late endocytic organelles that provide another means of vesicular transport of cholesterol to the inclusion. MVBs contain intraluminal vesicles derived from the invagination and budding of vesicles into the endosome in an ESCRT-dependent manner (Piper & Katzmann, 2007). MVBs can develop into late endosomes which can either fuse with lysosomes to break down their contents or release their contents into the extracellular space following fusion with the plasma membrane (Piper & Katzmann, 2007). By immunofluorescence, components of MVB membranes including transmembrane proteins CD63 and MLN64 and the lipid, lysobisphosphatidic acid (LBPA), were shown to localize to the inclusion, with CD63 even being observed in small vesicles within the inclusion (Beatty, 2006, 2008). Anti-CD63 antibodies altered cholesterol distribution and impaired inclusion growth, although

CD63 expression was not necessary for MVB association with the inclusion (Beatty, 2008). Pharmacological inhibition of MVB biogenesis with the small molecule U18666A, caused lysosomal cholesterol accumulation, which correlated with an inhibition of inclusion growth and fewer infectious progeny (Beatty, 2006). These data support that the chlamydial infection utilizes MVB trafficking for development (Fig. 1.3B).

Lipid droplets (LDs) form from the membrane of the endoplasmic reticulum and have been suggested to be a source of neutral lipids, like cholesterol, for the chlamydial infection (Cocchiaro et al., 2008; Kumar et al., 2006). Electron microscopy showed that LDs surround the inclusion, colocalizing with chlamydial proteins, Lda1 and Lda3; and in some cases LDs traverse the inclusion membrane (Cocchiaro et al., 2008; Kumar et al., 2006). Interestingly, Lda3 induces disassociation of adipocyte differentiation related protein (ADRP), which is a host protein that inhibits LD-degrading lipases (Cocchiaro et al., 2008). It is plausible that Lda3 disrupts ADRP function to promote LD degradation so that chlamydiae can utilize the lipids in membrane biosynthesis (Cocchiaro et al., 2008). Additional studies showed that inhibition of neutral lipid biosynthesis impaired *Chlamydia* development, supporting the importance of LD-derived lipids in chlamydial pathogenesis (Fig. 1.3B) (Cocchiaro et al., 2008).

1.10 Is cholesterol truly necessary for the chlamydial infection?

Although cholesterol transport to the chlamydial inclusions has been observed, there is still speculation about whether cholesterol is necessary for *Chlamydia* infection. There are a couple pieces of evidence to suggest that cholesterol is not required. First,

infection in DHCR24-/- mutant cells, which have a mutation in the final step of cholesterol synthesis, produced no defect in the chlamydial infection (Gilk et al., 2013). As DHCR24-/- mutants still produce the cholesterol precursor, desmosterol, it is possible that desmosterol is sufficient for the infection. It is also possible that desmosterol is converted into cholesterol by chlamydiae, but this has not been tested. Second, the majority of host cell cholesterol is found in the plasma membrane, but there are no studies that have implicated the plasma membrane as a source of cholesterol for the chlamydial infection. These examples cast doubts about cholesterol as a requirement for the chlamydial infection.

However, there is much more data that supports cholesterol being necessary for *Chlamydia* pathogenesis. Cholesterol is not commonly found in prokaryotes but it comprises 6% of the chlamydial membranes (Carabeo et al., 2003). As previously mentioned, *Chlamydia* have a reduced, but conserved genome that does not encode cholesterol synthesis machinery (Sigalova et al., 2019), meaning the infection depends on the host cell to provide this lipid. Also, disrupting cholesterol trafficking with inhibitors caused defects in inclusion growth and progeny production (Beatty, 2006). Another intracellular pathogen, *Eimeria bovis*, requires exogenous sterol uptake and intracellular cholesterol transport to promote development (Silva et al., 2022). This is also the case for other intracellular bacteria including *Coxiella, Anaplasma, Ehrlichia, and Rickettsia,* which all rely on cholesterol from their eukaryotic host for pathogenesis (Samanta et al., 2017). These data support the general requirement of cholesterol during intracellular

bacterial infections, which strongly suggests that cholesterol may also be important for *Chlamydia* infection.

Depending on availability, eukaryotic cells either acquire cholesterol through receptor-mediated uptake of low-density lipoprotein (LDL) or conduct endogenous cholesterol synthesis in the endoplasmic reticulum (Fig. 1.3A) (Maxfield & van Meer, 2010). If insufficient LDL is available in the media, the cells will initiate the latter process. For cells cultivated in FBS serum media, like in our studies, the primary source of cholesterol is acquired as LDL, which is trafficked through the endosomal-lysosomal pathway (Goldstein & Brown, 2015). In the endocytic compartment, acid lipases cleave the cholesterol esters to release free cholesterol for delivery to the late endosome (LE) (Subramanian & Balch, 2008). Carabeo *et al.* determined that *Chlamydia* obtained LDL-derived cholesterol and cholesterol made *de novo* in a Golgi-dependent manner (Fig. 1.3B) (Carabeo et al., 2003).

In the late endosome, Niemann-Pick C1 (NPC1) and NPC2 are the cholesterol binding proteins that are important for cholesterol transport (Fig. 1.3A) (Subramanian & Balch, 2008). NPC1 is a large, protein with 13-transmembrane domains and is found within the membrane of the LE. NPC2 is a smaller, glycosylated protein found in the lumen of the late endosome. The de-esterified cholesterol is first bound by NPC2, which then transfers the cholesterol to the N-terminal binding domain of NPC1. Next, NPC1 inserts cholesterol into the LE/lysosomal membrane for transport to cellular membranes, however the molecular mechanisms for this process are poorly understood (Luo et al., 2017). Defects in either NPC1 or NPC2 result in lysosomal accumulation of cholesterol

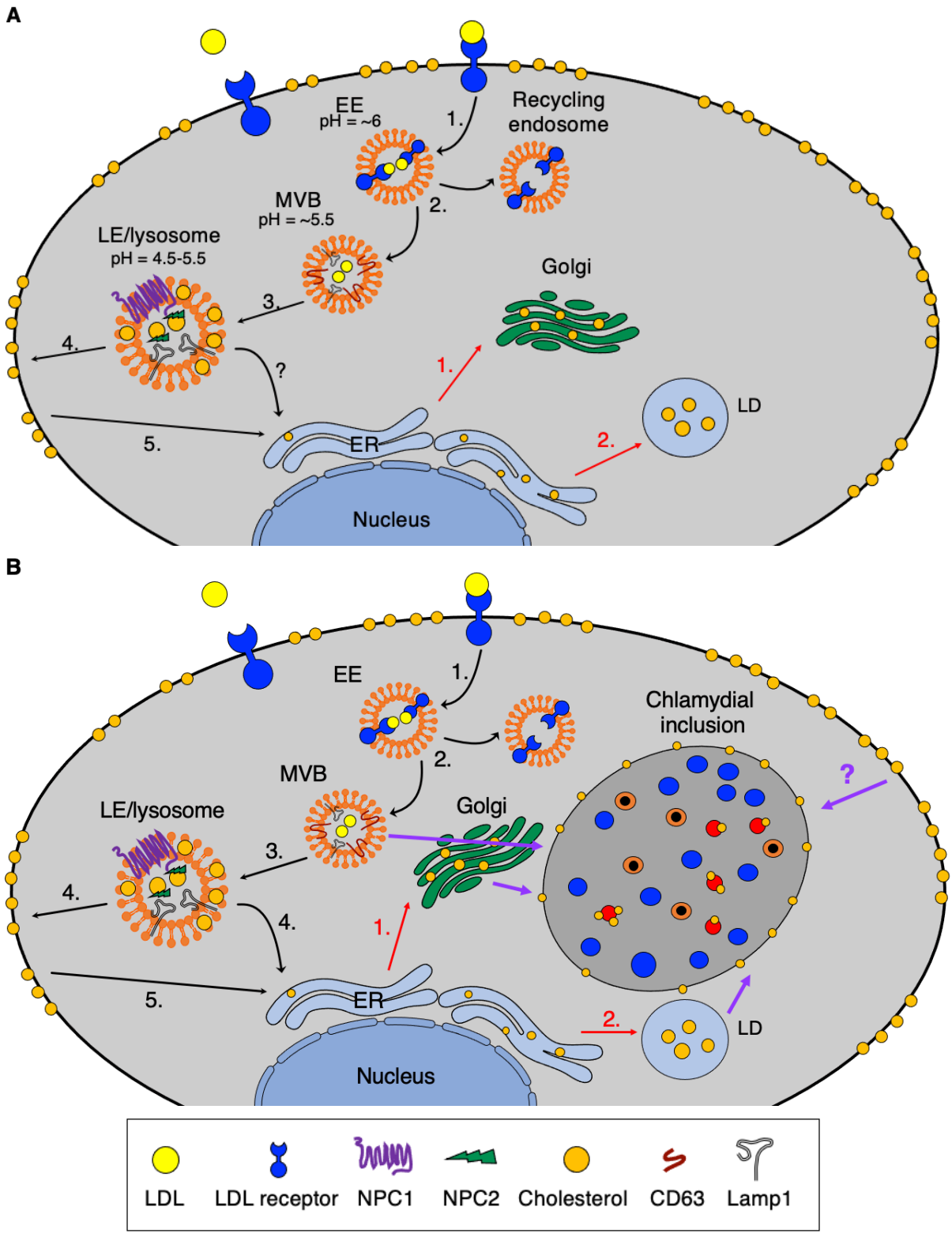
A
EE
pH = ~6
1.
Recycling
endosome
2.
MVB
pH = ~5.5
LE/lysosome
pH = 4.5-5.5
3.
Golgi
4.
?
1.
LD
5.
ER
2.
Nucleus
B
EE
1.
Chlamydial
inclusion
2.
MVB
?
LE/lysosome
Golgi
3.
4.
4.
1.
5.
ER
2.
LD
Nucleus
LDL
LDL receptor
NPC1
NPC2
Cholesterol
CD63
Lamp1

Figure 1.3. Trafficking of cholesterol acquired by LDL receptor-mediated endocytosis and endogenous cholesterol synthesis in uninfected and *C. trachomatis*-infected cells.
The black arrows indicate the pathway for eukaryotic host cell cholesterol acquired by LDL-receptor mediated endocytosis. The red arrows indicate the pathway for endogenous host cell cholesterol synthesis. The purple arrows indicate the pathways that the *Chlamydia* infection is known to intercept for acquiring cholesterol.
(A) Cholesterol trafficking in an uninfected HeLa cell. 1) Endocytic cholesterol acquisition begins when LDL binds to LDL receptor at the cell surface. 2) Once endocytosed, LDL is trafficked in the early endosome (EE) and is de-esterified in the more acidic compartment of multi-vesicular bodies (MVBs), which express CD63. Meanwhile, the LDL receptor is recycled to the cell surface by the recycling endosome. 3) Next, in the lumen of the late endosome (LE), the cholesterol-binding protein NPC2 binds cholesterol and transfers it to a second, cholesterol-binding transmembrane protein, NPC1. NPC1 integrates cholesterol into the LE membrane. 4/5) The LE fuses with the more acidic lysosome, which expresses Lamp1. Cholesterol is then transported to the plasma membrane followed by transport to the ER and Golgi. There is some evidence to suggest that cholesterol can also be transported to the ER directly from the lysosome, although this has been widely debated. When there is an insufficient amount of cholesterol in the extracellular environment, the cell will initiate endogenous cholesterol production. 1) Cholesterol is synthesized in the ER, which can then be trafficked to the Golgi for transport to cell membranes. 2) In cases where there is an abundance of cholesterol, the ER will store it in lipid droplets (LD).
(B) Cholesterol trafficking in a *C. trachomatis*-infected HeLa cell. The infection intercepts cholesterol from MVBs, the Golgi, and LDs. The plasma membrane is a rich source of cholesterol, but it is not known whether the inclusion can obtain cholesterol from this membrane directly.

and a 10-fold increase in intracellular cholesterol levels (Lange et al., 1998). Beatty *et al.* also showed that inhibition of NPC1 cholesterol transport with the drug U18666A caused defects in inclusion growth and RB-to-EB conversion (Beatty, 2006, 2008) (Fig. 1.3B). These data support the role of cholesterol in promoting the chlamydial infection, but it is still an area of active research and will be addressed further in chapter 5.

1.11 Studying *Chlamydia* infection *in vitro*

Chlamydia is a challenging organism to work with in the laboratory setting

because it cannot be grown in traditional bacteriological media and requires a eukaryotic host for propagation. Some chlamydial species such as *C. muridarum* have been successful for studies in mouse models, likely because the strain specifically infects mice and hamsters (De Clercq et al., 2013). As *C. trachomatis* infects humans and monkeys, there are no suitable mouse models because they require high inoculation titers and the infection resolves quickly (De Clercq et al., 2013). *C. trachomatis* genital infections are caused by serovars D-K, but studies of host cell-*C. trachomatis* interactions in our lab are typically performed *in vitro* with LGV serovar L2 because of its high infection efficiency (Bugalhão & Mota, 2019; Scidmore, 2006). Even so, chemical or mechanical assistance is necessary to increase infectivity.

The advantage of studying the *Chlamydia* infection *in vitro* is that there are well-established and commonly used assays to monitor the chlamydial developmental cycle. To monitor inclusion growth, infected samples are fixed and visualized by microscopy. For immunofluorescence, the inclusions are stained with antibodies targeting MOMP or Incs that will allow visualization of the inclusion and its membrane. Inclusion sizes can then be measured from immunofluorescence images manually or using computer programs. Another method of determining inclusion size is from electron microscopy (EM) images. Like immunofluorescence images, EM can provide a 2D image of a section of an infected cell, from which an outline of the inclusion can be made and quantified for the area. The advantage of this method is that it does not require antibodies to visualize the inclusion, although it is more labor intensive and costly than

standard immunofluorescence imaging. A limitation of both methods, however, is that they measure inclusion size on a 2D scale. Recently, there have been advancements of studying the chlamydial infection using 3D-electron microscopy (3D-EM), which uses serial sections of 2D images to reconstruct a 3D image of the inclusion vacuole (J. K. Lee et al., 2018). 3D-EM has been instrumental in monitoring volumetric changes in inclusion size over the course of the infection, as well as volumetric changes in the chlamydiae themselves (J. K. Lee et al., 2018).

Monitoring the number of infectious EBs produced is a great way to measure the biological success of the infection. Although EBs can be detected by EM, the EBs can still be defective in establishing a secondary infection because they are not “mature” (Núñez-Otero et al., 2021a). To measure infectious EBs, the *Chlamydia* field typically uses a progeny assay. For this assay, infected monolayers of cells are harvested and then sheared by freeze/thaw cycles followed by vigorous vortexing or sonication. This process breaks open the host cell and inclusion membranes to release the bacteria. Next, the chlamydiae are recovered and serially diluted to infect a fresh monolayer of cells. In our lab, after about 30 hours, the samples are fixed, stained for immunofluorescent visualization of the inclusion, and quantified for the number of inclusion forming units (IFUs). Thus, this assay measures the production of infectious offspring from a primary infection. However, the assay cannot determine whether any changes in infectious progeny are due to defects in RB-to-EB conversion or RB replication.

RB replication is less commonly reported in the literature, but equally important

because it can be used to determine the total number of *Chlamydiae,* not just infectious progeny. Quantifying the number of chlamydial genomes provides information about whether chlamydial genome replication is occurring and can be quantified by qPCR. However, because genome replication can also occur under conditions of persistence, one cannot assume that an increase in genomes coincides with an increase in chlamydiae. As mentioned, persistence is a state when an RB undergoes several rounds of genome amplification without cell division and no infectious progeny are produced (Beatty et al., 1994). To rule out that the increase in chlamydial genomes is due to persistence, qPCR assays should be conducted in conjunction with progeny assays and/or EM analyses to monitor the chlamydial forms.

1.12 Manipulating the chlamydial infection

Over the years, there have been many approaches to manipulate the chlamydial infection with **the goal** of understanding the mechanisms that promote *Chlamydia* development. Conditions such as temperature shifts (Tjiam et al., 1984; Theunissen et al., 1993; Chiarelli et al., 2020), siRNA knockdown (Heuer et al., 2009; Lucas et al., 2015), genetic manipulations (Bastidas & Valdivia, 2016; Wolf et al., 2019), and inhibitor treatments (Hackstadt et al., 1995; Beatty, 2006; Muschiol et al., 2006; Muñoz et al., 2021) have helped identify the metabolic processes and protein targets necessary for the chlamydial infection. However, each of these experimental manipulations has its advantages and its drawbacks.

siRNA knockdown is beneficial in that there are libraries of commercially

available siRNAs targeted for numerous host cell proteins that produce efficient knockdown. A drawback of siRNAs is that maintaining knockdown of the protein throughout the 48-72-hour *Chlamydia* developmental cycle can pose a challenge and may require multiple rounds of protein knockdown. Another challenge is that a protein may not ever be efficiently knocked down by siRNA, which means other approaches such as CRISPR or inhibitors need to be implemented.

Historically, there has been a lack of genetic tools available for studying chlamydial genetics. The greatest challenge is that *Chlamydia* is an intracellular pathogen and delivery of DNA into chlamydiae must traverse the host plasma membrane, inclusion, and chlamydial membrane. In the past decade, innovations such as CRISPRi, genetic transformation, allelic exchange, and transposon mutagenesis have all become successful methods of manipulating the chlamydial genome (Banerjee & Nelson, 2021).

Inhibitors are particularly useful in that they can be easily added and replenished in the media at any timepoint during the infection. Also, the commercial availability of thousands of inhibitors at relatively low prices makes these experiments more accessible. One of the drawbacks of investigating inhibitors of chlamydial targets is that their efficacy depends on the ability of the small molecule to traverse both host and *Chlamydia* membranes. However, many inhibitor studies have successfully manipulated the chlamydial infection by targeting a host cell function. It is also important to properly titrate the inhibitor to find the tolerable concentrations for the host cell under infection conditions. If the inhibitor is not tested for toxicity, defects in the infection could be

caused by a dying host cell rather than the efficacy of the inhibitor. Another drawback of inhibitors is that they may exhibit off target effects, which makes it challenging to discern the specific target contributing to a phenotype. Thus, to validate a target's role in the infection, inhibitor studies can be complimented with siRNA knockdown.

1.13 Assessing how the *Chlamydia* field measures defects in the *Chlamydia* infection through inhibitor studies.

Inhibitors are the most widely applied tool to understand the development of the chlamydial infection. There are currently over seven hundred publications of anti-chlamydial small molecule inhibitors, and many have led to the discovery of host and bacterial targets important for the chlamydial infection. I provide an extensive assessment of the effects of anti-chlamydial inhibitors, which has never been done before. **My goal** was to identify what host cell and chlamydial pathways, when blocked by inhibitors, caused the most defects in chlamydial development. From these analyses, we can determine which pathways are potential therapeutic targets.

Generally, inhibitors against lipid and protein synthesis/trafficking, host enzymes, inflammation, and a number of other cellular functions have been effective host cell targets to decrease the chlamydial infection (Table 1.1). For example, inhibitors iAkt (Capmany et al., 2019), T863 (Sharma et al., 2018), nafamostat mesylate (Inman & Chiu, 2012; Peng et al., 2020), Adalimumab (Njau et al., 2009), and PipN3/N4 (Reimer et al., 2016) blocked multiple parts of chlamydial development including inclusion growth, RB replication, and RB-to-EB conversion. These inhibitors are beneficial tools in

determining effective pathways and targets that are necessary during infection. With regards to chlamydial targets, inhibitors of type III secretion, chlamydial enzymes, metabolism, and chelating agents produced anti-chlamydial effects (Table 1.2). Specifically, inhibition of the chlamydial T3SS with C1 or INP0400 blocked inclusion growth, RB replication, and RB-to-EB conversion, highlighting the T3SS as a valuable target to inhibit chlamydial pathogenesis (Bailey et al., 2007; Claywell et al., 2018; Muschiol et al., 2006, 2009; Slepenkin et al., 2007; Wolf et al., 2006).

Although these tables provide an easy way to narrow down effective inhibitors of *Chlamydia* infection, there are many measurements missing that are important for characterizing these defects. There are several steps during chlamydial development that can be altered by inhibitors such as inclusion formation, inclusion growth, RB replication, RB-to-EB conversion, EB "maturation," and inclusion lysis (Fig. 1.4). However, many reports focus on investigating defects in inclusion growth and RB-to-EB conversion because they are easier to quantify and measure (Tables 1.1-1.2) (Abdelsayed et al., 2014; Beatty, 2006, 2008; Carabeo et al., 2002; Claywell et al., 2018; Cockburn et al., 2019; J. L. Li et al., 2018; Marwaha et al., 2014; Recuero-Checa et al., 2016; Ripa & Mårdh, 1977; Sabet et al., 1984; Saleeb et al., 2018; Seleem et al., 2020; Slepenkin et al., 2007). Inhibitor studies including sulfonated polymers (Gallegos et al., 2019), azoramide (Walenna et al., 2020), benzylidene acylhydrazides (Bao et al., 2014), salicylidene acylhydrazides (Ur-Rehman et al., 2012), W1227933 and W1774182 (Grishin et al., 2018) conduct one or two assays to measure effects on the chlamydial infection, but do not fully characterize these effects, meaning many steps in chlamydial

development that could be affected are not tested (“NT”) (Tables 1.1-1.2). Although some studies include more extensive analyses, a majority report a progeny defect without identifying effects on chlamydial replication, which can also contribute to fewer progeny (Tables 1.1-1.2). Some publications also indirectly report effects on replication by EM (Muschiol et al., 2006; Zigangirova et al., 2016). However, a limitation of EM analyses is that they provide information about the chlamydiae from a 2D section of the inclusion, which was shown to be an inadequate reflection of the chlamydial population in the entire inclusion (J. K. Lee et al., 2018). Another aspect of inhibitor treatment that is rarely considered is whether it alters the length of the *Chlamydia* developmental cycle, which is the case for several host cell inhibitors (Table 1.1). Further rationale for improving these inhibitor studies will be addressed in chapter 3.

Table 1.1. Inhibitors that target eukaryotic cell processes and their effects on the chlamydial infection.

The following is a list of published inhibitors of *Chlamydia* infection that directly target a eukaryotic host cell pathway. The inhibitors are categorized based on the type of pathway that is affected. The effects of these inhibitors are classified based on their ability to alter 1) inclusion growth, 2) RB replication, 3) RB-to-EB conversion, 4) EB maturation, and 5) inclusion lysis. A check mark indicates that a defect was observed, "No effect" means there was no observed effect, and "NT" means the developmental process was not tested.

		Effects on the chlamydial infection					
	Inhibitor	**1. Inclusion growth**	**2. RB replication**	**3. RB-to-EB conversion**	**4. EB maturation**	**5. Inclusion lysis**	**Source**
Lipid synthesis and/or trafficking	U18666A	✓	NT	✓	NT	NT	Beatty, 2006; 2008
	Desipramine	✓	NT	✓	NT	NT	Cockburn, 2019
	ACSL inhibitors	✓	NT	✓	NT	NT	Recuero-Checa, 2016
	Myriocin	No effect	NT	✓	NT	✓	Robertson, 2009
	iAkt	✓	✓	✓	NT	NT	Capmany, 2019
	T863	✓	✓	✓	NT	NT	Sharma, 2017
	mevastatin	✓	✓	NT	NT	NT	Bashmakov, 2010
	4-HCAA	✓	NT	✓	NT	NT	Peters, 2015
	Triacsin C, 2-Fluoropalmitic acid (2-FPA), Rosiglitazone	✓	NT	✓	NT	NT	Kumar, 2006; Recuero-Checa, 2016; Soupene, 2017
	AACOCF3	NT	NT	✓	NT	NT	Su, 2004
Protein synthesis and/or trafficking	BFA	✓	NT	No effect	NT	NT	Hackstadt, 1995; 1996
	Cyclohexamide	✓	NT	✓	NT	NT	Ripa, 1977; Sabet, 1984; Grieshaber, 2020
Enzymes	Nafamostat Mesylate	✓	✓	✓	NT	NT	Inman, 2012; Peng, 2020
	SC-560 and PTPBS	✓	NT	✓	NT	NT	Yan, 2008
	z-Val-Phe-CHO, z-Leu-Nle-CHO	✓	✓	✓	NT	NT	Itoh, 2019
	GM6001	✓	NT	✓	NT	NT	Balakrishnan, 2009
	PI15	No effect	✓	✓	NT	NT	Prusty, 2018
	U0126, VX-11e, BVD-523, LJH685, and LJI308	✓	NT	✓	NT	NT	Xue, 2021
	Rotterlin	✓	✓	NT	NT	NT	Lei, 2012; Shivshankar, 2020
	Compound D7	✓	✓	NT	NT	NT	Johnson, 2009
Inflammation	Resveratrol and curcumin	NT	NT	NT	NT	✓	Deby-Dupont, 2005
	Andrographilide	✓	NT	✓	NT	NT	Hua, 2015
	aspirin	✓	NT	✓	NT	NT	Yoneda, 2003; Tiran, 2002
	Maraviroc, celastrol and azelastine	✓	✓	✓	NT	NT	Kuratli, 2020
Additional inhibitors	melatonin and serotonin	✓	NT	✓	NT	NT	Rahman, 2005
	pyocyanin	✓	NT	✓	NT	NT	Jian Lin Li, 2018
	PipN3 and PipN4	✓	✓	✓	NT	NT	Reimer, 2016
	sulfated pentagalloyl glucoside (SPGG); sulfonated polymers PSS and SPS	NT	NT	✓	NT	NT	Gallegos, 2019
	Adalimumab	✓	✓	✓	NT	NT	Naju, 2009
	phenoxazine derivate, Phx-3	✓	✓	✓	NT	NT	Uruma, 2005
	sodium azide and antimycin	✓	NT	✓	NT	✓	Gill, 1970
	azoramide	NT	NT	✓	NT	NT	Walenna, 2020
	acylated sulfonamides	✓	NT	✓	NT	NT	mojica,2017; Marwaha, 2014
Plant-derived inhibitory compounds	Capsaicin	✓	✓	✓	NT	NT	Yamakawa, 2018
	Biochanin A	✓	NT	✓	NT	✓	Hanski, 2014

Table 1.2. Inhibitors that target *Chlamydia* and their effects on the chlamydial infection.

The following is a list of all the known published inhibitors of *Chlamydia* infection that directly target a chlamydial pathway. The inhibitors are categorized based on the type of pathway that is affected. The effects of these inhibitors are classified based on their ability to alter 1) inclusion growth, 2) RB replication, 3) RB-to-EB conversion, 4) EB maturation, and 5) inclusion lysis. A check mark indicates that a defect was observed, "No effect" means there was no effect, and "NT" means the developmental process not tested.

		Effects on the chlamydial infection					
	Inhibitor	1. Inclusion growth	2. RB replication	3. RB-to-EB conversion	4. EB maturation	5. Inclusion lysis	Source
T3SS Inhibitors	C1	✓	✓	✓	NT	NT	Wolf, 2006; Claywell, 2018
	CL-55	✓	✓	✓	NT	NT	Zigangirova, 2012; 2016
	INP0341	✓	NT	✓	NT	NT	Slepenkin, 2007
	INP0400	✓	✓	✓	NT	NT	Muschiol, 2006; Slepenkin, 2007; Slepkin, 2020; Muschiol, 2009; Bailey, 2007
	INP0010	✓	✓	NT	NT	NT	Keyser, 2008
	W1227933 and W1774182	✓	NT	NT	NT	NT	Grishin, 2017
	Salicylidene acylhydrazides	NT	NT	✓	NT	NT	Ur-Rehman, 2012
	Benzylidene Acylhydrazides	✓	NT	✓	NT	NT	Bao, 2014
	INP0007	NT	NT	NT	NT	NT	He, 2015; Slepenkin, 2007
	INP0007	✓	NT	NT	NT	NT	Prantner, 2009
	INPs 0341, 0149, 0161, 0029, 0007, 0400, 0269	✓	✓	✓	NT	NT	Chu, 2010
Enzymes	MDSA and derivatives	✓	NT	✓	NT	NT	Claywell, 2018
	JO146 and JCP83 (designed CtHtrA inhibitors)	✓	✓	✓	NT	NT	Huston 2013; Gloeckl, 2013; Marsh, 2017; Agbowuro, 2019; Hwang, 2021; Ong, 2015; Lawrence, 2016
	A01 (designed CtHtrA inhibitor)	✓	✓	✓	NT	NT	Zhou, 2019
	P2-modified proline analogues	NT	NT	✓	NT	NT	Hwang, 2022
	primary alcohol (1-Butanol)	NT	No effect	✓	NT	NT	Nelson, 2006
	3'-pyridyl oxindole, compund D7	✓	✓	✓	NT	NT	Johnson 2009
	benzal-N-acylhydrazones (BAH)	NT	NT	✓	NT	NT	Zhang, 2019
	WEHD-fmk	✓	✓	✓	NT	NT	Christian, 2011
Metabolism	KSK120	✓	✓	✓	NT	NT	Engström 2014; 2015
	KSK213	No effect	No effect	No effect	✓	NT	Nuñez-Otero, 2021
	Activator of cylindrical protease (ACP) derivatives	✓	NT	✓	NT	NT	Seleem, 2020
	LPC-011	✓	No effect	✓	NT	NT	Cram, 2017
	docosahexaenoic acid (DHA)	✓	NT	✓	NT	NT	Dudiak, 2021
Antibiotics	N-acylhydrazones, CF0001 and CF0002	✓	NT	✓	NT	NT	Zhang, 2017
	IFNγ	✓	No effect	✓	NT	No effect	Geibel, 2019
	FK506 and rapamycin	✓	NT	✓	NT	NT	Lundemose, 1993
Chelating Agents	8-hydroxyquinoline-ciprofloxacin	NT	NT	✓	NT	NT	Vu, 2018
	3-isoxazolidone derivatives	✓	NT	✓	NT	NT	Abdelsayed, 2014

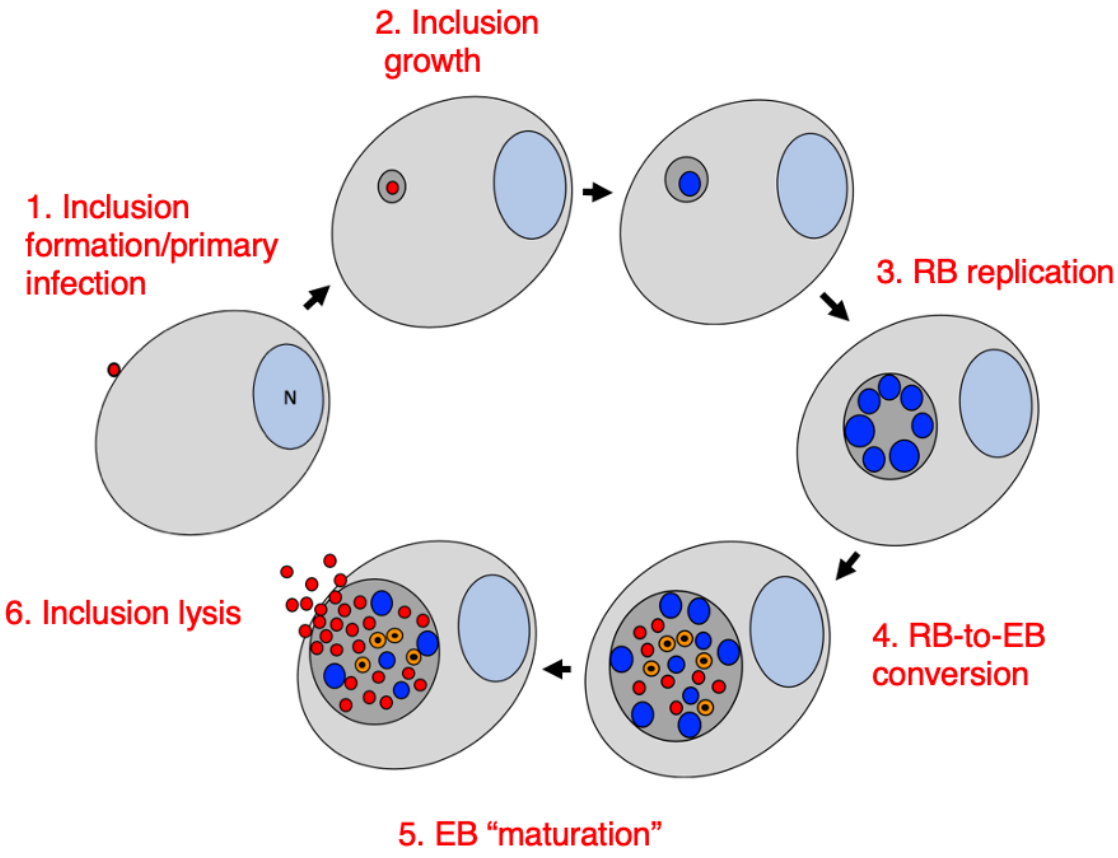

Figure 1.4. Inhibitors can alter the *Chlamydia* infection at several points during development. Inhibitors have been shown to alter: 1) inclusion formation during a primary infection, 2) inclusion growth, 3) RB replication, 4) RB-to-EB conversion, 5) EB “maturation,” defined as EBs capable of a secondary infection, and 6) inclusion lysis.

CHAPTER 2: MATERIALS AND METHODS

"The true method of knowledge is experiment." - William Blake, Poet

2.1 Pharmacological compounds

Table 2.1 Pharmacological compounds used in these studies. These small molecule inhibitors and other compounds are presented with the final concentrations optimized for *C. trachomatis* infection conditions. All compounds were reconstituted in dimethyl sulfoxide (DMSO).

Compound	Source	Catalog #	Final concentration
Brefeldin A (BFA)	Fisher Scientific	AAJ62340MA	1 µg/ml
KSK120	Sven Bergström, Umeå University, Umeå (gift)	----------	10-15 µM
MK2206	Selleckchem	S1078	3 µM
Compound C	Sigma Aldrich	171260	2 µM
H89	Cayman Chemical	130964-39-5	12.5 µM
D/D solubilizer	TakaRa	635054	1 µM
Filipin I	Sigma Aldrich	11078-21-0	500ug/ml
U18666A	Fisher Scientific	NC9623905	15 µM
Itraconazole	Fisher Scientific	501362449	3.75 µM
Astemizole	ToCris	348950	3.75 µM
Y27632 dichloride	ToCris/ABCAM	ab120129	25 µM
SB 747651A dihydrochloride	ToCris	4630	2.5 µM
PF-4708671	MedChem Express	HY-15773	1 µM
PF543 hydrochloride	ToCris	575410	20 µM
Bafilomycin	Selleckchem	88899-55-2	200 nM
Chloroquine	Millipore/Sigma Aldrich	50-63-5	20 µM

2.2 Antibodies

Table 2.2 Antibodies used in these studies. The following is a table of the antibodies, sources, and dilutions used for applications in immunofluorescence and western blot.

Antibody Target	Species	Source	Catalog #	Dilution
MOMP	Mouse	Dr. Ellena Peterson (gift) (Pal et al., 2005)	----	1:30,000
Hc1	Rabbit	Dr. Ted Hackstadt (gift) (Grieshaber et al., 2006)	----	1:1,000
Hc2	Rabbit	Dr. Ted Hackstadt (gift) (Grieshaber et al., 2006)	----	1:1,000
OmcB	Rabbit	Dr. Guangming Zhong (gift) (Qi et al., 2011)	----	1:1,000
GM130	Mouse	BD Transduction Laboratories	610822	1:5,000
pPKC substrate	Rabbit	Cell Signaling	2261S	1:1,000
GAPDH	Mouse	Santa Cruz Biotechnology	sc-47724	1:2,000
α-tubulin	Rabbit	Sigma	T5168	1:5,000
Rabbit IgG Alexa Fluor 488	Donkey	Invitrogen	A21206	1:1,000
Mouse IgG Alexa Fluor 555	Donkey	Invitrogen	A31570	1:1,000
Rabbit IgG LI-COR IRDye 680	Goat	Fisher Scientific	926-680-71	1:10,000
Mouse IgG LI-COR IRDye 800	Goat	Fisher Scientific	926-32210	1:10,000

2.3 Cell culture

HeLa, RPE-1, and MEF cell lines were purchased from ATCC and cultured at 37°C and 5.0% CO_2 in Dulbecco's modified Eagle medium (DMEM) (11995-065; Gibco) supplemented with 10% fetal bovine serum (FBS) (S11550; Atlanta Biologicals). mpkCCD WT and PKA knockout cell lines were a generous gift from Mark Knepper (National Institutes of Health, Bethesda, MD) and were grown in DMEM supplemented with 10% FBS. C1 HeLa cells stably expressing GFP-tagged FM4-hGH were kindly

provided by Andrew Peden (University of Sheffield, England). All experiments were conducted in HeLa cells unless stated otherwise.

2.4 *Chlamydia* infection

Monolayers of HeLa cells were infected with *C. trachomatis* serovar L2, strain L2/434/Bu (ATCC VR-902B), at a multiplicity of infection (MOI) of 3 in SPG (200 mM sucrose, 20 mM sodium phosphate, and 5 mM glutamate, pH 7.2) and centrifuged at 700 × *g* for 1 h at room temperature. After centrifugation, the inoculum was removed and replaced with 500 µl of DMEM supplemented with 10% FBS. *C. trachomatis* infections in other cell lines were carried out under the same conditions. Infections with the RST5 CPAF WT and RST17 CPAF chlamydial mutant, a generous gift from Dr. Raphael Valdivia (Duke University), were performed following the same infection protocol.

2.5 *Chlamydia* infections with inhibitors

Inhibitors were added to infected monolayers immediately after the 1-hour centrifugation step. The inhibitor was present in the medium for the duration of the infection. For replenishment studies, fresh inhibitor medium was added at 24 hpi.

2.6 Immunofluorescence microscopy

Cells, grown and infected on glass coverslips, were fixed in either cold 4% paraformaldehyde or 100% ice-cold methanol for 10 min. Cells were permeabilized and

incubated in blocking buffer (2% FBS, 0.1% Triton) for 30 min at room temperature. *C. trachomatis* was visualized with a monoclonal mouse antibody against the major outer membrane protein (MOMP). Coverslips were mounted with ProLong Glass antifade containing NucBlue to stain DNA (P36985; Invitrogen). Immunofluorescence microscopy images were acquired on a Zeiss Axiovert Observer microscope (#1029641704). Inclusion areas were quantified by manual tracing using ImageJ software.

2.7 Viability assay

Toxic effects of the inhibitor on uninfected host cells were assessed with the MTT assay per the manufacturer's protocol (ab211091; Abcam).

2.8 Infection efficiency

HeLa cells infected with *C. trachomatis* at an MOI of 3 were treated with inhibitors starting at 1 h post infection (hpi). At 32 hpi, samples were fixed in ice-cold methanol, permeabilized, blocked, and then stained for MOMP. The number of cells containing an inclusion was quantified from 10 different fields using a 63× objective. The data were expressed as a percentage of cells with an inclusion, which is reflective of infection efficiency.

2.9 qPCR

The number of chlamydial genomes per infected HeLa cell was measured by qPCR. A

plasmid containing the *C. trachomatis euo* gene was used to generate a standard curve from which the *Chlamydia* copy number was calculated. PCRs with primers to a host cell gene (GAPDH) were performed to generate a PCR product that was used to calculate the total number of host cells. The total number of *Chlamydia genomes* per cell was calculated by normalizing *Chlamydia* copy number (EUO) to the respective GAPDH values. Primer sequences for EUO were 5′-*TTATTCCGTGGGACAAGTGG*-3′ (forward primer) and 5′-*TGCAAGACTTTTCCCTTTGC*-3′ (reverse primer). Primer sequences for GAPDH were 5′-*GGCGCTCACTGTTCTCTCCC*-3′ (forward primer) and 5′-*CGCAAGGCTCGTAGACGCG*-3′ (reverse primer). Each qPCR utilized SsoAdvanced universal SYBR green supermix (1725271; Bio-Rad) and was run on a Bio-Rad thermocycler.

2.10 Progeny assay

C. trachomatis-infected cells were treated with inhibitors starting at 1 hpi. At the indicated time point after infection, cells were washed with 1× PBS, which was then replaced with 500 µl cold SPG. Cells were lysed by freezing at –80°C for 30 min, followed by thawing at 37°C for 15 min and vigorous vortexing. Cell lysates were serially diluted in SPG and used to reinfect fresh monolayers of HeLa cells in the absence of inhibitor. At 27 hpi, cells were fixed in ice-cold methanol, and numbers of inclusion forming units were determined via immunofluorescence microscopy using an antibody to MOMP. The number of inclusions was determined from 10 fields of view observed with a 20× objective. For analyses to determine progeny per cell, the number of

infectious progeny (IFUs) was divided by the number of host cells present at the start of the infection. The number of host cells was quantified by manual counting of trypsinized cells on a hemocytometer.

$\underline{\text{Progeny}_{max}}$ is defined as the maximal number of progeny detected by progeny assay. The time point of Progeny_{max} coincides with the last time point intact inclusions for a particular condition are observed. Thus, the time point of Progeny_{max} can be used as a proxy for the time point of the onset of inclusion lysis.

2.11 Western blotting

Cell lysates were prepared by lysing cells directly in 2% SDS (Johnson et al., 2015), followed by boiling of the samples at 95°C for 5 min. Equal volumes of lysate were loaded, separated by SDS-PAGE, and transferred onto nitrocellulose membranes. Membranes were blocked with 5% bovine serum albumin (BSA) in 1× Tris-buffered saline containing 0.1% Tween 20 (TBS-T). The membranes were imaged on an Odyssey CLx Li-COR machine.

2.12 Electron Microscopy

MK2206 and Compound C-treated samples

C. trachomatis-infected HeLa cells were washed once with 1X PBS and trypsinized at 37°C for 5 minutes. Samples were centrifugated at 300xg for 5 minutes, washed gently with 5 ml of 1XPBS, and centrifugated for another 5 minutes. Infected cells were

resuspended in 1 ml of fixative (EM-grade 2% paraformaldehyde (100503-917; VWR), EM-grade 2.5% glutaraldehyde (NC9861069; Fisher Scientific) in 0.1 M cacodylate buffer and incubated rocking at room temperature for two hours. After pelleting the cells at 300xg for 5 minutes, the fixative was removed, replaced with 0.1 M cacodylate buffer, and stored at 4°C. Samples were processed in the Molecular Microbiology Imaging Facility at the Washington University School of Medicine in St. Louis.

H89-treated samples

C. trachomatis-infected HeLa cells were fixed with 2% EM-grade paraformaldehyde (100503-917; VWR) and 2.5% EM-grade glutaraldehyde (NC9861069; Fisher Scientific) for 30 min at room temperature and then overnight at 4°C. MK2206 and Compound C samples were processed and imaged at the Molecular Microbiology Imaging Facility at the Washington University School of Medicine in St. Louis. H89 samples were processed and imaged by the Electron Microscopy Core Imaging Facility at the University of Maryland School of Dentistry.

2.13 Protein transport assay

C1 HeLa cells stably expressing GFP-tagged FM4-hGH were infected with *C. trachomatis* at an MOI of 3 and grown in the presence or absence of 12.5 µM H89 starting at 1 hpi. Infected cells were treated for up to 100 min with D/D solubilizer at a final concentration of 1 µM, fixed, and analyzed by fluorescence microscopy. As a positive control, infected cells were incubated with 100 µM H89, a concentration known

to inhibit protein transport to the cell surface (Aridor & Balch, 2000), for 2 h prior to solubilizer addition.

2.14 C_6-NBD ceramide lipid transport assay

This lipid transport assay was performed as described previously (Moore, 2012). In brief, HeLa cells, seeded on coverslips and infected with *C. trachomatis* at an MOI of 3, were grown in the presence or absence of 12.5 µM H89. To compare the effect of H89 on lipid transport for inclusions of similar size, control samples were assayed at 24 hpi and H89 samples at 36 hpi. At the indicated time points post infection, cells were shifted to 4°C for 30 min and washed twice with ice-cold Eagle minimal essential medium (EMEM; 50188268FP; Fisher Scientific). They were then incubated with EMEM supplemented with 0.035% defatted BSA (9048-46-8; Fisher Scientific), 5 µM C_6-NBD ceramide (NC0339630; Fisher Scientific), and H89. After a 60-min incubation at 4°C, which facilitated C_6-NBD ceramide labeling, unincorporated C_6-NBD ceramide was removed by washing twice with EMEM. Cells were then incubated with EMEM containing 0.75% defatted BSA and H89 for the times indicated at 37°C, followed by staining with 4′,6-diamidino-2-phenylindole (DAPI) and mounting for immediate observation by fluorescence microscopy. As a positive control, cells were treated with brefeldin A, which inhibits ceramide transport to the inclusion (Hackstadt et al., 1995), from 21 to 24 hpi, followed by sample harvesting and analysis at 24 hpi.

2.15 Fluorescent EGF uptake assay

HeLa cells were plated for a confluency of 70%. The following day, samples were infected and incubated with DMSO or 12.5 µM H89. At 27 hpi, samples were washed twice with 1XPBS and replaced with serum free media containing DMSO or 12.5 µM H89 an incubated for an additional 3 hours. As controls for a block in EGF endocytosis, samples were treated with 5 µM Erlotinib or incubated on ice for 3 hours. At 30 hpi, media was reserved and 0.50 µg/ul of GFP-EGF (green) was added. Samples were fixed in 4% paraformaldehyde at the times indicated.

2.16 Transferrin uptake and pulse chase assay

Uptake assay

HeLa cells were plated for a confluency of 70%. The following day, samples were infected and incubated with DMSO or 12.5 µM H89. At 29 hpi, samples were washed twice with 1XPBS and replaced with serum starved DMEM+0.2% BSA media with DMSO or 12.5 µM H89 for 2 hours. At 31 hpi, media was reserved, and fluorescent transferrin (25 µg/ml) was added. Samples were fixed in 4% paraformaldehyde at the times indicated. As controls for a block in transferrin uptake, samples were pretreated with 50 µM H89 in serum free media for 1 hour prior to transferrin addition or incubated on ice.

Pulse chase assay

HeLa cells were plated for a confluency of 70%. The following day, samples were serum

starved in DMEM+0.2% BSA media with DMSO or 12.5 μM H89 for 3 hours at 37C. Media was reserved, and fluorescent transferrin (25 μg/ml) was added. Samples were incubated for an additional hour, washed twice with 1XPBS, and replaced with serum media. Samples were fixed in 4% paraformaldehyde at the times indicated. As controls for a block in transferrin uptake, samples were pretreated with 50-100 μM H89 in serum free media for 1 hour prior to transferrin addition or incubated on ice.

2.17 LysoTracker assay

HeLa cells were plated for a confluency of 70% on glass-bottom dishes. The following day, the media was removed, samples were washed twice with 1X PBS and replaced with 10% FBS DMEM serum media (no phenol red) in the presence or absence of 12.5 μM H89. 24 hours later, media was reserved and 50 nM of LysoTracker was added. Samples were incubated for an additional 2 hours and imaged live at the times indicated.

2.18 Cholesterol depletion and re-addition

HeLa cells were plated in 10% FBS DMEM media for infection the next day. Following the spin infection, *C. trachomatis*-infected HeLa cells were incubated in media supplemented with either 10% or 10% lipoprotein deficient fetal bovine serum (880100-1; Kalen Biomedical LLC). For conditions with cholesterol re-addition, 250X cholesterol lipid concentrate was added to the media (12531018; Thermo Fisher Scientific).

2.19 Statistical analysis

For each experiment, at least 3 independent biological replicates were performed, and results are presented as either means ± standard deviations (SD) or means ± standard error (SE). Data were analyzed by unpaired, two-tailed *t* tests on GraphPad Prism software, version 9.

CHAPTER 3: Differential effects of small molecule inhibitors on the intracellular *Chlamydia* infection

Note: Data has been accepted for publication in *mBio,* 2022. All the data and figures for this publication were generated myself.

"As always in life, people want a simple answer . . . and it's always wrong."

– Susan Greenfield, Ph.D. in Pharmacology

3.1 Abstract

Chlamydia are obligate intracellular bacteria that reside within a membrane-bound compartment called the chlamydial inclusion inside a eukaryotic host cell. These pathogens have a complex biphasic developmental cycle, which involves conversion between a replicating, but non-infectious, reticulate body (RB) and an infectious elementary body (EB). Small molecule inhibitors have been reported to have deleterious effects on the intracellular *Chlamydia* infection, but these studies have typically been limited in terms of assays and time points of analysis. We compared published and novel inhibitors and showed that they can differentially alter inclusion size, chlamydial number and infectious EB production, and that these effects can vary over the course of the intracellular infection. Our results provide the justification for analysis with multiple assays performed either at the end of the infection or over a time course. We also show that this approach has the potential to identify the particular step in the developmental

cycle that is impacted by the inhibitor. We furthermore propose that the magnitude of inhibitor-induced progeny defects is best quantified and compared by using a new value called maximal progeny production ($Progeny_{max}$). As a demonstration of the validity of this systematic approach, we applied it to inhibitors of Akt and AMPK, which are host kinases involved in lipid synthesis and cholesterol trafficking pathways. Both inhibitors reduced EB production, but Akt disruption primarily decreased RB-to-EB conversion while AMPK inhibition paradoxically enhanced RB replication.

3.2 Introduction

Chlamydia is the most common bacterial cause of sexually transmitted infection in the U.S. (Batteiger and Tan, 2019). Over 1.8 million cases of chlamydial infection are reported to the CDC each year, and this number is continually increasing (Centers for Disease Control and Prevention., 2019). There is no vaccine to prevent infection, which leaves surveillance testing and antibiotic treatment as the main management strategies to combat this public health challenge (Workowski, 2021). Small molecules have been reported to have anti-*Chlamydia* activity *in vitro*. While these inhibitors have the potential to be developed into antibiotics, they are also powerful tools for mechanistic studies of this wide-spread infection.

Chlamydia are obligate intracellular bacteria that replicate within an infected host cell via an unusual biphasic developmental cycle (Moulder, 1991). The infection begins with uptake of an elementary body (EB), the infectious form of the bacterium, into a eukaryotic host cell. Around 6-8 hours post infection (hpi), the EB converts into a

reticulate body (RB), which is the metabolically active, dividing, but non-infectious form of *Chlamydia*. After multiple rounds of RB replication, RBs asynchronously convert into EBs, which are released from the host cell either by lysis or inclusion extrusion to infect new host cells (Hybiske & Stephens, 2007). The length of the developmental cycle varies with *Chlamydia* spp., but for *C. trachomatis*, EBs are first produced at about 24 hpi and the developmental cycle lasts about 48 hours.

In an infected host cell, RBs and EBs are contained within a membrane-bound vacuole called the chlamydial inclusion. This compartment grows over time until it occupies most of the host cytoplasm and can be readily detected by light microscopy. Its membrane is composed of lipids and cholesterol, which are acquired from the host cell (Beatty, 2008; Carabeo et al., 2003; Hackstadt et al., 1995, 1996), but the mechanisms by which *Chlamydia* hijacks these molecules are not completely understood. The inclusion membrane also contains approximately 50 chlamydial inclusion membrane proteins (Incs) that mediate interactions with host organelles (Derré, 2015, 2017; C. A. Elwell et al., 2011; C. A. Elwell & Engel, 2012).

During the intracellular *Chlamydia* infection, there is a 1,000-fold increase in both the number of chlamydiae and the volume of the inclusion (J. K. Lee et al., 2018). Detailed quantitative and volumetric analyses have shown a tight correlation between chlamydial number and inclusion size over the entire course of a wildtype infection (J. K. Lee et al., 2018). Similarly, a correlation between chlamydial genome copy number and inclusion growth has been reported (Brothwell et al., 2021). As inclusion size can be readily monitored by immunofluorescence microscopy, it has often been used as a

surrogate measure for the overall infection.

Numerous small molecules are reported to have anti-chlamydial activity in a cell culture model of *Chlamydia* infection, as determined by measurements of inclusion size by immunofluorescence microscopy and/or EB production in progeny assays. Another, less frequently used assay is the quantification of chlamydial genome copy number by qPCR, which determines the total number of bacteria, but does not distinguish between RBs and EBs. Typically, these assays are performed at one or two time points during the intracellular infection, but the time points of analysis vary between studies. The dynamic nature of this biphasic developmental cycle raises several questions: 1) What are the best assays and time points to measure the effects of an inhibitor on the intracellular infection? 2) Do analyses at one or two time points accurately reflect the overall effects on the infection? 3) How can an inhibitor be analyzed if it alters the length of the developmental cycle? 4) How can the effects of different inhibitors be compared?

To answer these questions, we systematically studied how several published and novel chlamydial inhibitors alter the chlamydial infection. For each inhibitor, we determined the time point corresponding to the end of the infection, which allowed us to measure changes in the length of the developmental cycle. We then quantified inhibitor-induced alterations of inclusion growth, chlamydial replication and progeny production over the course of the intracellular infection. Our experiments showed that 1) small molecule inhibitors can have temporal and differential effects on the intracellular infection, 2) the magnitude of a progeny defect can be quantified and compared through a new value called $Progeny_{max}$, and 3) our approach can provide mechanistic insights

into the specific step in the *Chlamydia* developmental cycle that is disrupted by an inhibitor.

3.3 Results

We began our study with a head-to-head comparison of two small molecule inhibitors that were reported to alter the intracellular *Chlamydia* infection. KSK120 is an inhibitor of bacterial glucose metabolism that has been reported to delay inclusion growth and decrease progeny production (Engström et al., 2014, 2015). Brefeldin A (BFA), a known inhibitor of host cell protein transport, has been found to produce smaller inclusions without disrupting progeny production (Hackstadt et al., 1995, 1996). We infected HeLa cells with *C. trachomatis* serovar L2 and treated with the respective inhibitor at 1 hour post infection (hpi). At 30 hpi, which is a late time in the intracellular infection, we measured inclusion size by immunofluorescence microscopy and performed progeny assays, which use a secondary infection to quantify the number of infectious EBs. Both KSK120 and BFA produced smaller inclusions compared to untreated controls (Fig. 3.1A-B). However, KSK120 caused a large, 277-fold reduction in progeny, while BFA had no significant effect (Fig. 3.1C); both findings are consistent with published data (Engström et al., 2014; Hackstadt et al., 1996). However, these discordant effects on inclusion size and progeny demonstrate how a single assay may not adequately measure the effects of an inhibitor on the *Chlamydia* infection.

We next examined the consequences of KSK120 and BFA treatments on inclusion size over the course of the developmental cycle (Fig. 3.2). Inclusions in

KSK120-treated cells were initially smaller, but then grew to a similar size as control cell inclusions (Fig. 3.2A-B), consistent with previous studies (Engström et al., 2014, 2015). In contrast, BFA treatment caused a 2-fold reduction in inclusion size at all time points (Fig. 3.2A-B). These results demonstrate that small molecule inhibitors can have effects on inclusion growth that may not be uniform over the course of the intracellular infection. Moreover, they revealed the limitations of a single time point analysis and the hazards of extrapolating from measurements taken partway through the developmental cycle.

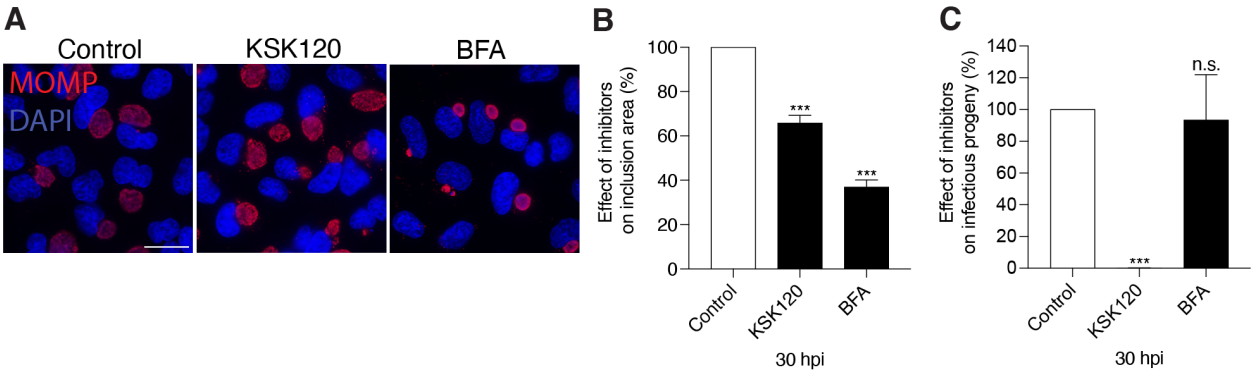

Figure 3.1. Inhibitors have discordant effects on the *Chlamydia* infection.
(A) Immunofluorescence images of *Chlamydia trachomatis* L2-infected HeLa cells treated with KSK120 or Brefeldin A (BFA) inhibitors starting at 1 hpi. Samples were fixed 30 hours post infection (hpi). To visualize the chlamydiae, samples were stained with antibodies to MOMP (red), while chlamydial and host DNA was detected with DAPI (blue). Scale bar is 10 µm.
(B) For each sample, the average inclusion area from 33-34 inclusions was normalized against the average inclusion area from the same number of control inclusions. The data are expressed as percentage of control. The results from three independent experiments are shown. The data are presented as means ± SE; ***, $P<0.001$.
(C) A progeny assay was performed to determine the number of infectious EBs from intact inclusions for control and inhibitor-treated HeLa cells at 30 hpi. Values of the inhibitor-treated conditions were normalized to their respective controls and are expressed as a percentage of control samples. Data are presented as means ± SE ($n=3$); ***, $P<0.001$; n.s. = data not statistically significant.

Our microscopy-based time course analysis also revealed that inhibitors can alter the length of the chlamydial developmental cycle. For control or KSK120 treatment, intact inclusions were visible up to 60 hpi, followed by widespread lysis of the inclusion and the host cell (Fig. 3.2A). In contrast, inclusions in BFA-treated cells only remained intact up to 48 hpi (Fig. 3.2A) and then underwent lysis. Thus, BFA appears to shorten the developmental cycle. These data raise the question of when to analyze and compare the effects of inhibitors if the length of the developmental cycle is altered.

To address this issue, we measured infectious progeny at 6 to 12-hour intervals over the time course of the infection to generate a one-step growth curve. For all inhibitors examined, progeny production increased to a peak and then gradually decreased at very late times (Fig. 3.3A-B). However, peak progeny production, which we called "$Progeny_{max}$", varied in time, occurring at 60 hpi for control and KSK120-treated cells, but at 48 hpi for BFA-treated cells. For all inhibitors, $Progeny_{max}$ coincided with the time point when we first detected host cell lysis, but most of the infected cells were still intact by light microscopy (data not shown). Compared to untreated control cells, $Progeny_{max}$ for KSK120- and BFA- treated cells were reduced by 83-fold (Fig. 3.3A) and 9-fold (Fig. 3.3B), respectively.

As a progeny defect could be due to effects on chlamydial replication or RB-to-EB conversion, we determined the number of chlamydial genomes by qPCR to assess possible effects on chlamydial replication. KSK120 treatment decreased the total number of chlamydiae by 16-fold, while BFA had no significant effect (Fig. 3.3C-D). Comparing the effects on chlamydial replication and infectious progeny production at

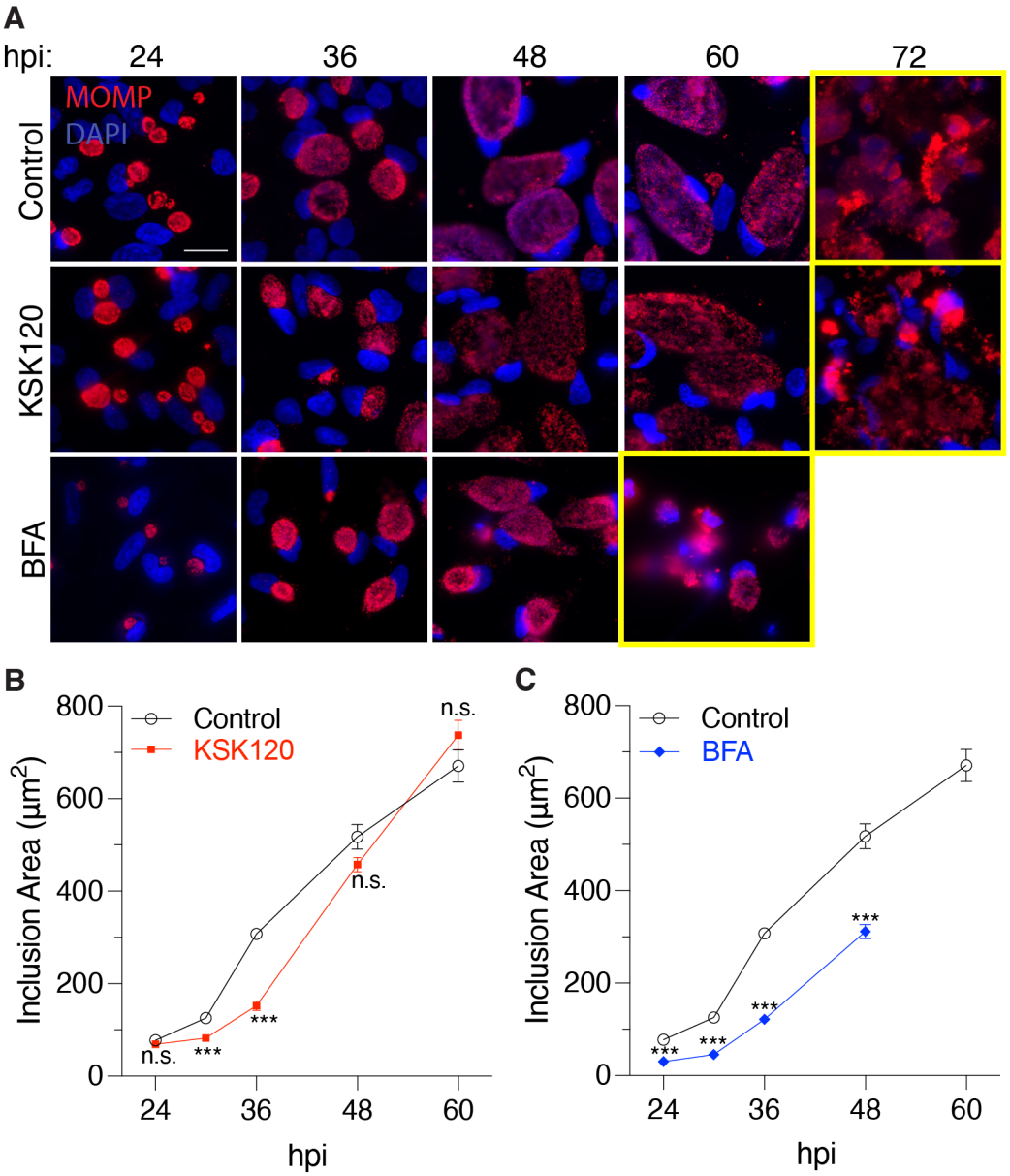

Figure 3.2. The effects of inhibitors on inclusion size can change during the time course of infection.

(A) Immunofluorescence images of *Chlamydia trachomatis* L2-infected HeLa cells treated with KSK120 or BFA inhibitors starting at 1 hpi. Samples were fixed at the times indicated and stained with antibodies to MOMP (red) and DAPI (blue). Scale bar is 10 µm. Yellow boxes indicate the time point when the onset of inclusion lysis is observed.

(B) The average area of 100 inclusions was measured for KSK120-treated cells at each time point. The data from one representative experiment are presented as means ± SE; ***, $P<0.001$; n.s. = data not statistically significant.

(C) Same as in (B) but for BFA-treated cells. The data from one representative experiment are presented as means ± SE; ***, $P<0.001$.

the time point of Progeny$_{max}$ revealed that KSK120 has deleterious effects on both RB replication and RB-to-EB conversion (Fig. 3.3A and C) (Engström et al., 2014, 2015). BFA, in contrast, had no effect on RB replication but primarily reduced progeny production, consistent with a defect in RB-to-EB conversion (Fig. 3.3B and D). Overall, our analysis shows that KSK120 and BFA disrupt different steps in development.

We then applied our systematic approach to two novel inhibitors that block synthesis and transport of host lipids and cholesterol, which are incorporated into both the inclusion and the chlamydial membrane (Beatty, 2008; Carabeo et al., 2003; C. A. Elwell & Engel, 2012). As the Golgi is a known source of lipids for the *Chlamydia* infection (Derré, 2017; C. A. Elwell & Engel, 2012; Hackstadt et al., 1995, 1996), we used MK2206 to inhibit Akt kinase activity, which is critical for lipid trafficking through the Golgi (Capmany et al., 2019). MK2206 treatment did not alter the length of the developmental cycle (Fig. 3.4A-C), inclusion growth (Fig. 3.4A-B) or chlamydial replication (Fig. 3.4D). However, at the time point of Progeny$_{max}$, MK2206 treatment showed a significant 29-fold reduction in progeny, consistent with a defect in RB-to-EB conversion (Fig. 3.4C). This conclusion was supported by EM analysis at 42 hpi (Fig. 3.4E). Quantifications of the chlamydial forms in the EM images showed a similar number of RBs for control and MK2206-treated samples (Fig. 3.4F). However, with MK2206, there was a small increase in IB numbers and a 2-fold decrease in the number of EBs (Fig. 3.4F). We also noted unusual-looking IBs, which are RBs in the process of converting into EBs, that were abnormally large with multiple dense nuclei (Fig. 3.4E). Together, these data suggest that Akt kinase activity promotes RB-to-EB conversion.

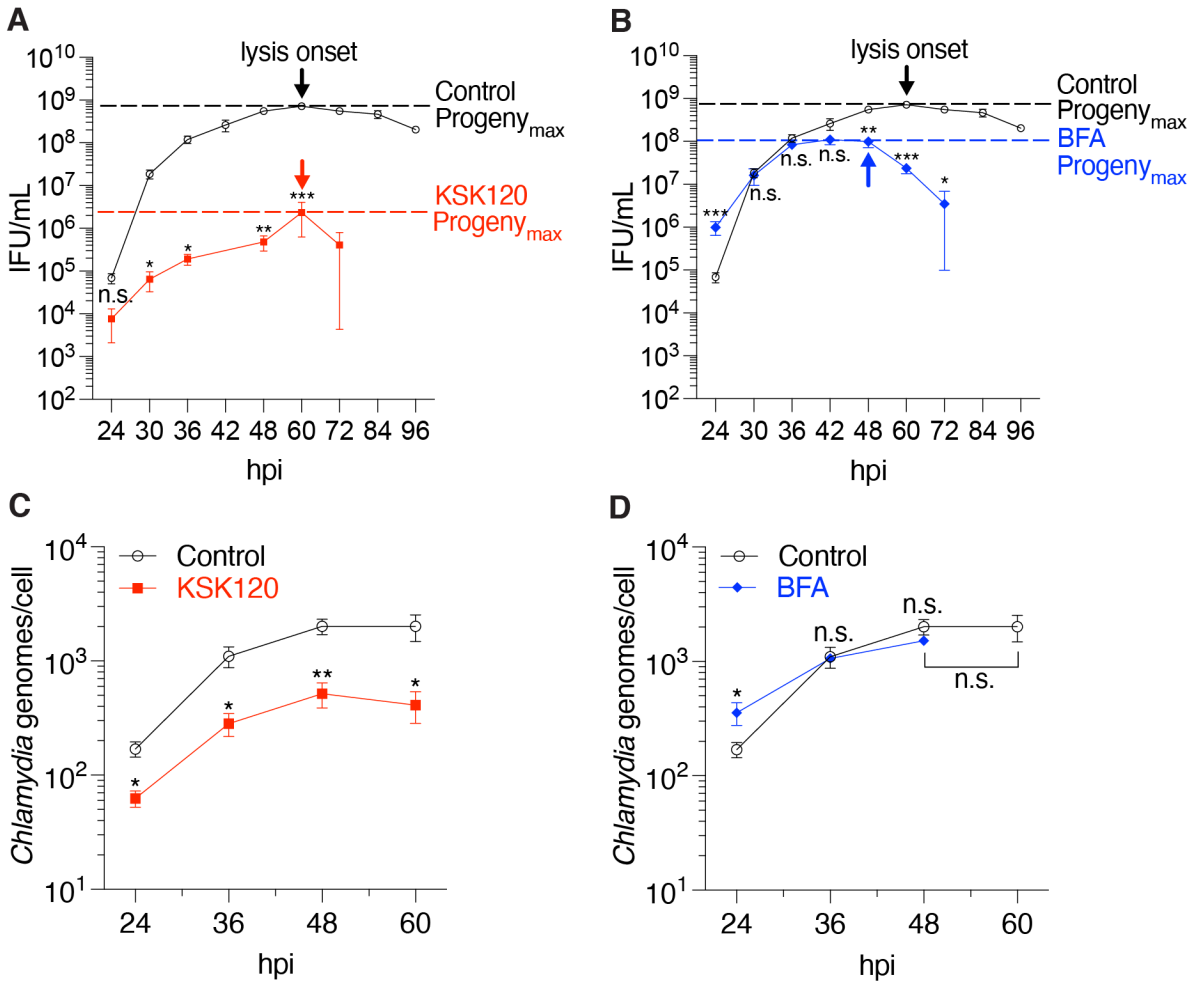

Figure 3.3. Progeny defects can result from effects on different steps of the *Chlamydia* developmental cycle.

(A) A progeny assay time course was used to determine the maximal number of infectious progeny ($Progeny_{max}$) yielded from intact inclusions in KSK120-treated cells. The onset of inclusion lysis is indicated by arrows. The horizontal dashed lines represent $Progeny_{max}$. The lysis onset also corresponds with $Progeny_{max}$. Data are presented as means ± SE (n=3); *, P<0.05; **, P≤0.01; ***, P<0.001; n.s. = data not statistically significant.

(B) Same as in (A), but for BFA-treated cells. Data are presented as means ± SE (n=3); *, P<0.05; **, P≤0.01; ***, P<0.001; n.s. = data not statistically significant.

(C) The number of chlamydial genomes for infected KSK120-treated HeLa cells was determined by qPCR at the indicated time points. Data are presented as means ± SE (n=3). *, P<0.05; **, P≤0.01.

(D) Same as in (C), but for BFA-treated HeLa cells. Data are presented as means ± SE (n=3). *, P<0.05; n.s. = data not statistically significant.

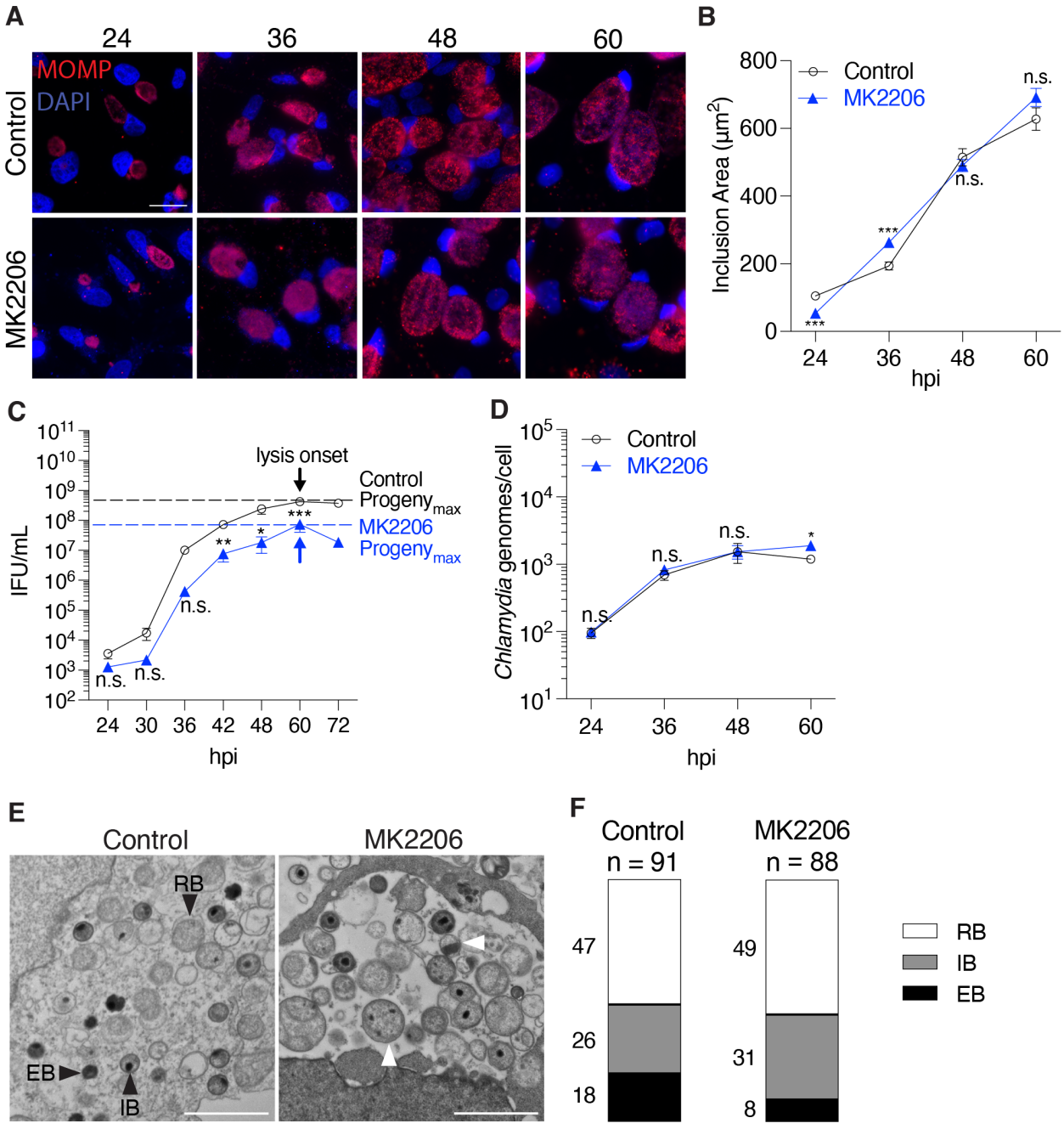

Figure 3.4. MK2206 may cause progeny defects through inhibition of RB-to-EB conversion.

(A) Immunofluorescence images of *Chlamydia trachomatis* L2-infected HeLa cells treated with DMSO or MK2206 starting at 1 hpi. Samples were fixed at the times indicated and stained with antibodies to MOMP (red) and DAPI (blue). Scale bar is 10 μm

(B) The average inclusion area from 100 inclusions was measured for each condition at each time point. The data from one representative experiment are presented as means ± SE;. ***, $P<0.001$; n.s. = data not statistically significant.

(C) A progeny assay time course was used to determine the $Progeny_{max}$ yielded from intact inclusions under MK2206-treated conditions. Arrows indicate the onset of inclusion lysis, when $Progeny_{max}$ was determined. Data are presented as means ± SE ($n=3$); *, $P<0.05$; **, $P\leq0.01$; ***, $P<0.001$; n.s. = data not statistically significant.
(D) The number of chlamydial genomes for infected MK2206-treated HeLa cells was determined by qPCR at the indicated time points. Data are presented as means ± SE ($n=3$). *, $P<0.05$; n.s. = data not statistically significant.
(E) Electron micrographs (EM) of infected cells treated with DMSO or MK2206 from 1 to 42 hpi. Scale bar, 2 µm. Chlamydial developmental forms are indicated: EB, elementary body; IB, intermediate body; and RB, reticulate body. Abnormal IBs with multiple dense chromatin foci are indicated with white arrowheads.
(F) A total of 100 chlamydial forms (RB, IB, and EB) was quantified from an EM image of a single inclusion for each condition. Infection and treatment conditions are described in part E.

We also tested Compound C, an inhibitor of the host cell kinase AMPK, which limits host cholesterol synthesis and promotes the breakdown of this important membrane component (Steinberg & Carling, 2019). Compound C did not alter the length of the chlamydial developmental cycle and slightly increased inclusion size (Fig. 3.5A-C). However, at the $Progeny_{max}$ (60 hpi), we observed a 4-fold increase in chlamydial genomes (Fig. 3.5D). As progeny production at this time point was similar as in control cells, we conclude that Compound C may enhance replication, but also limit RB-to-EB conversion. Consistent with this conclusion, electron micrographs showed that inclusions in Compound C-treated cells contained more RBs and fewer EBs than control inclusions (Fig. 3.5E). Quantifications of the chlamydial forms from EM images show that there is an increase in RB number for Compound C-treated samples (Fig. 3.5F). While there was no difference in the number of IBs between control and Compound C samples, there was about a 4-fold decrease in the number of EBs with Compound C (Fig. 3.5F).

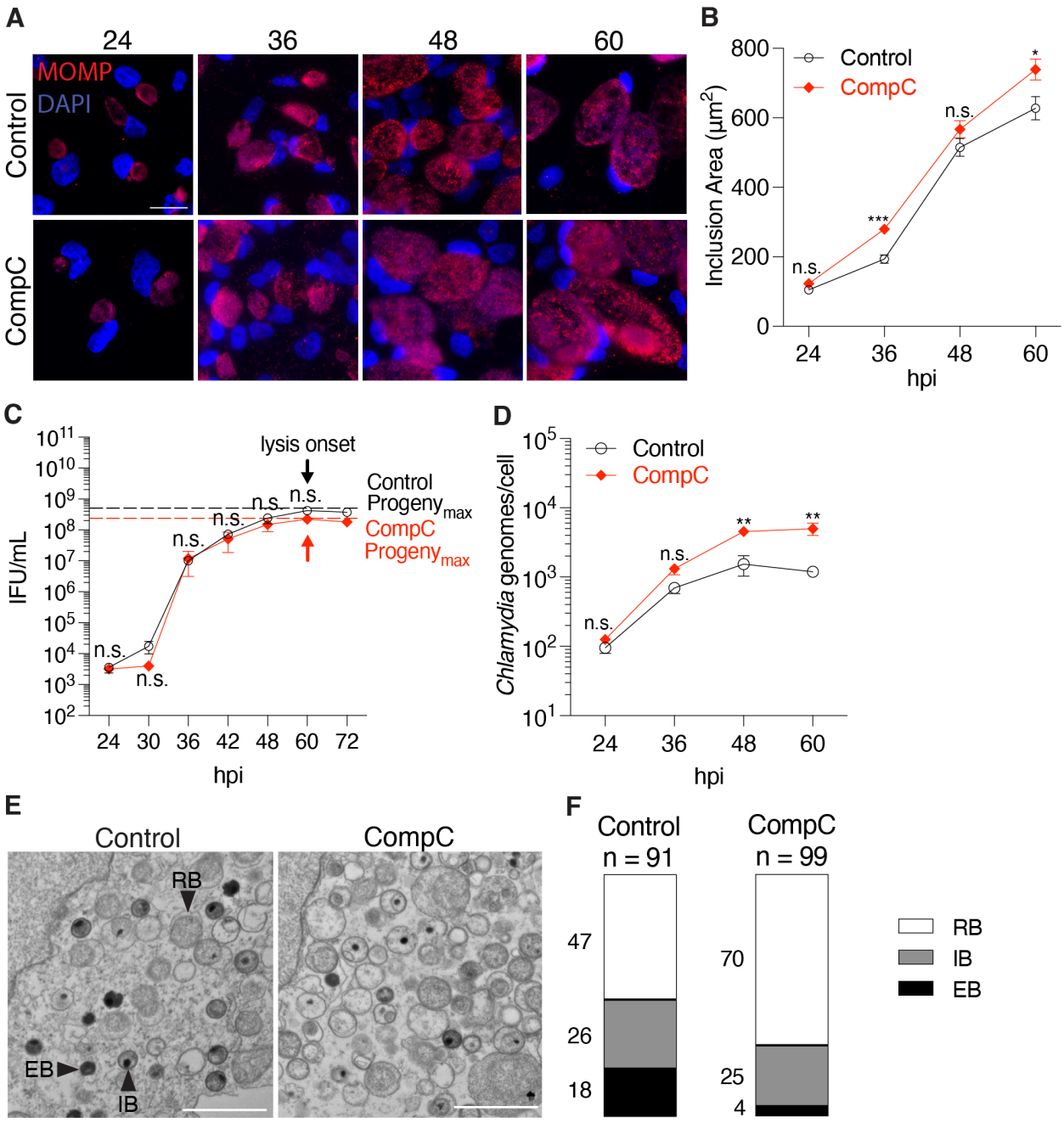

Figure 3.5. Compound C (CompC) inhibitor increases chlamydial replication.
A) Immunofluorescence images of *Chlamydia trachomatis* L2-infected HeLa cells treated with DMSO or CompC starting at 1 hpi. Samples were fixed at the times indicated and
stained with antibodies to MOMP (red) and DAPI (blue). Scale bar is 10 µm
(B) The average inclusion area from 100 inclusions was measured for each condition at each time point. The data from one representative experiment are presented as means ± SE;. *, $P<0.05$; ***, $P<0.001$; n.s. = data not statistically significant.
(C) A progeny assay time course was used to determine the $Progeny_{max}$ yielded from

intact inclusions with CompC-treated conditions. Arrows indicate the onset of inclusion lysis, at which $Progeny_{max}$ was measured. Data are presented as means ± SE (n=3); n.s. = data not statistically significant.
(D) The number of chlamydial genomes for infected CompC-treated HeLa cells was determined by qPCR at the indicated time points. Data are presented as means ± SE (n=3). **, $P \leq 0.01$; n.s. = data not statistically significant.
(E) Electron micrographs (EM) of infected cells treated with CompC from 1 to 42 hpi. Scale bar, 2 µm. Chlamydial developmental forms are indicated: EB, elementary body; IB, intermediate body; and RB, reticulate body.
(F) A total of 100 chlamydial forms (RB, IB, and EB) was quantified from an EM image of a single inclusion for each condition. Infection and treatment conditions are described in part E.

To put these results into context, we used $Progeny_{max}$ to compare the magnitude of the anti-chlamydial effects of these inhibitors (Fig. 3.6A). For example, MK2206 and BFA each caused about a 10-fold decrease in progeny, while H89 and KSK120 reduced progeny by 35- and 83-fold, respectively. These effects were much more severe than what we observed for Compound C, which produced a modest 3-fold reduction in progeny, in the same range as the CPAF mutant, RST17 (Fig. 3.6A), a well-characterized *C. trachomatis* loss-of-function mutant (Snavely et al., 2014). This analysis demonstrates how $Progeny_{max}$ can be used to quantify and compare the effects of different inhibitors and other manipulations on a productive chlamydial infection. Furthermore, the infection efficiency of the primary chlamydial infection was measured for each condition. None of the conditions affected the percentage of infected cells, supporting that the decrease in progeny was not caused by an inhibition of the initial infection (Fig. 3.6B).

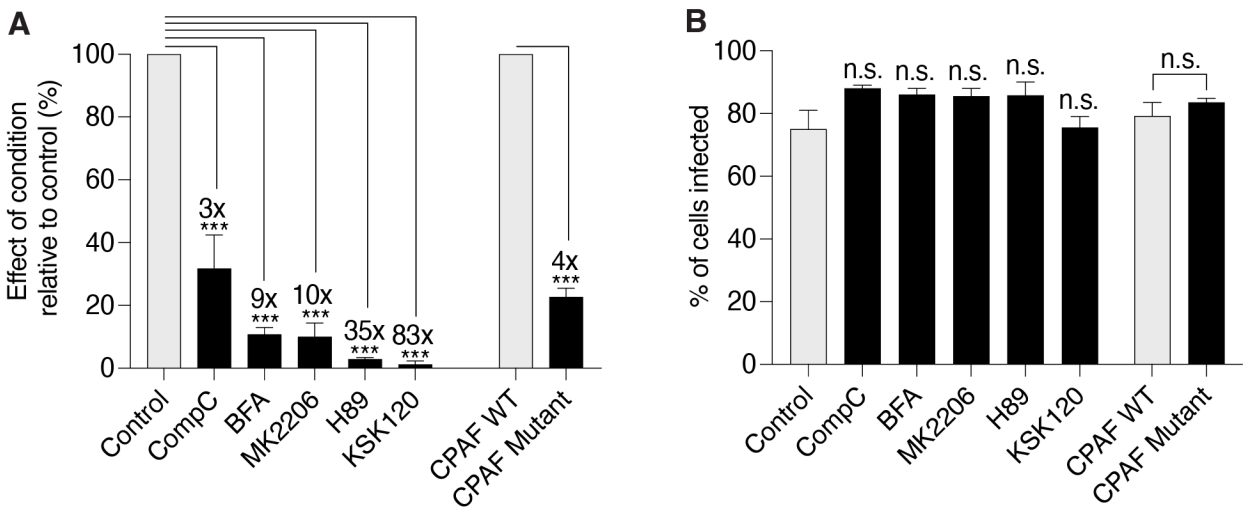

Figure 3.6. Experimental manipulations can alter Progeny$_{max}$ to different degrees, assuming no initial disruption of infection efficiency.
(A) The maximal number of infectious progeny (Progeny$_{max}$) for infected samples under each condition was normalized to their respective control (control and CPAF WT =100%). Data are expressed as a percentage to indicate relative effect of the condition. The fold change reduction in progeny is included above the error bars. Data are presented as means ± SE (n=3); ***, P<0.001.
(B) HeLa cells were infected on coverslips and treated with inhibitors from 1 to 48 hpi. Infection efficiency was determined by calculating the percentage of HeLa cells with an inclusion. n.s. = data not statistically significant.

Finally, we used our data to examine the relationship between inclusion size and chlamydial number (Fig. 3.7). At the time point of lysis onset, KSK120-treated cells had inclusions of normal size but few chlamydiae. In contrast, inclusions in BFA-treated cells were smaller, but chlamydial number was unaffected. Compound C caused a completely different effect by increasing chlamydial number without greatly affecting inclusion size. These findings demonstrate that inhibitors can disrupt the linear relationship between inclusion growth and the increase in chlamydial number observed during a wildtype *C. trachomatis* infection (J. K. Lee et al., 2018) in unpredictable ways.

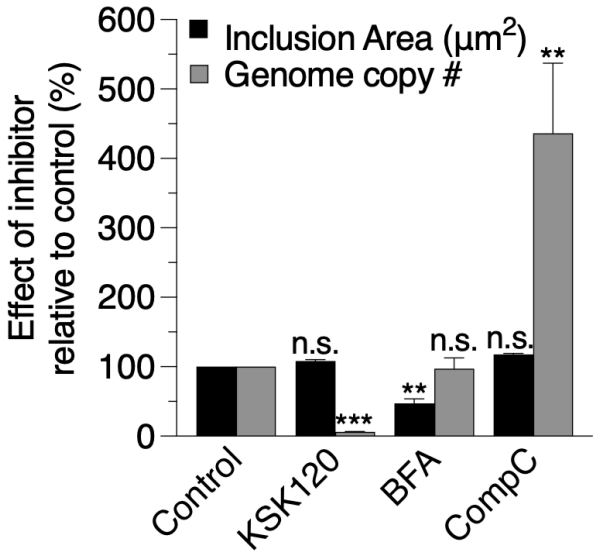

Figure 3.7. Inclusion size and chlamydiae numbers in an inclusion do not always correlate.
Inclusion areas and numbers of chlamydial genomes for inhibitor-treated samples were determined at the time of lysis onset. For control, KSK120, and Compound C lysis onset was at 60 hpi. For BFA, this time point was 48 hpi. Values from three separate experiments were normalized to untreated controls (control = 100%) and are expressed as a percentage to indicate the relative effect of the inhibitors. The data are presented as means ± SE ($n=3$); *, $P<0.05$; **, $P\leq0.01$; ***, $P<0.001$; n.s. = data not statistically significant.

3.4 Discussion

In this study, we present a systematic approach to analyze and compare the effects of small molecule inhibitors on the intracellular *Chlamydia* infection. We show that inhibitors can produce discordant effects on inclusion growth, chlamydial replication and infectious progeny production, providing strong justification for analyzing an inhibitor with multiple assays. We also report that inhibitors may not have uniform effects throughout the developmental cycle, raising the issue of when to analyze inhibitor treatment during the 48-72-hour *Chlamydia* developmental cycle. As a solution,

we introduced $Progeny_{max}$ as a new measure that allows the effects of inhibitors on a productive *Chlamydia* infection to be quantified and compared. We also demonstrate how our approach can reveal the step in the developmental cycle that is affected by an inhibitor and thereby provide novel mechanistic insights into the regulation of this infection.

Our experiments reveal the limitations of analyzing the effects of an inhibitor at one or two time points partway through the intracellular infection. For example, KSK120 produced smaller inclusions early on that then grew to the same size as control inclusions, consistent with a delay, rather than a block, in inclusion growth (Fig. 3.2) (Engström et al., 2015). With BFA and MK2206, progeny production was normal at early time points, but there were progeny defects at late times in the infection (Fig. 3.3B and 3.4A). This late temporal effect of BFA may explain why this commonly used protein transport inhibitor was not previously noted to cause a reduction in chlamydial progeny (Hackstadt et al., 1995, 1995).

We propose that the end of the intracellular infection, marked by the onset of inclusion and host cell lysis, may be the best time point for inhibitor analysis. Less than 10% of total *C. trachomatis* EB production is completed by 28 hpi (J. K. Lee et al., 2018), and thus measurements of progeny production at or prior to this time point may not accurately represent an overall progeny defect. In addition, progeny assays performed after the onset of host and inclusion lysis may undercount the number of progeny, presumably because EBs from lysed host cells are lost into the supernatant and not recovered. We found that inclusion size and infectious progeny were highest at

the time point when host cell lysis was first detected in a few cells by light microscopy. This time point must be experimentally determined because an inhibitor can alter the length of the developmental cycle, as was the case with BFA.

Our findings provide strong justification for the use of a time course analysis as a comprehensive and suitable approach for studying an inhibitor of the *Chlamydia* infection. The effect of KSK120 in causing an initial delay in inclusion growth, or the late progeny defects with BFA and MK2206 would not have been observed without a time course analysis. In a similar fashion, Clarke and colleagues used a time course analysis to show that the absence of the *C. muridarum* plasmid delayed inclusion growth and progeny production (Skilton et al., 2018). Furthermore, Sharma *et al.* observed that depletion of lipid droplets decreased progeny production at 24 hpi, but increased it at 48 hpi (Sharma et al., 2018). Thus, even though a time course analysis involves more work, it can provide additional information and even mechanistic insights into the effect of an inhibitor on the *Chlamydia* infection.

A key feature of our study is the introduction of $Progeny_{max}$ as a standardized measure to quantify and compare progeny defects in a *Chlamydia* infection. $Progeny_{max}$ measures maximal production of infectious EBs rather than EBs produced at some interim time point in the intracellular infection. As $Progeny_{max}$ is not measured at a fixed time point, it allows inhibitors to be compared even if they alter the length of the developmental cycle. The concept of $Progeny_{max}$ is generalizable and can be applied to effects on progeny production caused by other experimental interventions, including different growth conditions, chlamydial mutants, and genetic manipulation or protein

knockdown of host factors. Our comparison of $Progeny_{max}$ values for several inhibitors revealed that the magnitude of a progeny defect can vary widely, with some inhibitors causing a large, > 10-fold defect (Fig. 3.6). While it is likely that large progeny defects are deleterious *in vivo*, the significance of small progeny defects is less clear. Such smaller defects may require further investigations of the inhibitor in an animal model of *Chlamydia* infection.

The use of novel inhibitors revealed that host kinases involved in lipid transport and cholesterol metabolism are involved in the *Chlamydia* infection. Our studies with MK2206 suggest that Akt-mediated transport of host lipids to the inclusion is necessary for RB-to-EB conversion, but not for chlamydial replication. A previous study reported that disruption of Akt activity caused a defect in inclusion growth at 24 hpi, but did not examine late time points (Capmany et al., 2019). Our experiments showed that inclusions from MK2206-treated cells were small early on but eventually grew to normal size. In contrast, AMPK inhibition appeared to enhance chlamydial replication. Thus, the known role of AMPK in promoting cholesterol catabolism and decreasing lipid synthesis may negatively regulate RB replication by limiting lipid availability. Together, these findings indicate that host lipids and cholesterol may play central roles in both RB replication and RB-to-EB conversion. Further analysis of MK2206 and Compound C may help with the development of novel anti-chlamydial compounds and allow mechanistic investigations into the role of host lipids and cholesterol in the *Chlamydia* infection.

In summary, we describe an improved approach to investigate the effects of small molecule inhibitors on the intracellular *Chlamydia* infection. Taking potential effects of inhibitors on the length of the intracellular infection and discordant effects on the inclusion and the chlamydial developmental cycle into account, we propose that inhibitor analysis should be performed with multiple assays at the end of the infection, when host cell lysis has just begun. Additional mechanistic understanding may be obtained with a time course analysis and from comparing effects on different steps in the developmental cycle, such as RB replication and RB-to-EB conversion. Our analysis of two novel inhibitors provides new insights into the roles of host lipids and cholesterol in the *Chlamydia* infection. Overall, this approach for studying anti-chlamydial inhibitors may lead to new therapeutic strategies for treating the highly prevalent infections caused by this pathogenic bacterium.

CHAPTER 4: The Small Molecule H89 Inhibits *Chlamydia* Inclusion Growth and Production of Infectious Progeny

Note: Data are published in *Infection and Immunity,* 2021; DOI: 10.1128/IAI.00729-20. All the data and figures for this publication were generated myself. Experimental design was aided by Dr. Kevin Wang and Dr. Lauren Sheehan.

"There are two possible outcomes: if the result confirms the hypothesis, then you've made a measurement. If the result is contrary to the hypothesis, then you've made a discovery." – Enrico Fermi, PhD in Physics

4.1 Abstract

Chlamydia is an obligate intracellular bacterium and the most common reportable cause of human infection in the United States. This pathogen proliferates inside a eukaryotic host cell, where it resides within a membrane-bound compartment called the chlamydial inclusion. It has an unusual developmental cycle, marked by conversion between a replicating form, the reticulate body (RB), and an infectious form, the elementary body (EB). We found that the small molecule H89 slowed inclusion growth and decreased overall RB replication by 2-fold but caused a 25-fold reduction in infectious EBs. This disproportionate effect on EB production was mainly due to a defect in RB-to-EB conversion and not to the induction of chlamydial persistence, which is an altered growth state. Although H89 is a known inhibitor of specific protein kinases

and vesicular transport to and from the Golgi apparatus, it did not cause these anti-chlamydial effects by blocking protein kinase A or C or by inhibiting protein or lipid transport. Thus, H89 is a novel anti-chlamydial compound that has a unique combination of effects on an intracellular *Chlamydia* infection.

4.2 Introduction

Chlamydia is a genus of pathogenic bacteria that is of high importance to public health. In the U.S., more than 1.8 million cases of chlamydial infection are reported to the CDC each year (Centers for Disease Control and Prevention, 2019). Almost all of these cases are genital infections due to *Chlamydia trachomatis*, which is the most common etiology of bacterial sexually transmitted disease (Batteiger and Tan, 2019). *C. trachomatis* also causes trachoma, which is the most common form of infectious blindness (Batteiger and Tan, 2019). A related species, *C. pneumoniae,* causes community-acquired pneumonia.

All *Chlamydia* species are obligate intracellular bacteria that share an unusual biphasic developmental cycle (Moulder, 1991). The elementary body (EB) is the infectious form that binds and enters a eukaryotic host cell, where it remains within a membrane-bound vacuole called the chlamydial inclusion. By 6-8 hours post infection (hpi), the EB converts into a reticulate body (RB), which is the metabolically active and replicating form of the bacterium. The RB population then expands through multiple rounds of division. Starting at about 24 hpi, individual RBs asynchronously convert into EBs, but the mechanisms and signals that regulate RB-to-EB conversion are not known.

Between 40-72 hpi, depending on the species, EBs are released from the host cell by sequential lysis of the inclusion and host cell (Snavely et al., 2014), or by extrusion of the inclusion from the intact host cell (Hybiske & Stephens, 2007).

The chlamydial inclusion is a dynamic organelle with a membrane that is made up of host-derived lipids and chlamydial proteins. It originates from an endocytic vesicle that expands 1,000-fold in volume during the intracellular infection (J. K. Lee et al., 2018). This dramatic growth in inclusion size and inclusion membrane surface area depends on the acquisition of lipids from the host cell (C. A. Elwell & Engel, 2012; Moore, 2012; Moore et al., 2008). The inclusion membrane also contains about 50 chlamydial proteins called Incs, which are integral membrane proteins that mediate interactions with the host cell (Moore & Ouellette, 2014; Weber et al., 2015). Host proteins are also recruited to the vicinity of the inclusion (Elwell & Engel, 2012; Rzomp et al., 2003), but there are only few reports documenting their insertion into the inclusion membrane (Hasegawa et al., 2009).

Chlamydia obtains lipids by hijacking membrane trafficking pathways of the host cell (Derré, 2015, 2017; C. A. Elwell & Engel, 2012; Heuer et al., 2009). For example, in an infected cell, post-Golgi vesicles are rerouted to deliver host sphingolipids and cholesterol, but not proteins, to the inclusion and the bacteria (Carabeo et al., 2003; Hackstadt et al., 1995, 1996). Also, vesicles that mediate anterograde and retrograde transport between the ER and the Golgi are important for the infection (Derré et al., 2007; Dickinson et al., 2019; Park et al., 2018). It remains unclear how vesicular trafficking pathways are diverted, and how they deliver host lipids to the inclusion.

The small molecule H89 has been used as a tool for investigating vesicular transport pathways. This isoquinoline sulfonamide was initially identified as a selective inhibitor of Protein kinase A (PKA), although it has since been found to inhibit at least eight other cellular serine/threonine kinases (Bain et al., 2007; Davies et al., 2000; Jamora et al., 1999; Limbutara et al., 2019; Lochner & Moolman, 2006; Murray, 2008). Interestingly, this small molecule was found to disrupt vesicular transport pathways, including post-Golgi and ER-to-Golgi transport, in a PKA-dependent and -independent manner, respectively (Aridor & Balch, 2000; T. H. Lee & Linstedt, 2000; Muñiz et al., 1997).

In this study, we tested the effects of H89 on a *Chlamydia* infection. We show that H89 treatment of *C. trachomatis*-infected cells delayed inclusion growth but produced larger-than-normal inclusions. In addition, H89 altered the chlamydial developmental cycle by limiting RB-to-EB conversion. Mechanistic analyses revealed that these phenotypes were not caused by inhibiting PKA or PKC activity, or by disrupting vesicular transport of host lipids or proteins.

4.3 Results

H89 slows the growth of the chlamydial inclusion.

We found that H89 treatment of *Chlamydia*-infected cells produced a concentration-dependent reduction in inclusion size (Fig. 4.1A-B). At 32 hpi, 25 µM H89 decreased inclusion area by 92% compared to control cells treated with vehicle, but this high concentration of H89 had significant cytotoxic effects on the host cell (Fig. 4.1C).

H89 at 6.25 µM, in contrast, had no significant effect on inclusion size (Fig. 4.1A-B). Instead, we used 12.5 µM H89 for all experiments described in this study, because it reduced inclusion size by 78% without affecting cell viability or the percentage of host cells with an inclusion, which is a measure of infection efficiency (Fig. 4.1A-D). H89 at 12.5 µM also decreased *C. trachomatis* inclusion size in retinal pigment epithelial (RPE-1) cells and in mouse embryonic fibroblasts (MEFs), demonstrating that this phenotype is not cell type specific (Fig. 4.1E).

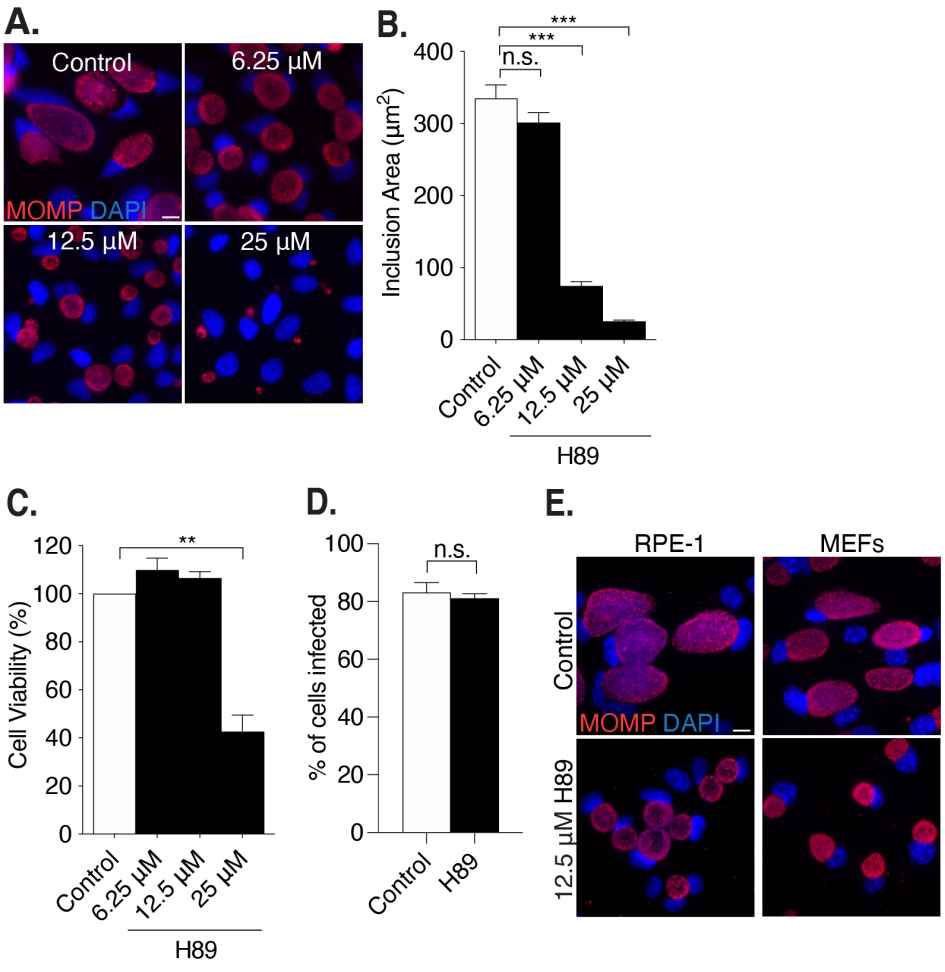

Figure 4.1. H89 decreases *C. trachomatis* inclusion size.
(A) HeLa cells grown on coverslips were infected with *C. trachomatis* L2 at an MOI of 3

and treated from 1 to 32 h post infection (hpi) with the indicated concentrations of H89. Control cells (control) were incubated in the equivalent volume of DMSO, which served as the solvent for H89. In these immunofluorescence images, chlamydiae are detected with antibodies to the major out membrane protein MOMP (red) and chlamydial and host DNA are stained with DAPI (blue). Scale bar, 10 µm.
(B) Quantification of the inclusion areas of the cells in panel A. One hundred inclusions were measured for each condition. Data from one representative experiment ($n=3$) are shown as means ± SD; ***, $P<0.001$. n.s. indicates the data are not statistically significant. (C) Viability of uninfected HeLa cells incubated with different concentrations of H89 for 32 h was assessed with an MTT cell viability assay. Data were normalized to the viability of untreated cells and are expressed as a percentage. Data are presented as means ± SD ($n=3$); **, $P\leq0.01$.
(D) HeLa cells were treated with 12.5 µM of H89 from 1 to 32 hpi. The percentage of HeLa cells with an inclusion was used to determine infection efficiency. n.s.: not statistically significant.
(E) Immunofluorescence images of retinal pigment epithelial cells (RPE-1) and mouse embryonic fibroblasts (MEFs) grown on coverslips, infected with *C. trachomatis* L2 at an MOI of 3, and treated with 12.5 µM H89 from 1 to 32 hpi. Scale bar, 10 µm.

We next investigated how H89 alters inclusion growth during the *Chlamydia* infection. We measured the greatest effect at 24 hpi, when inclusions were 5-fold smaller than that in untreated control cells (Fig. 4.2A-B). H89 also produced significantly smaller inclusions at 36 and 48 hpi. However, inclusions of H89-treated cells continued to grow so that at 48 hpi the difference in size was only 1.4-fold (Fig. 4.2A-B) compared to that of the control cells. These results indicate that H89 slows rather than blocks inclusion growth.

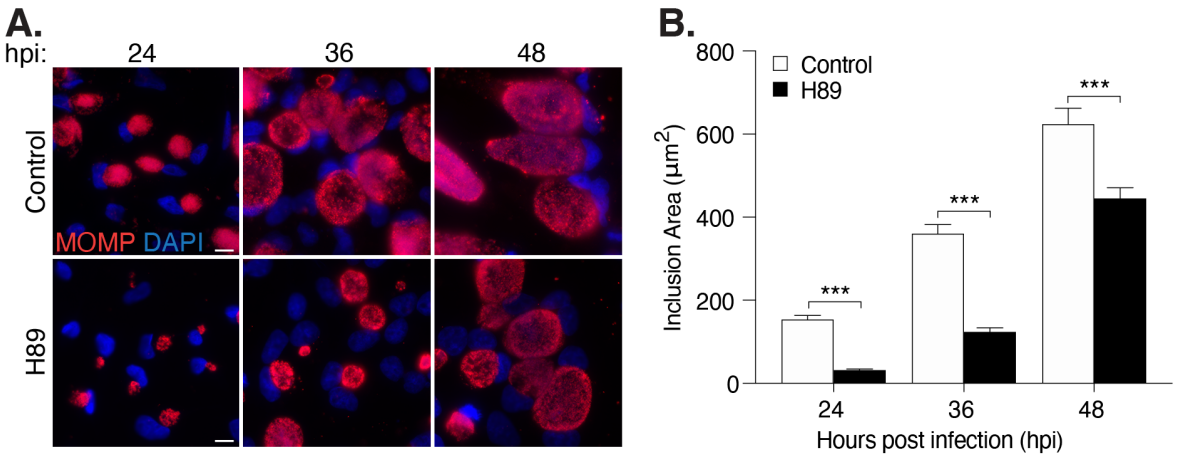

Figure 4.2. H89 delays *Chlamydia* inclusion growth.
(A) Immunofluorescence images of *Chlamydia trachomatis* L2-infected HeLa cells treated with H89 starting at 1 hpi. Samples were fixed at the indicated time points. Chlamydiae were stained with antibodies to MOMP (red), while chlamydial and host DNA was detected with DAPI (blue). Scale bar is 10 µm.
(B) Quantification of inclusion surface areas for the cells in panel A. One hundred inclusions were measured for each condition. Data from one representative experiment are presented as means ± SD ($n=3$); ***, $P<0.001$.

H89 alters the chlamydial developmental cycle

We performed a series of experiments to examine the effect of H89 on *Chlamydia* development. We first used quantitative PCR (qPCR) to quantify the number of chlamydial genomes within each infected cell as a measure of chlamydial replication. Compared to control cells, H89 treatment decreased the number of chlamydial genomes by about 2-fold from 12 to 48 hpi (Fig. 4.3A-B). These data show that H89 reduced chlamydial replication consistently throughout the infection by a small but measurable amount.

As qPCR does not distinguish between RBs and EBs, we used progeny assays to measure the effect of H89 on the production of infectious EBs. Prior to 24 hpi, the number of progeny with or without H89 treatment was very small (<1 inclusion-forming

units [IFU]/cell; data not shown). However, starting at 24 hpi, which is the time when EBs are first detected (J. K. Lee et al., 2018), H89 greatly decreased the production of progeny. For example, at 36 hpi, H89 treatment caused a 112-fold reduction from 1,914 to 17 progeny/cell, and at 48 hpi, H89 treatment caused a 25-fold reduction from 3,200 to 130 progeny/cell (Fig. 4.3C). Replenishing H89 at 24 hpi did not have additional inhibitory effects on inclusion size or progeny (data not shown), further confirming that H89 retained its activity over the course of the infection. Thus, our results show that the effects of H89 on infectious progeny are more than 10-fold greater than those on total chlamydial numbers (Fig. 4.3D).

We next investigated if H89 causes this disproportionate reduction in infectious chlamydiae by disrupting RB-to-EB conversion. As chlamydial late genes are expressed during RB-to-EB conversion (Rosario & Tan, 2020), we monitored the expression of the late gene product OmcB, which is an outer membrane protein only present in EBs (Belland et al., 2003; Shaw et al., 2000). Immunofluorescence microscopy analysis detected fewer OmcB-positive foci in inclusions of H89-treated cells than in controls at all three time points (Fig. 4.4A). Similarly, Western blots showed that OmcB levels, after normalization to the loading control, glyceraldehyde-3-phosphate dehydrogenase (GAPDH), were reduced in H89-treated cells by 73% at 36 hpi and 48% at 48 hpi (Fig. 4.4B-C). Protein levels of MOMP, an outer membrane protein expressed by all chlamydial forms, were not significantly reduced by H89 at these time points when normalized to GAPDH (Fig. 4.4B and D). H89 also reduced the expression of two other late gene products, Hc1 and Hc2, which are both involved in DNA condensation and EB

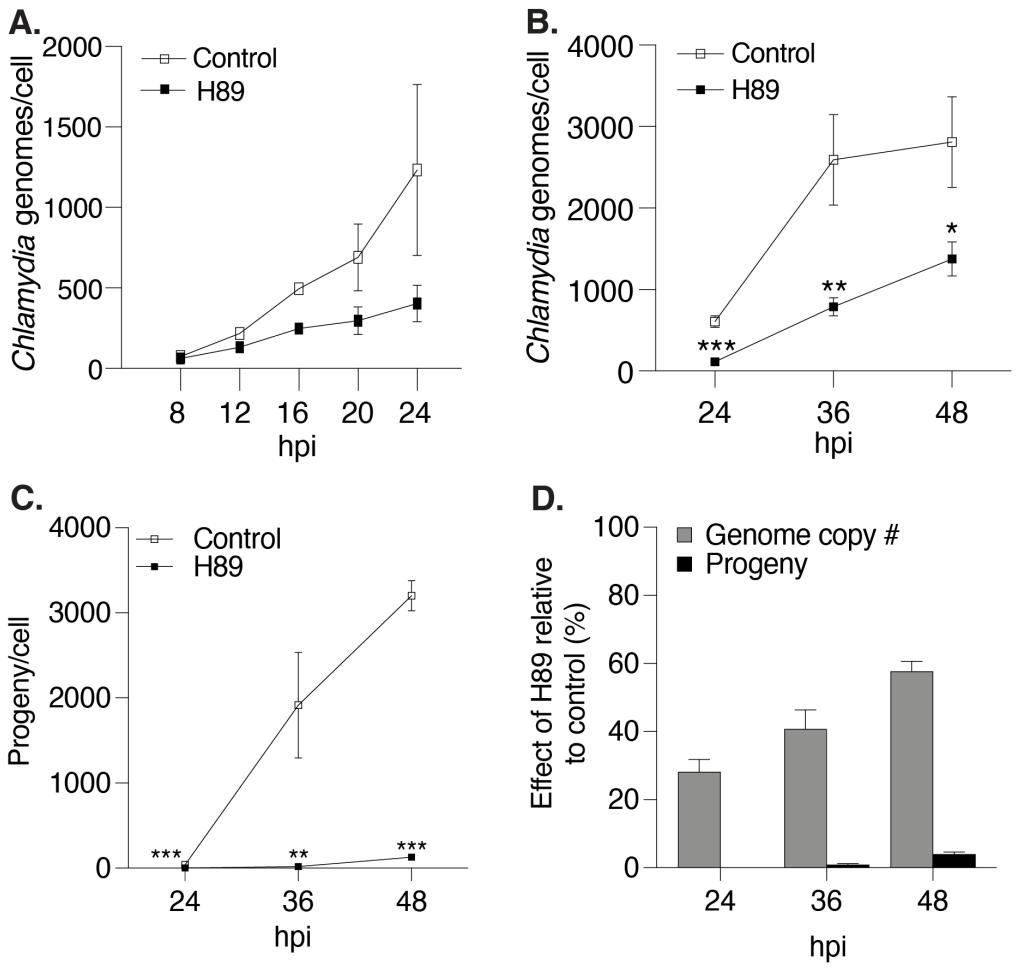

Figure 4.3. H89 causes a greater effect on infectious progeny than on chlamydial replication.

(A) The number of chlamydial genomes in infected, H89-treated HeLa cells was determined via qPCR at the indicated time points from 8-24 hpi and normalized to the number of host cells. Data are presented as means ± SD ($n=3$).

(B) The number of chlamydial genomes in infected, H89-treated HeLa cells was determined via qPCR at the indicated time points from 24-48 hpi and normalized to the number of host cells. Data are presented as means ± SD ($n=3$). **, $P \leq 0.01$; ***, $P \leq 0.001$.

(C) The number of infectious EBs was determined in a progeny assay for infected control and H89-treated HeLa cells at the indicated time points and normalized to the number of host cells. Data are presented as means ± SD ($n=3$); **, $P \leq 0.01$; ***, $P < 0.001$.

(D) The numbers of chlamydial genomes and infectious progeny in H89-treated samples were normalized to their untreated control counterparts (control = 100%) and expressed as a percentage to indicate relative effect of H89.

production (Fig. 4.4E) (Belland et al., 2003). These results provide evidence that H89 decreases the expression of late chlamydial genes.

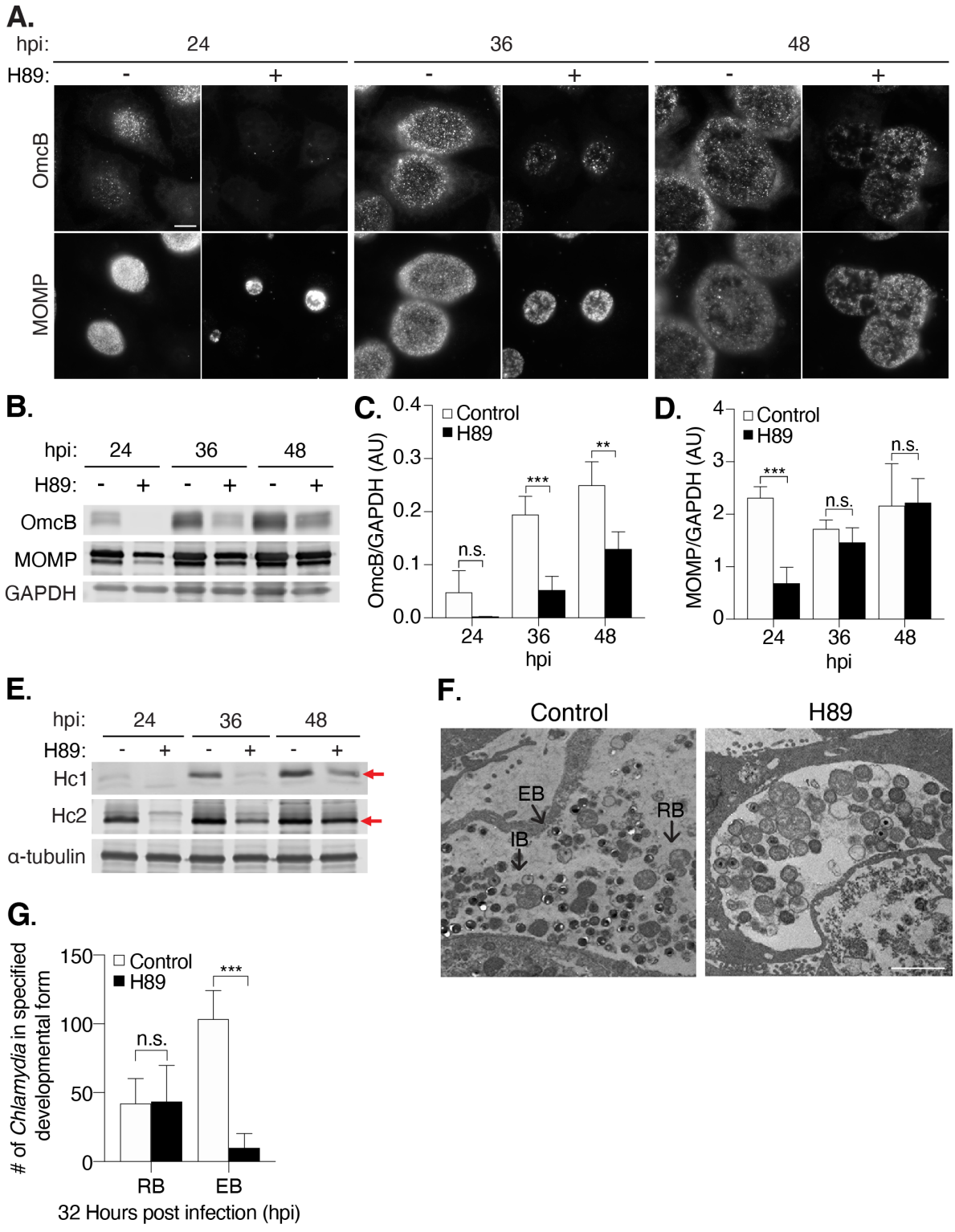

Figure 4.4. H89 delays expression of an EB-specific protein and reduces the number of EBs.
(A) *C. trachomatis* L2-infected HeLa cells were treated with H89 at 1 hpi and imaged at the indicated time points. EBs were stained with antibodies to OmcB, while all chlamydial developmental forms were detected with antibodies to MOMP. Scale bar, 10 µm.
(B) Western blot analysis of total cell lysates from infected cells treated as described for panel A. The levels of OmcB and MOMP are shown. GAPDH served as a loading control. A representative blot is shown ($n=4$).
(C) Quantification of OmcB protein levels from the Western blots in panel B. OmcB levels were normalized to the GAPDH loading control. The data are presented as arbitrary units (AU) and means ± SD ($n=4$); **, $P \leq 0.01$; ***, $P \leq 0.001$. n.s. indicates that the data are not statistically significant.
(D) Quantification of MOMP protein levels from the Western blots in panel B. MOMP levels were normalized to the GAPDH loading control. Data are presented as arbitrary units (AU; mean ± SD) ($n=4$); ***, $P \leq 0.001$. n.s. indicates the data are not statistically significant.
(E) Lysates of infected HeLa cells treated with H89 starting at 1 hpi were analyzed by western blotting at the indicated time points. The levels of histone-like proteins Hc1 and Hc2 (both indicated with a red arrow), as well as the general chlamydial surface protein MOMP are shown. α-tubulin served as a loading control.
(F) Electron micrographs (EM) of infected cells untreated or treated with H89 from 1 to 32 hpi. Scale bar, 2 µm. The different chlamydial developmental forms are indicated: EB, elementary body; IB, intermediate body; and RB, reticulate body.
(G) The numbers of EBs and RBs, detected by EM in 32-hpi inclusions of control and H89-treated infections, were quantified. The data are presented as means ± SD for control ($n=7$ inclusions) and H89 ($n=8$ inclusions) treatments; ***, $P \leq 0.001$; n.s., not statistically significant.

As a complementary method to assess RB-to-EB conversion and EB production, we examined the effect of H89 on *C. trachomatis*-infected cells by electron microscopy (Fig. 4.4F). At 32 hpi, control cells contained a mixture of RBs, IBs, and EBs, as previously noted (J. K. Lee et al., 2018). In contrast, H89-treated cells and control cells had equivalent numbers of RBs but a 10-fold reduction in EBs (Fig. 4.4G). We did not detect aberrant bodies, which are abnormally large RBs present during the altered growth state of chlamydial persistence, which can be induced by tryptophan deprivation

or antibiotic exposure (Panzetta et al., 2018). We conclude that H89 reduces the number of infectious progeny by limiting RB-to-EB conversion.

12.5 µM H89 treatment does not alter vesicular trafficking of proteins or lipids in *Chlamydia*-infected cells

We next examined if the anti-chlamydial effects of H89 were due to disruption of ER-to-Golgi and post-Golgi apparatus transport. For these studies, we used C1 HeLa cells, in which protein trafficking can be easily observed because they stably express the green fluorescent protein (GFP)-tagged FM4-hGH transport reporter (Gordon et al., 2010). FM4-hGH accumulates in the ER, but the addition of the D/D solubilizer promotes transport of the reporter from the ER to the Golgi apparatus and then to the plasma membrane for secretion.

H89 at 12.5 µM did not alter protein trafficking in *Chlamydia*-infected C1 HeLa cells, as determined by fluorescence microscopy. At time zero, each condition had 100% GFP reporter localization at the ER (Fig. 4.5A-B). In nearly 100% of control and H89-treated cells, the GFP reporter left the ER after solubilizer addition and reached the Golgi apparatus by 20 min (Fig. 4.5A-B). After 100 min, the reporter was released from the cell, as measured by loss of the GFP signal (Fig. 4.5A-B). In contrast, FM4-hGH remained in the ER in >97% of cells treated with 100 µM H89, a concentration that is known to block protein trafficking (Fig. 4.5B) (Aridor & Balch, 2000). To control for the smaller inclusion size of H89-treated cells, we also compared H89-treated cells at 36 hpi with untreated control cells at 24 hpi (Fig. 4.6A-B) and found that protein secretion

occurred independently of the size of inclusions in H89-treated cells.

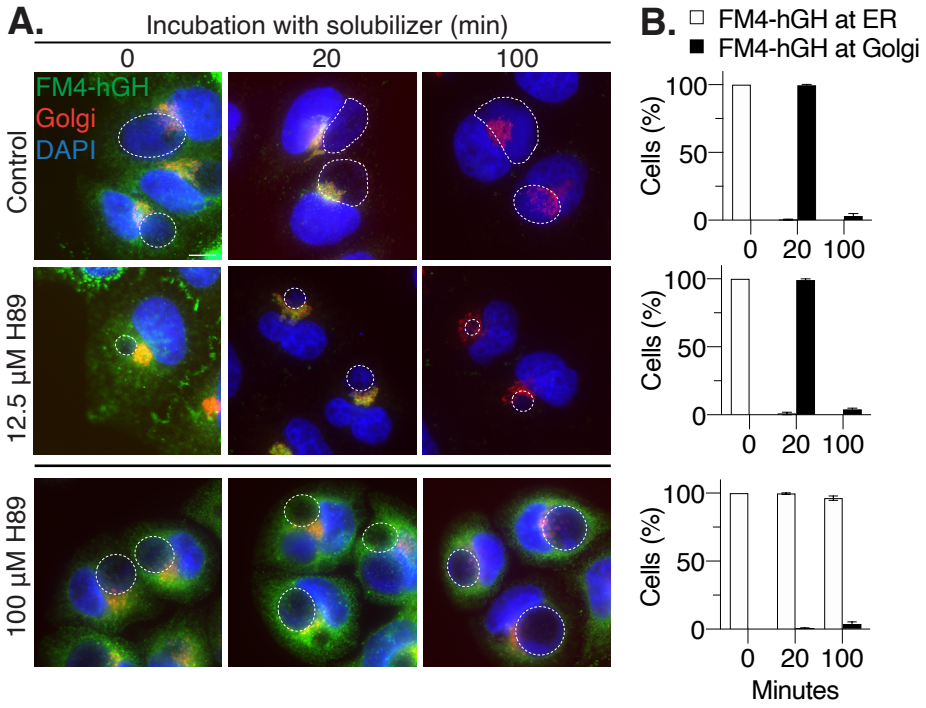

Figure 4.5. H89 at 12.5 µM does not alter ER-to-Golgi or post-Golgi apparatus trafficking in *Chlamydia*-infected cells.
(A) C1 HeLa cells, which express the GFP-tagged transport reporter protein FM4-hGH (green), were infected and treated with H89 at 1 hpi. At 32 hpi, cells were incubated with solubilizer for 0, 20, or 100 min and then fixed and processed for fluorescence microscopy analysis. The Golgi apparatus was visualized with antibodies to GM130 (red), and chlamydial and host DNA were stained with DAPI (blue). The bottom panel shows a control sample in which infected C1 HeLa cells were treated with 100 µM H89 from 30 to 32 hpi before the addition of solubilizer at 32 hpi. Chlamydial inclusions are outlined with white, dashed lines. Scale bar, 10 µm.
(B) The number of cells with GFP-tagged FM4-hGH at either the ER or the Golgi apparatus was normalized to the control and expressed as a percentage for the indicated time points after solubilizer addition (minutes). The data are presented as means ± SD ($n=3$).

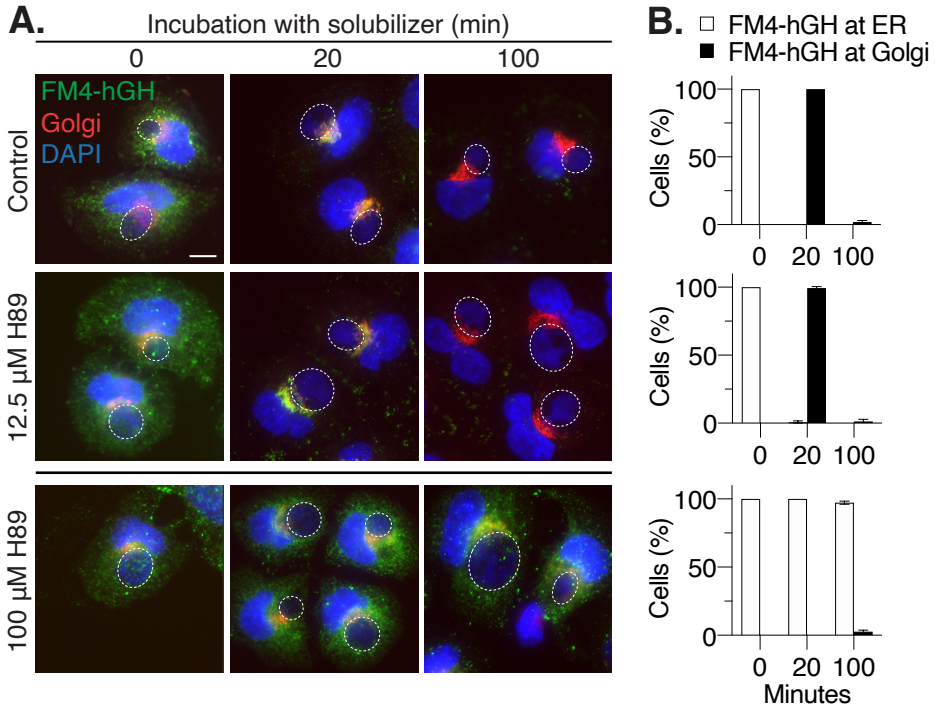

Figure 4.6. 12.5 M H89 does not alter ER-to-Golgi or post-Golgi trafficking in *Chlamydia*-infected cells, regardless of inclusion size.
(A) C1 HeLa cells, which express the GFP-tagged transport reporter protein FM4-hGH (green), were infected in the presence of H89 and incubated with solubilizer for 0, 20 or 100 minutes at the indicated time points post infection. To account for differences in inclusion size, we compared the effect of the H89 inhibitor on protein transport for 12.5 µM H89-treated samples at 36 hpi and control samples at 24hpi. The bottom panel shows a control sample in which infected C1 HeLa cells were treated with 100 µM H89 from 22 to 24 hpi, prior to the addition of solubilizer at 24 hpi. The Golgi was visualized with antibodies to GM130 (red), and chlamydial and host DNA were stained with DAPI (blue). Chlamydial inclusions are outlined with white, dashed lines. Scale bar: 10 µm. (B) The number of cells with GFP-tagged FM4-hGH at either the ER or the Golgi was normalized to the control and expressed as a percentage for the indicated time points post solubilizer addition (minutes). The data are presented as mean ± SD (n=3).

We also tested if 12.5 µM H89 disrupts the vesicular delivery of lipids to the inclusion and chlamydiae. In a well-established ceramide transport assay, the fluorescent ceramide analog C_6-NBD ceramide is converted into C_6-NBD sphingomyelin in the Golgi apparatus and then incorporated into the inclusion membrane and chlamydiae (Hackstadt et al., 1995, 1996). To account for the reduced inclusion size of

H89-treated cells, we performed this assay at 36 hpi for H89-treated samples and 24 hpi for controls (Fig. 4.7). At 0 min, C_6-NBD ceramide was in the cytosol, only faintly present in the Golgi apparatus, and absent from the inclusion. After 20 min, fluorescent sphingomyelin was at the Golgi apparatus but was also detected in bacterial membranes of control and H89-treated cells. As a positive control, we showed that brefeldin A (Hackstadt et al., 1995), which inhibits trafficking to the inclusion, blocked C_6-NBD ceramide delivery. We conclude that 12.5 µM H89 is unlikely to block inclusion growth and EB production by disrupting host protein or lipid transport pathways.

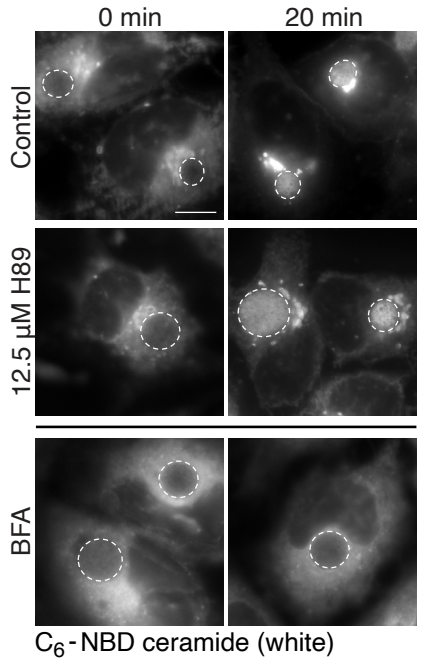

Figure 4.7. 12.5 M of H89 does not inhibit lipid transport to the inclusion.
Fluorescence images of the NBD-ceramide transport assay in *C. trachomatis* L2-infected HeLa cells. Two time points of this assay are shown. To account for differences in inclusion size, we compared NBD-ceramide transport for 12.5 µM H89-treated samples at 36 hpi and control samples at 24hpi. The bottom panel shows a control sample in which infected cells were treated with 5 µM BFA from 21 to 24 hpi prior to ceramide addition. DAPI (not shown) was used to identify the chlamydial inclusions, which are outlined with white, dashed lines. Scale bar: 10 µm.

H89 does not inhibit PKA or PKC activity in *Chlamydia*-infected cells

We tested if H89 altered chlamydial infection through its known inhibitory effects on protein kinase A (PKA). For this experiment, we compared *C. trachomatis* infection in the stable PKA knockout cell line mpkCCD (KO) and its wild-type (WT) counterpart (Limbutara et al., 2019). H89 caused a similar decrease in inclusion size and progeny for both PKA KO and wild-type cells (Fig. 4.8A-B). We verified that infection efficiency in PKA KO cells was similar to that in wild-type cells (data not shown).

We also investigated if H89 has negative effects on *Chlamydia* infection by inhibiting protein kinase C (PKC), another known H89 target in host cells. PKC is relevant to the *Chlamydia* infection because phosphorylated PKC substrates have been detected at the inclusion membrane (Davies et al., 2000; Sah et al., 2019). However, immunofluorescence microscopy analysis showed that phosphorylated PKC substrates were still present at the inclusion in H89-treated cells (Fig. 4.8C). Thus, the H89-induced phenotypes in *Chlamydia*-infected cells are unlikely to be caused by inhibition of PKA or PKC activity.

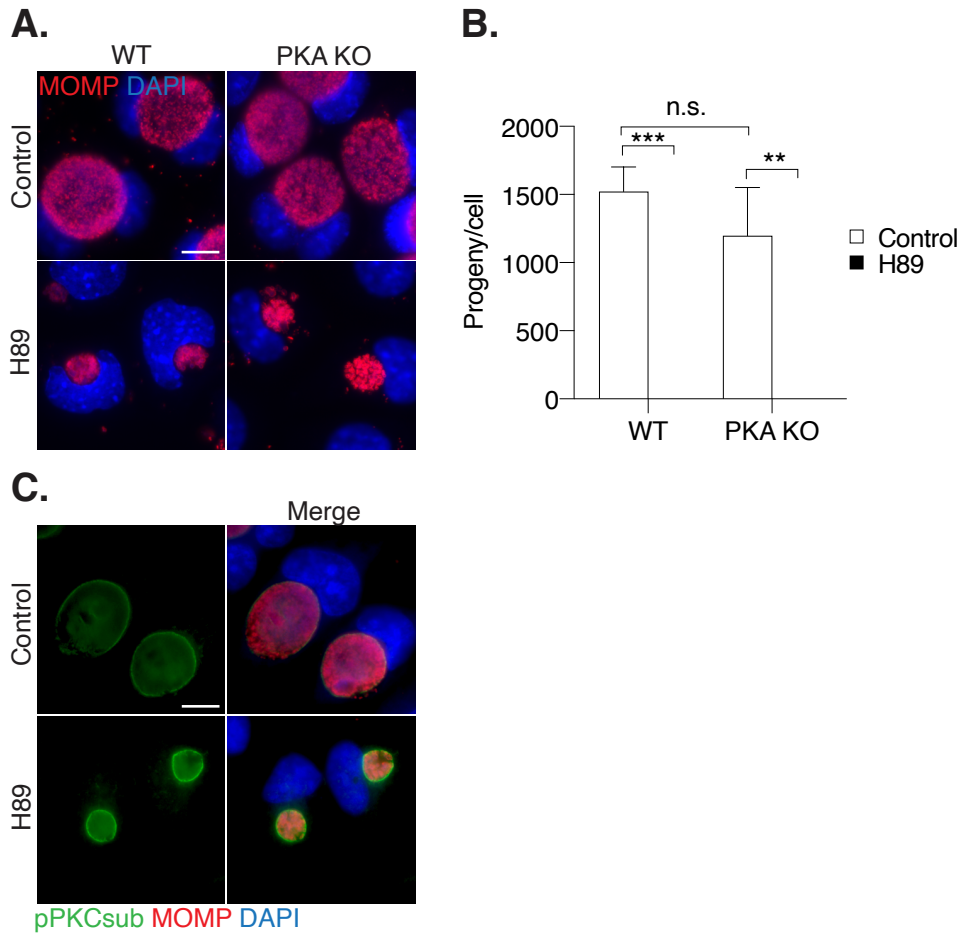

Figure 4.8. H89 effects on *Chlamydia* development are not due to inhibition of PKA or PKC.

(A) mpkCCD WT and PKA knockout (PKA KO) cell lines were infected with *C. trachomatis* L2 and either left untreated or treated with 12.5 µM H89 from 1 to 32 hpi. Cells were fixed and subjected to immunofluorescence microscopy analysis with antibodies to MOMP (red). Chlamydial and host DNA were stained with DAPI (blue). Scale bar, 10 µm.

(B) Production of infectious EBs (progeny assay) was measured for the cells treated as described for panel A, normalized to the number of host cells, and presented as means ± SD ($n=3$); **, $P \leq 0.01$; ***, $P < 0.001$; n.s., not statistically significant.

(C) Immunofluorescence images of *C. trachomatis* L2-infected HeLa cells fixed at 24 hpi and stained with an antibody that recognizes phosphorylated PKC substrates (green). Chlamydiae were detected with antibodies to MOMP (red). Chlamydial and host DNA were stained with DAPI (blue). Scale bar, 10 µm.

4.4 Discussion

In this study, we examined the effects of the small molecule H89 on intracellular *Chlamydia* infection. We found that this compound slowed inclusion growth and disrupted the chlamydial developmental cycle. H89 decreased the production of infectious progeny by causing a small reduction in RB replication and a much larger decrease in RB-to-EB conversion. The effects of H89 on the infection were not caused by inhibiting two known kinase targets or vesicular transport pathways.

The initial goal of this study was to use a pharmacological approach to examine the role of host vesicular transport during chlamydial infection. We chose H89, because this small molecule disrupts vesicular transport to and from the Golgi apparatus in uninfected cells at concentrations of up to 100 µM and incubation times of up to 2 h (Aridor & Balch, 2000; T. H. Lee & Linstedt, 2000; Muñiz et al., 1997). However, H89 treatment at these high concentrations over the 2-day course of the intracellular *C. trachomatis* infection was toxic to the host cell. Therefore, we used a concentration of 12.5 µM, which had no cytotoxic effects on the host cell and did not interfere with protein and lipid transport, but still altered both the chlamydial inclusion and developmental cycle.

Our data indicate that H89 slows, but does not abolish, inclusion growth. The treatment with this compound decreased inclusion size at all time points measured. The greatest size difference was at 24 hpi, but the inclusion size gradually caught up so that there was only a modest 1.4-fold difference at 48 hpi. A defect in host lipid acquisition is known to interfere with inclusion growth. While we showed that H89 did not alter

sphingomyelin transport to the inclusion, we cannot exclude the possibility that H89 interferes with the acquisition of other host lipids.

Many small molecules have been shown to inhibit the intracellular *Chlamydia* infection by reducing inclusion size and, in some cases, infectious progeny (Beatty, 2006; Claywell et al., 2018; Gloeckl et al., 2013; Hua et al., 2015; Kumar et al., 2006; J. L. Li et al., 2018; Muschiol et al., 2006). However, failure to produce progeny could be due to defects at various steps in the developmental cycle, including EB entry, EB-to-RB conversion, RB replication, and RB-to-EB conversion. KSK120, an inhibitor of *C. trachomatis* glucose metabolism, has been shown to primarily cause a defect in chlamydial replication (Engström et al., 2014, 2015). Studies on other inhibitors that decrease infectious progeny have not distinguished between effects on RB replication and RB-to-EB conversion, where the latter would only decrease the production of EBs but not RBs.

Our studies identified RB-to-EB conversion as the main step in the chlamydial developmental cycle that is inhibited by H89. *Chlamydia*-infected cells treated with H89 could support RB replication, albeit with a 2-fold reduction in total chlamydial numbers. However, the difference between this small replication defect and the 25-fold reduction in infectious progeny indicates a post-replication defect in EB production. Through multiple lines of evidence, we demonstrate that H89 disrupts RB-to-EB conversion. Specifically, we measured decreased expression of EB-specific gene products by Western blotting and microscopy analysis, detected fewer EBs relative to RBs by EM, and observed a reduced number of infectious EBs in progeny assays.

H89 did not interfere with RB-to-EB conversion by inducing chlamydial persistence. Agents such as gamma interferon and penicillin lead to persistence by causing a general block in RB-to-EB conversion with decreased late gene expression and EB production (Hogan et al., 2004; Panzetta et al., 2018). However, a cardinal feature of persistence is a concomitant replication defect that results in very large, nondividing RBs called aberrant bodies (Wyrick, 2010). In our EM studies of H89-treated cells, there were no aberrant bodies; instead, we only detected normal-appearing RBs and dividing RBs, which is consistent with ongoing RB replication.

H89 may exert its effects on *Chlamydia* infection through its known role as an inhibitor of specific host protein kinases. The best-characterized target of H89 is PKA, which regulates transcription, protein expression, and cell growth and differentiation (Chijiwa et al., 1990; Yan et al., 2016). In *Coxiella burnetii*, PKA promotes formation of the parasitophorous vacuole and production of infectious progeny (MacDonald et al., 2012, 2014). However, we found that PKA was not necessary for the *C. trachomatis* infection and that H89 still altered inclusion size and EB production in PKA knockout cells. PKC is another target of H89 (Bain et al., 2007; Davies et al., 2000). This kinase and its phosphorylated substrates are recruited to the chlamydial inclusion (Sah et al., 2019). However, H89 did not alter the localization of phosphorylated PKC substrates to the inclusion, suggesting that H89 acts through other kinases, including MSK1, S6K1, PKB, and ROCK-II (Davies et al., 2000; Limbutara et al., 2019; Lochner & Moolman, 2006; Murray, 2008). Notably, H89 was shown to reduce intracellular *Salmonella* growth by inhibiting PKB/AKT1 activity (Kuijl et al., 2007), but it is not known if these

host kinases have roles in inclusion growth and chlamydial development. In addition, H89 might inhibit chlamydial kinases, such as Pkn1, PknD, and Pkn5 (Belland et al., 2003; Claywell et al., 2016). Additional studies that are beyond the scope of the manuscript will explore the specific H89 target(s) whose disruption produces the strong phenotypes that we observed.

In conclusion, H89 treatment of *Chlamydia*-infected cells has inhibitory effects on both the chlamydial inclusion and the developmental cycle. Our detailed analysis showed that H89 reduces the production of infectious progeny by causing both a small decrease in RB replication and a much larger defect in RB-to-EB conversion. Conversion from an RB to an EB is a critical step for spreading the intracellular *Chlamydia* infection to a new host cell. However, to the best of our knowledge, no other pharmacological inhibitor has been shown to interrupt RB-to-EB conversion without causing chlamydial persistence. This distinct property makes H89 a useful tool that may lead to new anti-chlamydial therapeutic strategies.

CHAPTER 5: The anti-chlamydial effects of H89 are due to defects in lysosomal acidification and cholesterol transport

Note: We plan to submit these data for publication. The data and figures were generated with the help of undergraduate, Priscilla Nguyen, who I mentored during my graduate studies.

"The same few dozen organic molecules are used over and over again in biology for the widest variety of functions." – Carl Sagan, Ph.D. in Astronomy and Astrophysics

5.1 Abstract

The published, novel anti-chlamydial inhibitor, H89, has been effective in slowing inclusion growth and inhibiting RB-to-EB conversion. However, the question remains: How does H89 mediate its effects on the chlamydial infection? We previously measured several known pathways and targets known to be blocked by H89, but none were affected under our infection and inhibitor conditions. Based on *in vitro* biochemical assays, H89 is also reported to inhibit several other kinases. Thus, to identify the H89 target that contributes to the infection defects, we tested several of these kinases using an inhibitor approach. We found that H89 caused defects in the infection similar to the inhibition of sphingosine kinase 1 (SphK1), and both conditions caused lysosomal acidification defects, resulting in cholesterol accumulation. We also observed that H89 treatment decreased cholesterol at the inclusion membrane. Additionally, we

demonstrated that decreasing intracellular cholesterol levels negatively affects inclusion growth and progeny production. Together, our data support that cholesterol and proper cholesterol trafficking are necessary to promote the chlamydial infection.

5.2 Introduction

Investigating the mechanism of H89 inhibition of the *Chlamydia* infection.

As discussed in chapter 4, our lab published the use of a novel anti-chlamydial inhibitor called H89, and its inhibition of inclusion growth and RB-to-EB conversion was not mediated through several known H89 pathways and targets (Muñoz et al., 2021). At concentrations of 50 μM H89 or higher, H89 blocked ER-to-Golgi, and post-Golgi transport, but our 12.5 μM H89 treatment conditions were too low for this inhibition (Table 5.1) (Muñoz et al., 2021). Furthermore, H89 is reported to block protein kinases A and C (PKA and PKC), but H89 treatment of PKA knockout cells still caused the same defects on the infection, and PKC function was not altered by H89, suggesting that H89 does not mediate its effects through these kinases (Table 5.1) (Muñoz et al., 2021).

H89 is also reported to inhibit several “off target” kinases at a similar concentration to what was used in our studies (Davies et al., 2000; Lochner & Moolman, 2006). While investigating some of these kinase targets, we found that H89 blocks cholesterol trafficking, which had not been previously reported (Table 5.1). As sphingolipid acquisition by chlamydiae was not affected, these data show that not all lipids are affected by H89 (Table 5.1) (Muñoz et al., 2021). Cholesterol is a component of both the chlamydial and inclusion membranes (Carabeo et al., 2003) and is generally

essential in maintaining the integrity of cell membranes (Maxfield & Menon, 2006). Therefore, disrupting cholesterol transport may prevent cholesterol acquisition by chlamydiae, compromising the growth and structure of the chlamydial membranes. Our goal was to test whether the H89-mediated defects in cholesterol trafficking caused defects in cholesterol acquisition by chlamydiae and contributed to downstream defects in inclusion growth and RB-to-EB conversion.

Table 5.1. Investigating H89-mediated inhibition of host and chlamydial functions. Host cell and chlamydial pathways and targets were tested for inhibition by H89 at the concentration optimized for the chlamydial infection (12.5 μM). Light blue section represents published targets/pathways of H89. Orange section represents a novel pathway blocked by H89.

Host cell and chlamydial pathways and targets inhibited by H89:	**Inhibited at our H89 concentration (12.5 μM)?**
ER-to-Golgi protein transport (Aridor & Balch, 2000; Muñoz, 2021)	No
Post-Golgi secretion (Muñiz, 1997)	No
Protein kinases A and C (Davies, 2000; Lochner & Moolman, 2006; Murray, 2008)	No
Sphingolipid acquisition by *Chlamydia* (Muñoz, 2021)	No
Cholesterol trafficking (unpublished)	Yes
Other serine/threonine kinases (Lochner & Moolman, 2006; Murray, 2008)	???

As discussed in chapter 1, depending on cholesterol availability, eukaryotic cells use two methods to acquire cholesterol: 1) exogenous uptake through low density

lipoprotein (LDL) receptors and 2) endogenous *de novo* synthesis in the endoplasmic reticulum (Luo et al., 2019) (Fig. 1.3). Most cells grown *in vitro* have sufficient cholesterol present within the FBS serum media and so there is little to no endogenous cholesterol synthesis (Goldstein & Brown, 2015). Both *de novo*-synthesized and LDL-derived cholesterol traffic to the chlamydial inclusion in a microtubule dependent manner (Carabeo et al., 2003). Specifically, Peters *et al.* showed that the *C. trachomatis* infection required esterified cholesterol as inhibition of host Acyl-CoA: cholesterol acyltransferase (ACAT) resulted in smaller inclusions and fewer progeny (Peters & Byrne, 2015). Moreover, treatment with a bacterial synthesis inhibitor severely limited cholesterol uptake, supporting that cholesterol acquisition is a pathogen-directed event (Carabeo et al., 2003).

Also in chapter 1, I summarized the evidence for and against cholesterol as being necessary for the chlamydial infection. Cholesterol is one of most abundant lipids found in chlamydiae and at the chlamydial inclusion (Carabeo et al., 2003). As *Chlamydia* lack the genetic machinery to synthesize cholesterol, it must be acquired from its host cell environment by hijacking lipid trafficking pathways (C. A. Elwell & Engel, 2012). Surprisingly, MEF cells devoid of cholesterol had no defect on the chlamydial infection, but this may be because desmosterol, the nearly identical precursor of cholesterol, was still abundant (Gilk et al., 2013). Nevertheless, the presence of cholesterol in chlamydial membranes and the dependency of chlamydiae on rerouting host lipid trafficking provides evidence that cholesterol may be one of the essential lipids acquired to promote the *Chlamydia* infection.

5.3 Results

H89 causes a defect in cholesterol trafficking.

As cholesterol is an important component of chlamydial membranes, and the chlamydial infection is known to divert host lipid pathways to acquire these nutrients, we measured whether cholesterol transport was affected under H89 conditions. First, we treated uninfected HeLa cells with DMSO or H89 for 32 hours and used the cholesterol binding molecule, filipin, to monitor cholesterol localization. In DMSO-treated cells, we observed cholesterol at the plasma membrane, Golgi (data not shown), and the lysosome where it partially co-localized with the lysosomal marker LAMP1 (Fig. 5.1A). With H89-treatment, cholesterol accumulated within the host cell and was primarily localized within the lysosome (Fig. 5.1A). In fact, magnification of these images showed that with H89 treatment, the lysosomes were larger than in control samples and filled with cholesterol (Fig. 5.1A). The lysosomal accumulation of cholesterol was not cell type specific as it was also observed in RPEs, MEFs, and HFFs (data not shown).

To determine whether this H89-induced phenotype was also present with an infection, we monitored filipin staining for *C. trachomatis*-infected HeLa cells treated with H89 for 36 hours. Using line intensity scanning to measure the fluorescence intensity of filipin at the inclusion, we found that in addition to causing cholesterol accumulation within lysosomes, H89 decreased cholesterol levels in the inclusion membrane by 50% (Fig. 5.1B-C). Furthermore, with H89-treatment, cholesterol-containing lysosomes aggregated around the inclusions, which were smaller compared to control-treated samples as reported previously (Muñoz et al., 2021). These data suggest that H89

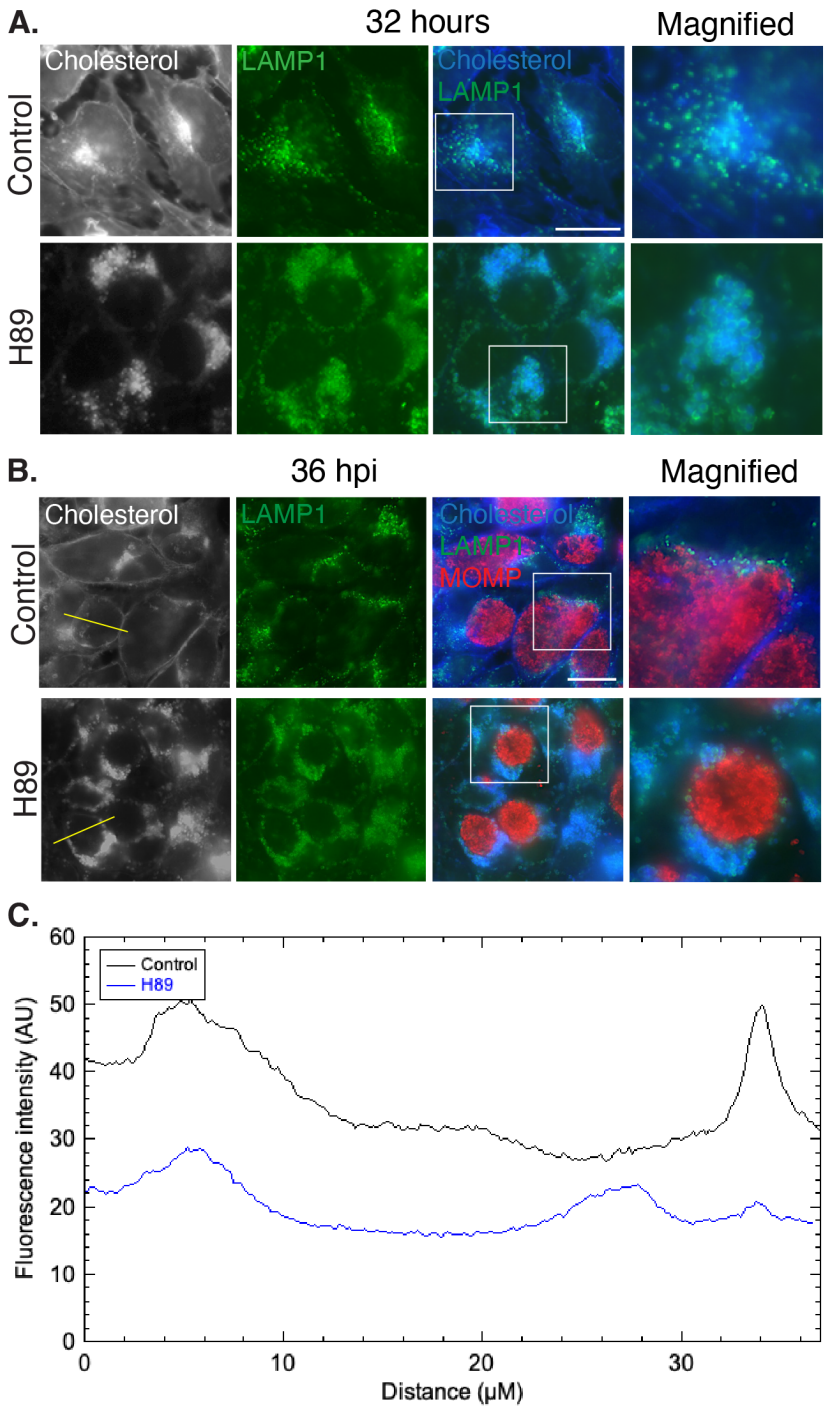

Figure 5.1. H89 causes an accumulation of cholesterol in the lysosome.
(A) Immunofluorescence images of uninfected HeLa cells treated for 32 hours in the presence or absence of H89. The fluorescent cholesterol-binding molecule filipin was used to visualize cholesterol (white/blue). Antibodies against LAMP1 were used to identify the lysosomes (green). White boxes indicate the portions of the image that have been magnified. Scale bar is 20 μm.
(B) Immunofluorescence images of *C. trachomatis*-infected HeLa cells treated for 36

hours in the presence or absence of H89. The fluorescent cholesterol-binding molecule filipin was used to visualize cholesterol (white/blue). Antibodies against LAMP1 were used to identify the lysosomes (green) and antibodies against MOMP were used to visualize chlamydiae (red). White boxes indicate the portions of the image that have been magnified. Scale bar is 20 μm.
(C) Line intensity scans were used to measure the fluorescence intensity (AU) of the filipin signal for DMSO control (black) and H89-treated (blue) samples in part B. Yellow line indicates where measurements were taken.

causes lysosomal accumulation of cholesterol in the eukaryotic cell and a reduction in inclusion membrane cholesterol levels by line intensity scanning. We were unable to measure cholesterol levels of chlamydiae using this same method, which is a challenge that was previously described (Carabeo et al., 2003).

H89 did not disrupt trafficking of exogenously acquired materials.

Under standard infection conditions, DMEM cell culture media is supplemented with 10% FBS, which is rich in nutrients including proteins, carbohydrates, electrolytes, and lipids such as cholesterol (Whitford & Manwaring, 2022). Consequently, most of the cholesterol used by the eukaryotic host cell is acquired through exogenous host cell uptake, rather than endogenous cholesterol synthesis (Brown & Sharpe, 2016). H89 has also been reported to block the endocytic uptake of materials such as transferrin (Cotlin et al., 1999) and EGF (Salazar & González, 2002) at concentrations ranging from 20-150 μM. We next tested whether H89 caused a general trafficking defect for exogenously acquired nutrients.

We first conducted transport assays with fluorescently labeled EGF and transferrin proteins to monitor their endocytic uptake by the eukaryotic host cell. Host

cell uptake of EGF is mediated by the EGF receptor (EGFR) and activation of EGFR has been shown to be required for *C. trachomatis* development (Patel et al., 2014). When EGF was added to the media of infected cells, EGF colocalized with EGFR within 5 minutes (Fig. 5.2A). After 20 minutes, for both the control and 12.5 μM H89 samples, EGF and EGFR colocalized in vesicles within the host cell (Fig. 5.2A). However, when samples were treated with the competitive inhibitor of the ATP binding site of EGFR, Erlotinib, or were incubated on ice, EGF remained at the host cell membrane (Fig. 5.2A) (Schettino et al., 2008).

Using a similar approach, we monitored the endocytic uptake of the iron-binding glycoprotein, transferrin. Transferrin trafficking is of interest because iron deficiency has been shown to negatively regulate inclusion growth and the production of infectious EBs (Al-Younes et al., 2001). Similarly, exogenous transferrin was observed in the host cell within 10 minutes for control and 12.5 μM H89 samples (Fig. 5.2B). However, when samples were treated with 50 μM H89 or were incubated on ice, little to no transferrin was observed within cells (Fig. 5.2B). Thus, 12.5 μM of H89 does not disrupt the uptake of materials that are known to promote the chlamydial infection.

In addition to measuring for defects in transferrin uptake, we also conducted a pulse chase assay to test whether H89 affected transferrin export. Fluorescently labeled transferrin was added to the media of uninfected HeLa cells and incubated for one hour. Next, the samples were washed and replaced with fresh media without transferrin. At 0 minutes, transferrin was visible within the host cell and by 40 minutes, most of the transferrin was undetectable (Fig. 5.2C). There were similar kinetics of transferrin

egress from the host cell under control and 12.5 µM H89 conditions, which suggests that our optimized concentration of H89 does not cause a general accumulation of exogenously acquired nutrients.

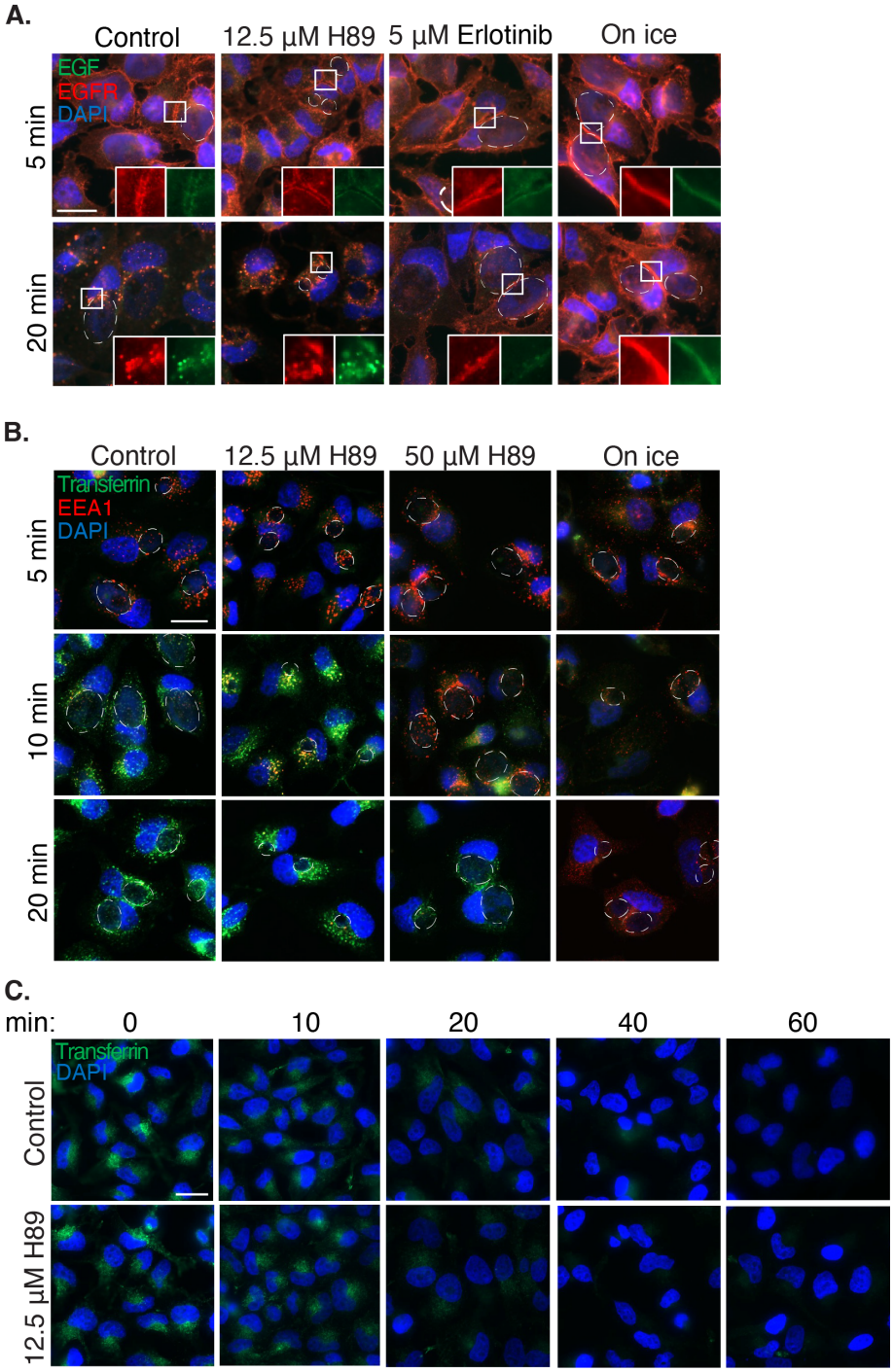

Figure 5.2. H89 does not broadly disrupt exogenous acquisition and trafficking of the chlamydial nutrients, EGF and transferrin.
(A) Immunofluorescence images of EGF uptake in *C. trachomatis*-infected HeLa cells treated with DMSO or 12.5 μM H89. At 27 hpi, samples were washed twice with 1XPBS and replaced with serum free media containing DMSO or 12.5 μM H89 for 3 hours. As controls for a block in EGF endocytosis, samples were treated with 5 μM Erlotinib or incubated on ice for 3 hours. At 30 hpi, media was reserved and 0.50 μg/ul of GFP-EGF (green) was added. Samples were fixed at the times indicated. Antibodies against EGFR (red) detected EGF receptor. Chlamydial and host DNA was detected with DAPI (blue). Chlamydial inclusions are outlined white, dashed lines. Inset shows zoomed in area for EGF and EGFR localization. Scale bar is 20 μm.
(B) Immunofluorescence images of a transferrin uptake in *C. trachomatis*-infected HeLa cells treated with DMSO or 12.5 μM H89. At 29 hpi, samples were washed twice with 1XPBS and replaced with serum starved DMEM+0.2% BSA media with DMSO or 12.5 μM H89 for 2 hours. At 31 hpi, media was reserved, and 25 μg/ml of fluorescent transferrin (green) was added. Samples were fixed at the times indicated. As controls for a block in transferrin endocytosis, samples were pretreated with 50 μM H89 in serum free media for only 1 hour prior to transferrin addition or incubated on ice. Antibodies against EEA1 (red) were used as an early endosomal marker. Chlamydial and host DNA was detected with DAPI (blue). Chlamydial inclusions are outlined with white, dashed lines. Scale bar is 20 μm.
(C) Immunofluorescence images of a transferrin pulse-chase assay in uninfected HeLa cells. Cells were serum starved in DMEM+0.2% BSA with DMSO or 12.5 μM H89 for 3 hours. Media was reserved and 25 μg/ml of fluorescent transferrin (green) was added. Samples were fixed at the times indicated. Host DNA was detected with DAPI (blue). Scale bar is 20 μm.

H89 mediated effects on cholesterol trafficking and the chlamydial infection resemble an NPC1 defect.

As H89 appeared to target cholesterol trafficking, we next asked whether cholesterol accumulation in the lysosome disrupts the chlamydial infection. The NPC1 inhibitor U18666A has been reported to cause cholesterol accumulation and correlates with inhibitory effects on inclusion growth and progeny production (Beatty, 2006, 2008). We then compared the cholesterol trafficking defects and inhibitory effects on the infection caused by U18666A and H89. In addition, we tested two other NPC1 inhibitors,

Itraconazole and Astemizole, which had not been previously tested during the *Chlamydia* infection (Cingolani et al., 2019; Lyu et al., 2018). Three NPC1 inhibitors showed the same lysosomal accumulation of cholesterol as H89 (Fig. 5.3A). To demonstrate that cholesterol accumulation is not a general defect induced by any inhibitor, we included another published chlamydial inhibitor, KSK120, and showed it does not cause cholesterol accumulation (Engström et al., 2014, 2015) (Fig. 5.3A).

We then conducted a side-by-side analysis of the inhibitors to compare their effects on different steps of chlamydial development. The H89 and NPC1 inhibitors produced at least a 20% inhibition of inclusion growth (Fig. 5.3B). They also all caused a significantly greater inhibitory effect on RB-to-EB conversion than chlamydial replication, consistent with an RB-to-EB conversion defect (Fig. 5.3B). Together, the data show a correlation between cholesterol retention within lysosomes and defects in the chlamydial infection.

Altering cellular cholesterol levels has negative effects on inclusion growth and progeny production.

It is plausible that the lysosomal accumulation of cholesterol limits cholesterol availability for chlamydiae. To test whether limiting cholesterol availability in the host cell inhibits the infection, we altered intracellular cholesterol levels. We conducted infections in 10% lipoprotein deficient serum media (LPDS), which has 40-fold lower levels of cholesterol than traditional serum media. Thus, LPDS will limit exogenous cholesterol uptake, the primary source of cholesterol for cells (Dietschy, 1984). We then measured inclusion growth, chlamydial replication, and infectious progeny because these were all

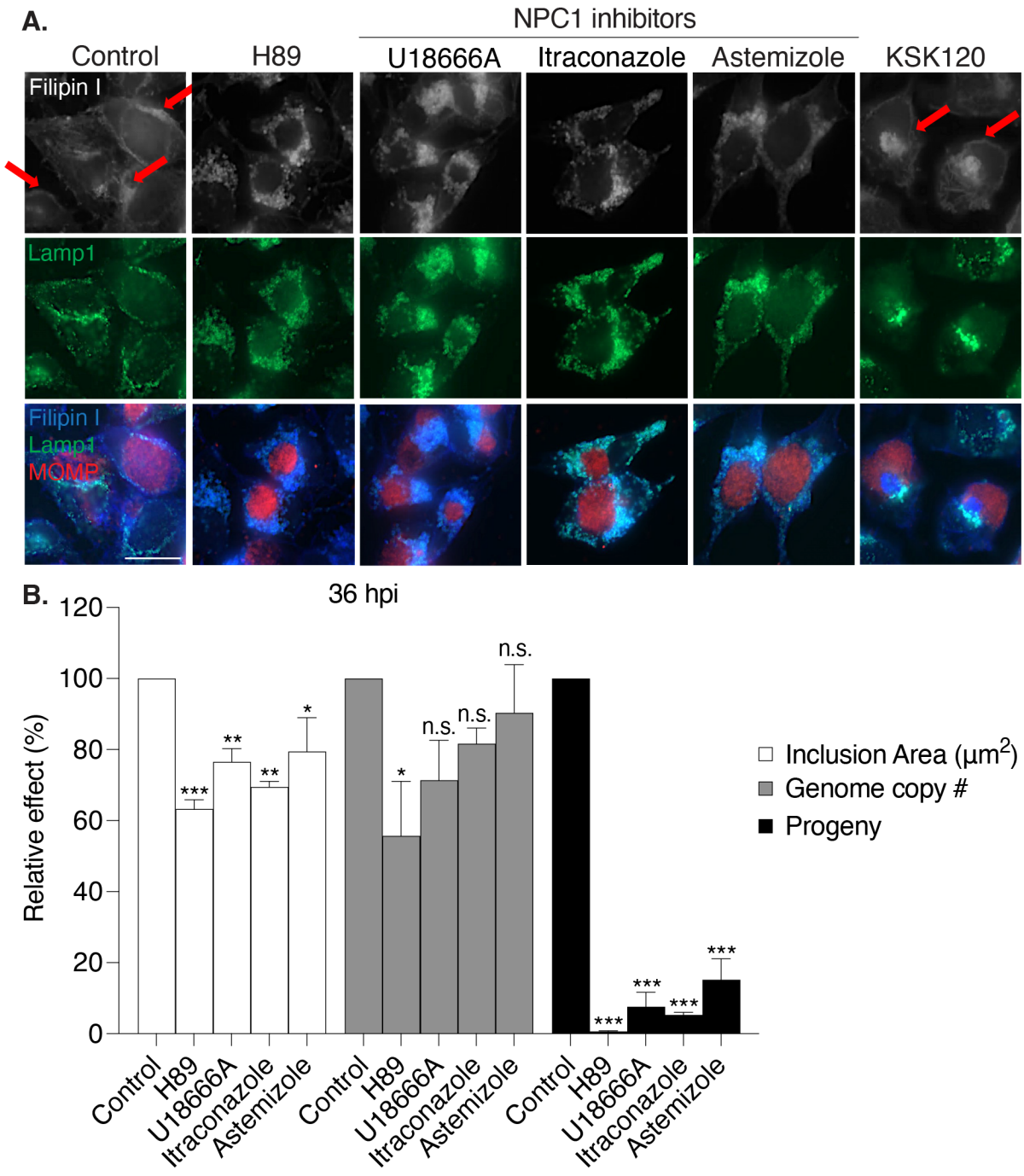

Figure 5.3. Lysosomal cholesterol accumulation correlates with defects in inclusion growth and progeny production.
(A) Immunofluorescence images of infected HeLa cells treated for 36 hours with inhibitors at the indicated concentrations: H89 (12.5 µM), U18666A (10 µM), Itraconazole (2.5 µM), Astemizole (2.5 µM), and KSK120 (10 µM). The fluorescent cholesterol-binding molecule filipin was used to visualize cholesterol (white/blue). Antibodies against LAMP1 were used to identify the lysosomes (green). Antibodies

against MOMP were used to visualize chlamydiae (red). Red arrows indicate cholesterol at membranes. Scale bar is 20 μm.
(B) Inclusion areas, numbers of chlamydial genomes, and progeny production for inhibitor-treated samples were determined at 36 hpi. A total of 100 inclusions across three experiments were measured. Values were normalized to untreated controls (control = 100%) and are expressed as a percentage. Data are presented as means ± SE ($n = 3$). *$P < 0.05$, **$P \leq 0.01$, ***$P < 0.001$; n.s. = data not statistically significant.

affected to some degree with H89 treatment. Overall, we found that LPDS-treated samples had a 2-fold reduction in inclusion size, genome copy number, and progeny production (Fig 5.4A-B). These data support that cholesterol-depleted media causes a modest inhibitory effect on the chlamydial infection.

We also decreased intracellular cholesterol levels using an inhibitor approach. Infections were incubated with DMHCA, a selective liver X receptor (LXR) agonist that promotes cholesterol efflux to decrease intracellular cholesterol levels (Magida & Evans, 2018; Vieira et al., 2020; Zhang et al., 2021). Fluorescence intensity measurements of filipin levels for each of the samples provide an indirect readout of cellular cholesterol levels. Compared to DMSO-treated controls, DMHCA caused a 2-3-fold decrease in membrane cholesterol levels (Fig 5.4C-D). We next measured the effect of decreased cholesterol levels on inclusion growth and showed that DMHCA caused a similar decrease in inclusion growth as H89 at both 32 and 48 hpi (Fig. 5.4E). Lastly, we report that both DMHCA and H89 caused a significant (>30-fold) reduction in progeny and a modest effect (≤3-fold) on the number of chlamydial genomes, reflective of an RB-to-EB conversion defect (Fig. 5.4F). Together, these data suggest that decreasing cellular cholesterol slows inclusion growth and delays chlamydial development.

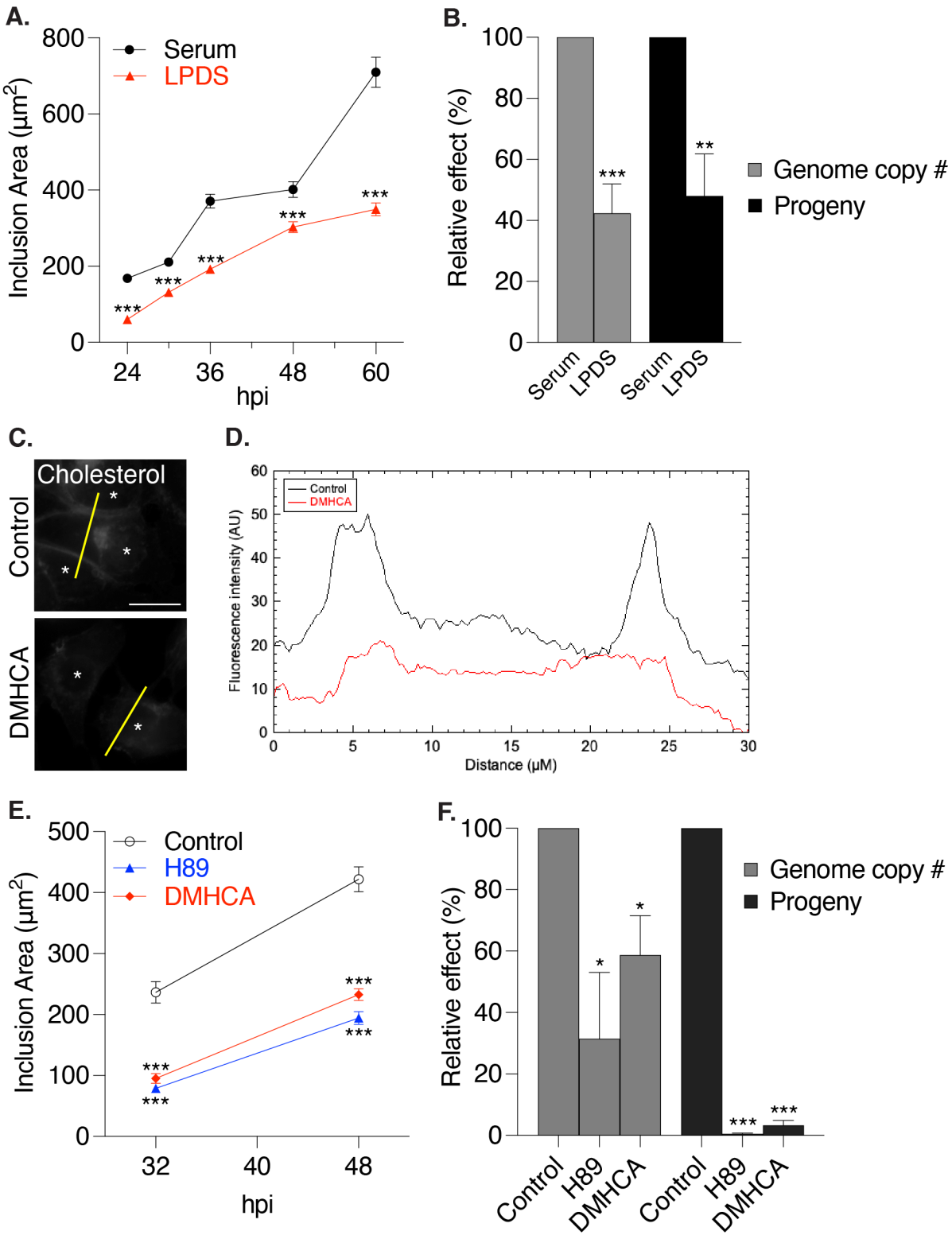
A.
Inclusion Area (μm²)
800
600
400
200
0
Serum
LPDS
***
24
36
48
60
hpi
B.
Relative effect (%)
100
80
60
40
20
0
***
**
Serum
LPDS
Serum
LPDS
Genome copy #
Progeny
C.
Cholesterol
Control
DMHCA
D.
Control
DMHCA
Fluorescence intensity (AU)
60
50
40
30
20
10
0
0
5
10
15
20
25
30
Distance (μM)
E.
Inclusion Area (μm²)
500
400
300
200
100
0
Control
H89
DMHCA
***
32
40
48
hpi
F.
Relative effect (%)
100
80
60
40
20
0
*
*
***
***
Control
H89
DMHCA
Control
H89
DMHCA
Genome copy #
Progeny

Figure 5.4. Decreasing intracellular cholesterol levels negatively affects inclusion growth and progeny production.
(A) Inclusion quantifications for infected HeLa cells incubated in normal 10% FBS serum media or 10% LPDS serum media. The average area of 100 inclusions was measured at each time point for each condition. The data from one representative experiment are presented as means ± SE; ***, $P<0.001$.
(B) The number of chlamydial genomes and infectious progeny produced from infected cells incubated in normal serum or LPDS-treated media was determined at 48 hpi. Values were normalized to the serum control (serum = 100%) and expressed as a percentage. The data are presented as mean ± SE (n=3); **$P\leq0.01$, ***$P<0.001$.
(C) Immunofluorescence images of infected HeLa cells treated for 32 hours with DMSO or DMHCA. The fluorescent cholesterol-binding molecule filipin was used to visualize cholesterol (white). Each inclusion is marked with an asterisk. Scale bar is 20 μm.
(D) Line intensity scans were used to measure the fluorescence intensity (AU) of the filipin signal for DMSO control (black) and DMHCA-treated (red) samples in part C. Yellow line indicates where measurements were taken.
(E) Inclusion quantification of infected HeLa cells treated with DMSO, H89, or DMHCA for the times indicated. The average inclusion area from 100 inclusions was measured for each condition at each timepoint. The data are presented as mean ± SE; ***$P<0.001$.
(F) The number of chlamydial genomes and infectious progeny in inhibitor-treated samples were determined at the time of lysis onset, which coincides with the time of $Progeny_{max}$ (control = 60 hpi, H89 = 72 hpi, and DMHCA = 48 hpi). Values were normalized to their untreated control counterparts (control = 100%) and expressed as a percentage. The data are presented as mean ± SE (n=3); *$P<0.05$, ***$P<0.001$.

<u>Cholesterol addition rescues H89 inhibitory effects on the chlamydial infection.</u>

We hypothesized that H89-treatment limited accessibility of cholesterol for chlamydiae and tested if adding cholesterol would rescue the defects on the infection. Exogenous cholesterol addition to the growth medium under H89-treatment significantly increased inclusion growth, while cholesterol addition under DMSO-treated samples had no effect (Fig. 5.5A-B). We then conducted a progeny assay time course to assess whether cholesterol addition would improve progeny production with H89. H89 samples reached $Progeny_{max}$ (refer to "$Progeny_{max}$" in Chapter 3) at around 72 hpi, which was

41-fold lower than the $Progeny_{max}$ of control samples at 60 hpi (Fig. 5.5C-D). Additionally, the control, control+cholesterol, and H89+cholesterol samples all produced a similar $Progeny_{max}$ value (Fig. 5.5C-D). Thus, exogenous cholesterol abrogated the progeny defect of H89. When chlamydial replication was also compared at the time point coinciding with lysis onset and $Progeny_{max,}$ cholesterol addition improved the number of chlamydial genomes in all conditions (Fig. 5.5D). Together, these data suggest that additional cholesterol can rescue chlamydial inclusion growth, enhance replication, and increase RB-to-EB conversion.

Screening for kinase targets of H89

Our previous studies with 12.5 μM H89 inhibitor showed that none of the known primary H89 targets were blocked at this concentration (Muñoz et al., 2021). *In vitro* studies report several additional kinase targets of H89 that are inhibited by at least 80% when used at a similar concentration (Limbutara et al., 2019; Lochner & Moolman, 2006; Murray, 2008). Our goal was to screen these kinase targets (ROCK-II, MKS1, S6K1, and AMPK) using an inhibitor approach to determine if any kinase(s) were necessary for the infection (Murray, 2008). Additionally, we included sphingosine kinase 1 (SphK1) because defects in this kinase are also known to cause lysosomal accumulation of cholesterol (Newton et al., 2020). For each inhibitor, we optimized the maximum tolerable concentration that still resulted in at least 80% cell viability by MTT assay (data not shown).

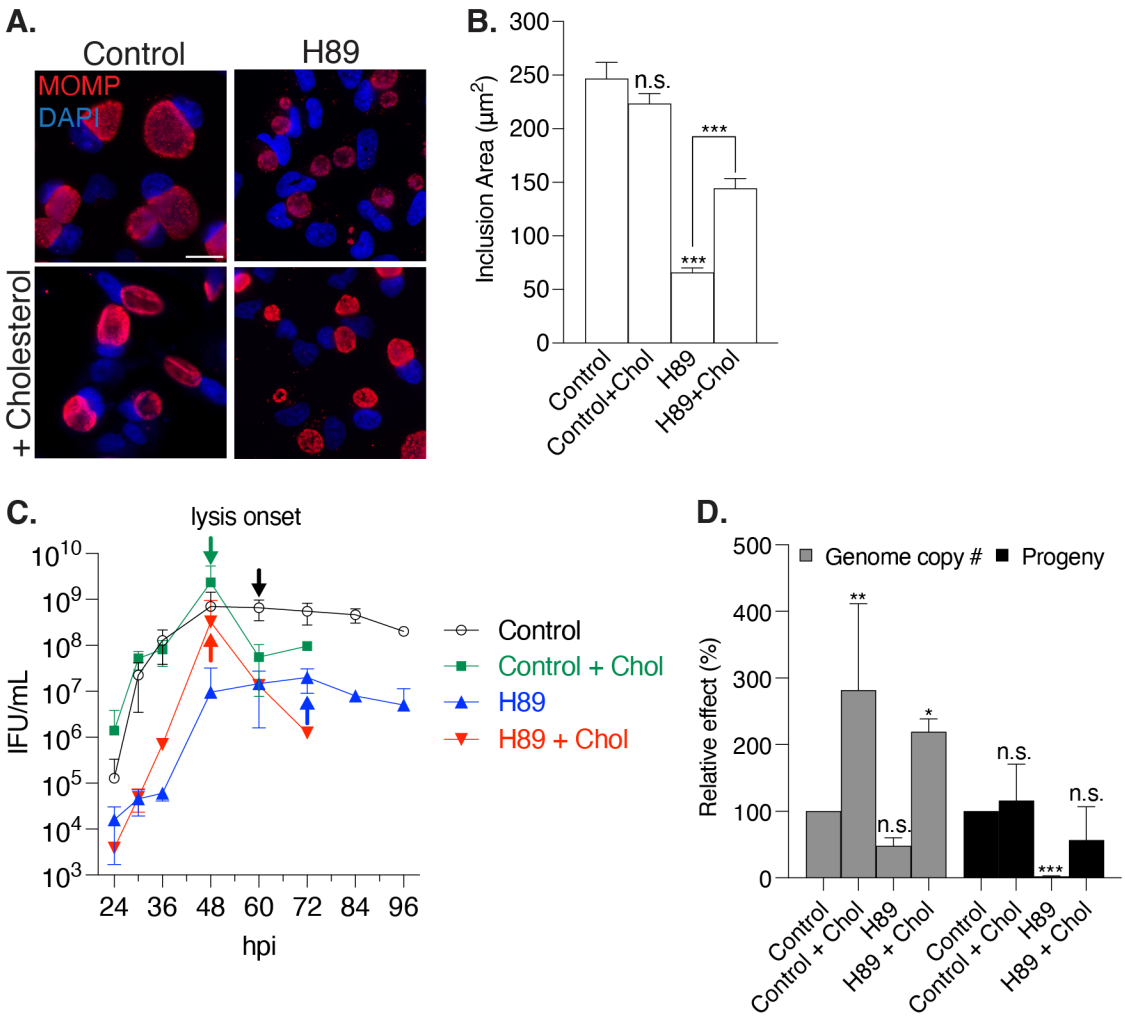

Figure 5.5 Cholesterol addition rescues the H89 defects on inclusion growth and progeny production.

(A) Immunofluorescence images of infected HeLa cells treated with or without 12.5 µM H89 for 32 hours in media supplemented with or without cholesterol. Chlamydiae are detected with antibodies to the major outer membrane protein MOMP (red) and chlamydial and host DNA are stained with DAPI (blue). Scale bar is 20 µm.

(B) Inclusion quantification from part A. The average inclusion area from 100 inclusions was measured for each condition at each timepoint. The data are presented as mean ± SE; ***P<0.001; n.s. = data not statistically significant.

(C) Measurements of progeny during the time course of infected DMSO or H89-treated HeLa cells incubated with or without exogenous cholesterol. Arrows indicate the onset of inclusion lysis and the time points when $Progeny_{max}$ was measured (control = 60 hpi, control+cholesterol = 48 hpi, H89 = 72 hpi, and H89+cholesterol = 48 hpi). Data are presented as means ± SE (n=3); Statistical significance was omitted due to crowding, but the data are compared in part D at the time point of lysis onset.

(D) The number of chlamydial genomes and infectious progeny were determined for each condition at the time of lysis onset. Values were normalized to the untreated

control (control = 100%) and expressed as a percentage. The data are presented as mean ± SE (n=3); *P<0.05, **P≤0.01, ***P<0.001; n.s. = data not statistically significant.

Our approach was to identify the kinase target that phenocopied the effects of H89 when inhibited. We found that only inhibition of S6K1 and SphK1 caused similar defects in inclusion size at 32 hpi compared to H89 (Fig. 5.6A). Also, none of the kinases produced a replication defect when inhibited (Fig. 5.6B). However, inhibition of S6K1, AMPK, and SphK1 all caused a significant decrease in progeny comparable to H89 (Fig. 5.6B). Since we were interested in cholesterol accumulation, we pursued the two kinase targets that, when inhibited, resulted in smaller inclusions and a progeny defect and then monitored for cholesterol localization in infected cells. We found that inhibition of SphK1 was the only other sample that produced the cholesterol accumulation defect (Fig. 5.6C). Overall, inhibition of SphK1 produced the most similar defects on the chlamydial infection compared to H89 at 32 hpi, with smaller inclusions, a significant defect in progeny production, and cholesterol accumulation (Fig. 5.6). Thus, SphK1 could be a kinase target of H89.

H89 may cause cholesterol accumulation and inhibitory effects on the infection by blocking sphingosine kinase function. We first confirmed that cholesterol accumulation occurred in both uninfected and infected cells with the SphK1 inhibitor PF543 (Fig 5.7A). A time course assay of inclusion growth showed that both H89 and PF543-treatment resulted in smaller inclusions throughout the infection, up until the point of lysis (Fig. 5.7B-C). Additionally, a time course assay of progeny production revealed that PF543 and H89 had at least a 10-fold decrease in $Progeny_{max}$ compared

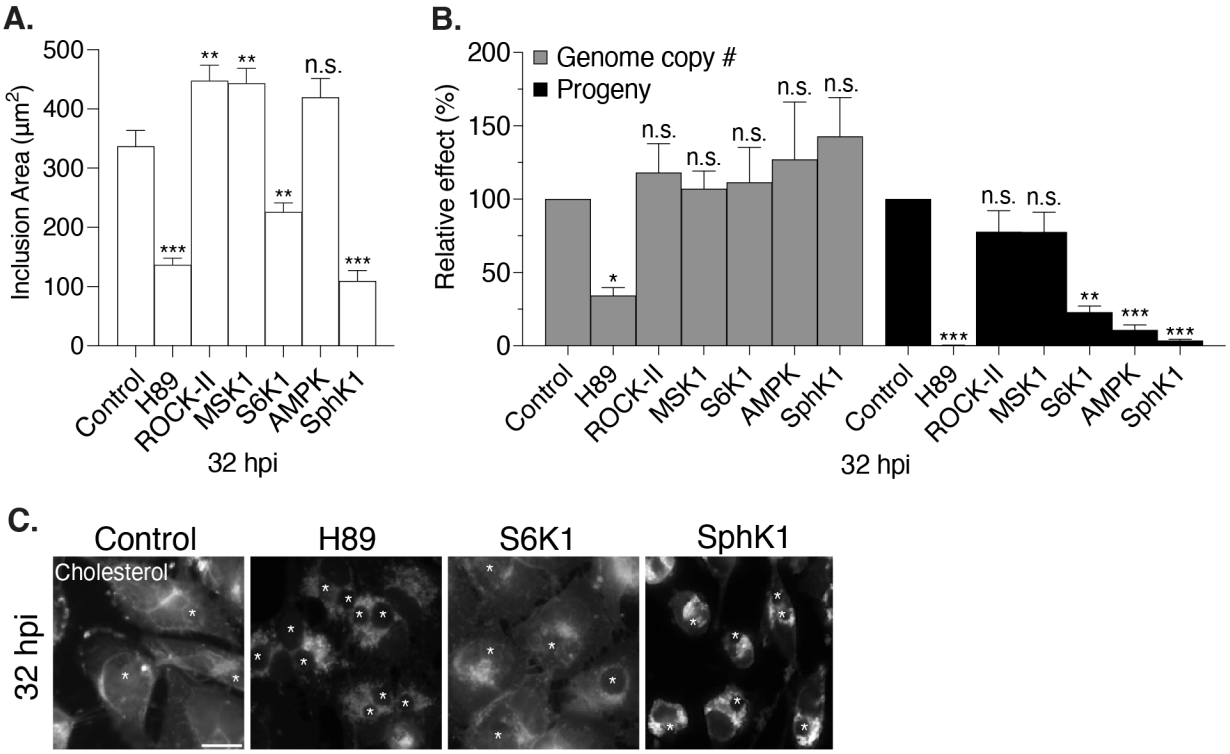

Figure 5.6. Screening for kinase targets of H89 using an inhibitor approach.
(A) Inclusion areas, numbers of chlamydial genomes, and progeny production for inhibitor-treated samples were determined at 32 hpi. Inhibitor concentrations used and their respective kinase targets: ROCK-II inhibitor Y27632 (25 μM); MSK1 inhibitor SB 747651A (2.5 μM); S6K1 inhibitor PF-4708671 (1 μM); AMPK inhibitor Compound C (2 μM); Sphingosine kinase 1 (SphK1) inhibitor PF543 (20 μM). H89 was used at 12.5 μM. For each sample, the average inclusion area from 50 inclusions was determined. Data are presented as means ± SE (n = 3). **P≤0.01, ***P<0.001; n.s. = data not statistically significant.
(B) The number of chlamydial genomes and infectious progeny in inhibitor-treated samples were determined at 32 hpi. Values were normalized to their untreated control counterparts (control = 100%) and expressed as a percentage. The data are presented as mean ± SE (n=3); *P<0.05, **P≤0.01, ***P<0.001; n.s. = data not statistically significant.
(C) Immunofluorescence images of infected HeLa cells treated for 32 hours with the indicated inhibitors. The fluorescent cholesterol-binding molecule filipin was used to visualize cholesterol (white). Each inclusion is indicated with a white asterisk. Scale bar is 20 μm.

to control samples (Fig. 5.7C). These data show that SphK1 activity promotes the chlamydial infection and provide more evidence that SphK1 may be a target of H89.

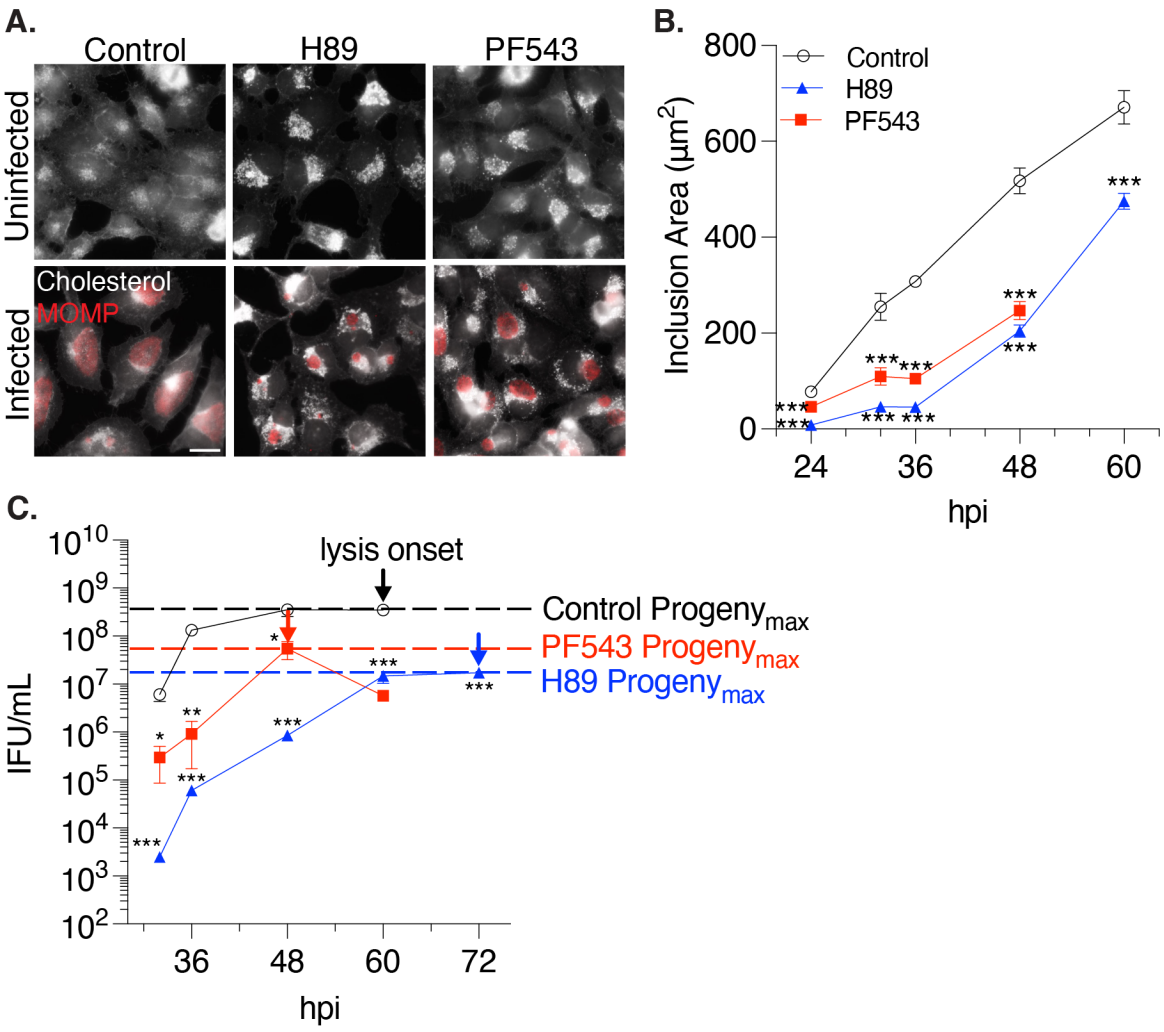

Figure 5.7. Inhibition of sphingosine kinase 1 function causes cholesterol accumulation and defects on the chlamydial infection.
(A) Immunofluorescence images of infected HeLa cells treated with DMSO, H89, or SphK1 inhibitor PF543 for 32 hours. The fluorescent cholesterol-binding molecule filipin was used to visualize cholesterol (white). Chlamydiae are detected with antibodies to the major outer membrane protein MOMP (red). Scale bar is 20 µm.
(B) Inclusion quantifications from conditions in part A. The average inclusion area from 100 inclusions was measured for each condition at each timepoint. The data are presented as mean ± SE; ***P<0.001.
(C) Measurements of progeny during the time course of infected HeLa cells incubated with the indicated inhibitors. Progeny$_{max}$ is indicated by a horizontal dashed line. Arrows indicate the onset of inclusion lysis. Data are presented as means ± SE (n=3); *P<0.05, **P≤0.01, ***P<0.001.

Our next goal was to determine if H89 affected SphK1 activity. We first conducted an *in vitro* kinase assay. Uninfected cells were treated with inhibitors for 24 hours, harvested by scraping, syringe lysed, and centrifugated to remove cellular debris. Sphingosine and ATP were added to 10 μl samples of supernatant and measured for SphK activity. Both H89 and the SphK1 inhibitor PF543 decreased SphK1 activity compared to control samples, as indicated by a greater amount of leftover ATP (Fig. 5.8A). As an additional control, the KSK120 inhibitor that does not target SphK1, was shown to have no significant effect on ATP consumption (Fig. 5.8A). We also monitored whether H89 affects SphK1 activity by monitoring M6PR protein expression, which is negatively regulated by SphK1 (Newton et al., 2020). Both H89 and PF543 increased protein expression of M6PR by western blot, although the affects appear to be mild (Fig 5.8 B-C). Thus, H89 may partially block sphingosine kinase activity.

To verify SphK1 as a true H89 target, we plan to infect SphK1 KO and WT cells in the presence and absence of H89-treatment. **I hypothesize** that the SphK1 mutants will result in smaller inclusions and fewer infectious progeny. Also, **I hypothesize** that H89 will not result in additional inhibitory effects on inclusion growth and progeny production in the SphK1 KO cells because the SphK1 target is missing. If there are additional defects on the infection, H89 either inhibits other kinases in addition to SphK1 or blocks another kinase(s) entirely. The combination of inhibitor and genetic approaches will help verify SphK1 as a target of H89.

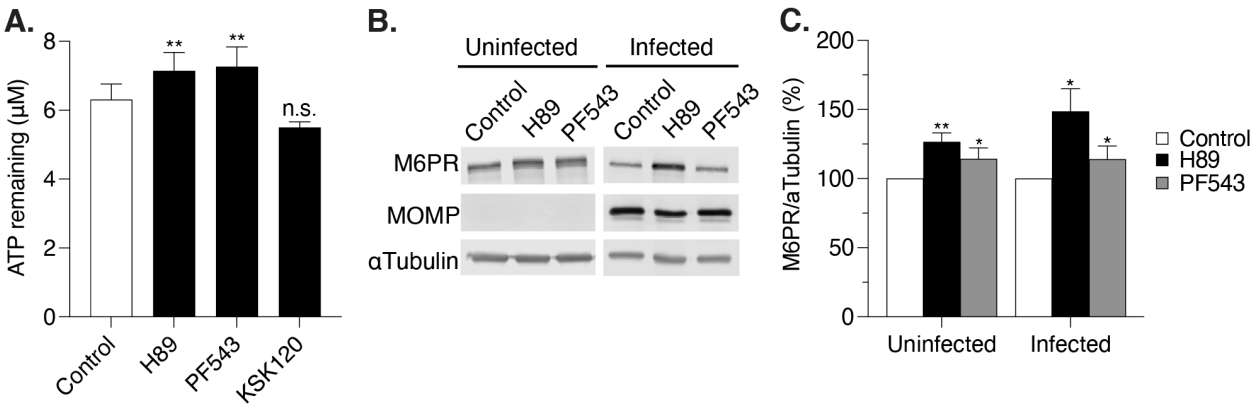

Figure 5.8. H89 decreases sphingosine kinase activity.
(A) *In vitro* sphingosine kinase assay for uninfected HeLa cells treated with DMSO, H89, or PF543 for 24 hours. Samples were syringe lysed and centrifugated to remove cellular debris. Purified sphingosine and ATP were added to 10 μl of supernatant. The amount of unused ATP remaining in the sample was measured. Data are presented as means ± SE (n=3); **P≤0.01; n.s. = data not statistically significant.
(B) Western blot of HeLa cells that were either left uninfected or infected with *C. trachomatis* and treated with DMSO, H89, or PF543 for 32 hours. Antibodies were used to detect M6PR, MOMP, and αTubulin.
(C) Quantifications of western blot samples treated as described in part B. For each sample, M6PR expression levels were normalized to αTubulin. Values are expressed as a percentage of the control (control = 100%). The data are presented as mean ± SE (n=3); *P<0.05, **P≤0.01.

H89 and SphK inhibitors are known lysosomotropic agents, meaning they cause an increase in lysosomal pH and decrease in lysosomal acidity (Ashfaq et al., 2011; Bae et al., 2012; Young et al., 2016). Our goal was to test whether H89 treatment under our conditions caused cholesterol accumulation by increasing the lysosomal pH. We treated uninfected HeLa cells for 24 hours with H89 and PF543 inhibitors, as well as chloroquine and bafilomycin, which are known to increase lysosomal pH (Fedele & Proud, 2020). The samples were then incubated with LysoTracker Red and imaged live for LysoTracker Red signal, which fluoresces in acidic environments. Line intensity scans showed that for all samples except the control, there was an overall decrease in

LysoTracker Red signal (Fig. 5.9 A-B). With PF543, there was about a 30% reduction in LysoTracker signal, and at least a 50% reduction with H89 (Fig. 5.9B). We included bafilomycin and chloroquine as positive controls for defective lysosomal acidification because they block the function of the lysosomal v-ATPase pump that regulates pH (Fig. 5.9B) (Fedele & Proud, 2020). We then showed that bafilomycin and chloroquine also cause lysosomal cholesterol accumulation during the chlamydial infection, like H89 (Fig. 5.9C). Our data demonstrate that H89 inhibits lysosomal acidification, which causes cholesterol retention within lysosomes.

Next, we tested whether these lysosomotropic agents caused defects in the chlamydial infection. H89, bafilomycin, and chloroquine, all caused a significant decrease in inclusion size when compared to DMSO-treated samples (Fig. 5.9D). Also, they all significantly reduced the number of infectious progeny by at least 10-fold and a modestly reduced the number of chlamydial genomes by 2-4-fold (Fig. 5.9D). Together, our data show that preventing lysosomal acidification is associated with a decrease in inclusion size, limited chlamydial replication, and considerably fewer progeny.

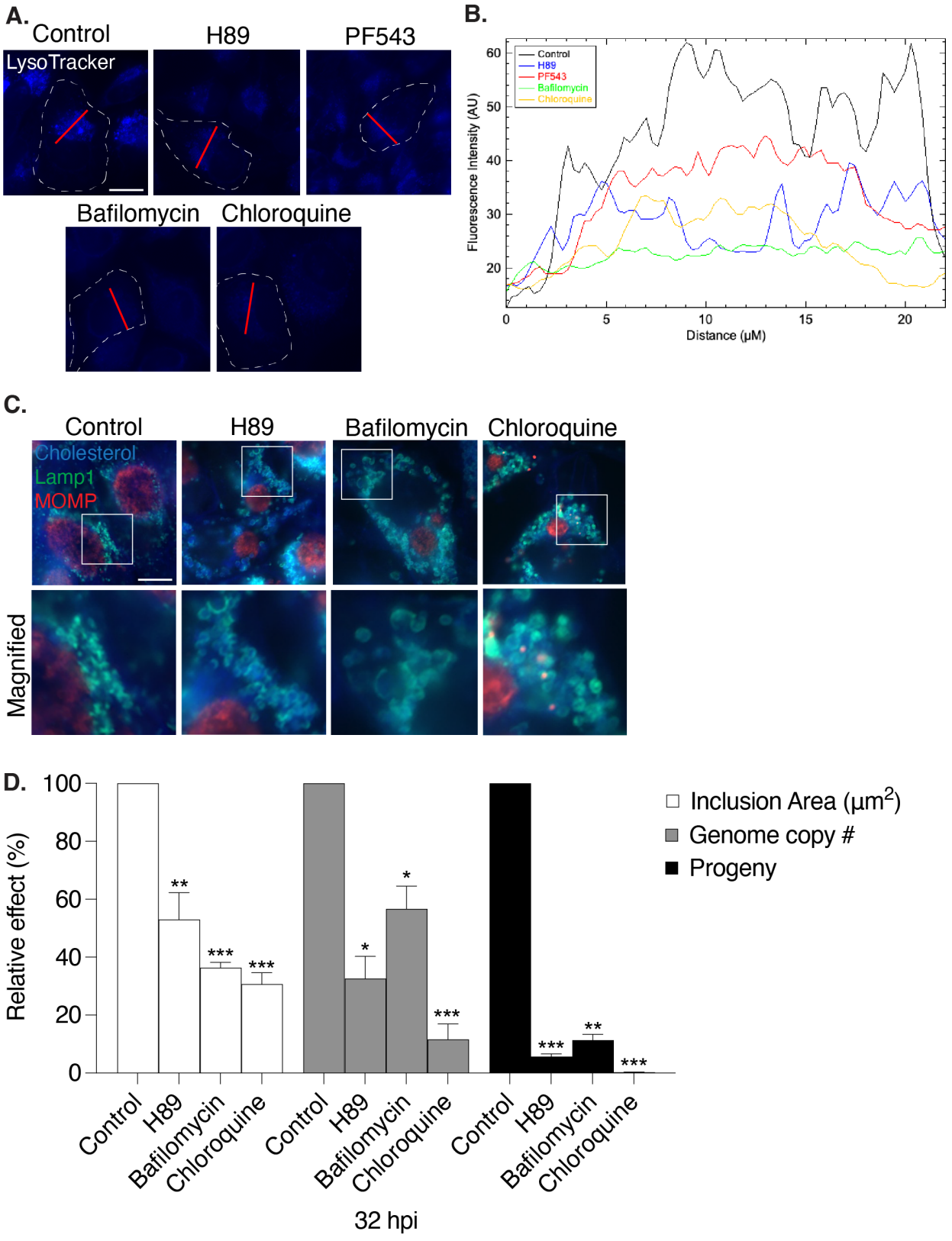
A.
Control
H89
PF543
LysoTracker
Bafilomycin
Chloroquine
B.
Control
H89
PF543
Bafilomycin
Chloroquine
Fluorescence Intensity (AU)
Distance (μM)
C.
Control
H89
Bafilomycin
Chloroquine
Cholesterol
Lamp1
MOMP
Magnified
D.
Relative effect (%)
Inclusion Area (μm2)
Genome copy #
Progeny
32 hpi

Figure 5.9. H89 causes defects in lysosomal acidification that are associated with defects on the chlamydial infection.
(A) Immunofluorescence images of uninfected HeLa cells treated with the indicated inhibitors for 24 hours and measured for lysosomal acidity with LysoTracker (50 nM) (blue). White dashed lines outline a single cell. The red line indicates the region of the cell measured for fluorescence intensity. Scale bar is 20 μm.
(B) Line intensity scans were used to measure the fluorescence intensity (AU) of LysoTracker signal for DMSO control (black), H89 (blue), PF543 (red), bafilomycin (green), and chloroquine (orange) conditions in part A.
(C) Immunofluorescence images of *C. trachomatis*-infected HeLa cells treated with the indicated inhibitors and fixed at 32 hpi. The fluorescent cholesterol-binding molecule filipin was used to visualize cholesterol (blue). Antibodies against LAMP1 were used to identify the lysosomes (green). Antibodies against MOMP was used to visualize chlamydiae (red). White boxes indicate the portions of the image that have been magnified. Scale bar is 10 μm.
(D) Inclusion areas, numbers of chlamydial genomes, and progeny production for inhibitor-treated samples were determined at 32 hpi. A total of 100 inclusions from three separate experiments were measured. For each experiment, values were normalized to untreated controls (control = 100%) and expressed as a percentage. Data are presented as means ± SE ($n = 3$). *$P < 0.05$, **$P \leq 0.01$, ***$P < 0.001$.

<u>Model for H89-mediated defects on cholesterol accumulation and the downstream consequences on the chlamydial infection</u>

We propose a mechanism for the anti-chlamydial effect of H89 (Fig. 5.10). Cholesterol accumulation in the lysosome is known to be caused by a cholesterol trafficking defect. We included the published NPC1 inhibitor of cholesterol trafficking U18666A, as well as two additional NCP1 inhibitors, Itraconazole and Astemizole, to support that cholesterol accumulation correlates with defects on the infection. Our data demonstrate that cholesterol accumulation has inhibitory effects on inclusion growth and RB-to-EB conversion, which supports published data (Beatty, 2006, 2008). We also provide some evidence to suggest that SphK1 may be one of many kinases inhibited by H89 to mediate these lysosomal defects. In support of this hypothesis, inhibition of

SphK1 with PF543 caused defects in lysosomal pH, cholesterol accumulation, and downstream defects in inclusion growth and progeny production. Thus, H89 likely inhibits *C. trachomatis* inclusion growth and the production of infectious progeny by decreasing lysosomal acidity and promoting cholesterol retention within lysosomes.

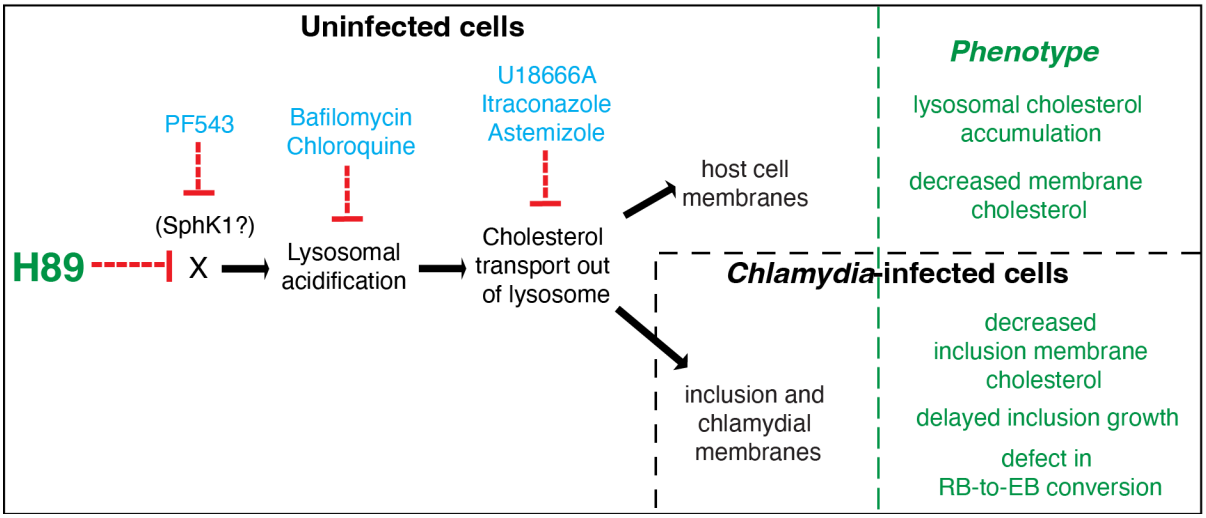

Figure 5.10. Model for H89-mediated defects on cholesterol trafficking through the inhibition of lysosomal acidification and the phenotypes observed in uninfected host cells and *Chlamydia*-infected cells.
The novel small molecule inhibitor H89 causes defects in lysosomal acidification similar to bafilomycin, chloroquine, and PF543 treatment. These inhibitors cause defects in cholesterol transport out of the lysosome like NPC1 inhibitors (U18666A, Itraconazole, and Astemizole). The phenotypes (green) of these inhibitors in uninfected cells are lysosomal cholesterol accumulation and decreased cholesterol levels in host cell membranes. For *Chlamydia*-infected cells, the cholesterol trafficking defect decreased cholesterol levels at the inclusion membrane, which correlated with delayed inclusion growth and a defect in RB-to-EB conversion. Mechanistically, H89 may inhibit SphK1 activity to mediate these effects, although the inhibition of other host cells kinases cannot be excluded.

5.5 Discussion

To investigate how H89 causes defects in the chlamydial infection, we discovered that H89 induces lysosomal cholesterol accumulation, which has not previously been reported. This defect in trafficking was only observed for cholesterol, as we did not observe defects in the endogenous uptake of EGF and transferrin, nor were there defects in transferrin trafficking out of the cell. However, the trafficking of other lipids through the endolysosomal pathway cannot be excluded. We showed that altering cholesterol levels within the host cell, either by decreasing serum cholesterol levels or promoting cholesterol efflux, produced defects in inclusion growth and infectious progeny production. As cholesterol trafficking defects are known to inhibit the chlamydial infection (Beatty, 2006, 2008), we screened for potential kinase targets and found that inhibition of SphK1 blocked the infection similarly to H89-treatment in addition to causing cholesterol accumulation. We also show preliminary data that H89 inhibits SphK1 activity and causes lysosomes to be less acidic. These findings are consistent with published data showing that bafilomycin, which decreases lysosomal acidity, causes a defect in inclusion growth and progeny production (Ouellette et al., 2011). Therefore, the cholesterol trafficking defects and subsequent defects on the chlamydial infection may be mediated through SphK1 inhibition.

Several pieces of evidence suggest that cholesterol is important for *Chlamydia* development. Firstly, Carabeo *et al.* showed that cholesterol is an integral part of the chlamydial inclusion and chlamydial membranes (Carabeo et al., 2003). Secondly, our data and studies from Beatty *et al.* show that causing lysosomal cholesterol

accumulation correlates with decreased inclusion growth and fewer infectious progeny (Beatty, 2006, 2008). Thirdly, decreasing intracellular cholesterol levels had inhibitory effects on the infection.

We showed that infections with cholesterol deficient LPDS media caused modest inhibitory effects on inclusion and progeny production. It is possible that a larger defect was not observed like with NPC1 inhibition because LPDS media was used only at the time of the infection. Host cells may still have residual cholesterol from being previously incubated in serum media. Another factor to consider is that endogenous cholesterol synthesis initiates when the cells are starved of cholesterol (Dietschy, 1984). We also found that blocking cholesterol synthesis in host cells with inhibitors in addition to using cholesterol-starved media was toxic after about 24-36 hours (data not shown). Therefore, this approach to decreasing cellular cholesterol levels was not ideal for studying the 48–72-hour chlamydial infection. For this reason, we used DMHCA, which decreases intracellular cholesterol levels by promoting cholesterol efflux. DMHCA-treatment caused smaller inclusions and fewer progeny to a similar extent as H89. Lastly, supplementing H89 infection conditions with cholesterol rescued progeny production and partially rescued inclusion growth, suggesting the infection needed cholesterol. These data provide many examples to support that *Chlamydia* depend on cholesterol to promote the infection.

The experiments conducted by Gilk *et al.* provide a counterargument for the importance of cholesterol during the infection. They generated a MEF cell line with a mutation in DHCR24, which is necessary for the final step of cholesterol synthesis in

converting desmosterol into cholesterol (Gilk et al., 2013). Although no cholesterol could be produced, desmosterol was still present and only differs from cholesterol by a double bond in its carbon chain. As cholesterol and desmosterol are nearly identical in structure and desmosterol can be used as a substitute in cell membranes (Rodríguez-Acebes et al., 2009), desmosterol may be sufficient for inclusion growth and progeny production. To test this, we propose repeating the experiments conducted in figure 5.5 and instead of adding cholesterol to the media, we would add desmosterol. If cholesterol and desmosterol can be used interchangeably by chlamydiae, we hypothesize that desmosterol would rescue inclusion growth, replication, and progeny production to the same extent as cholesterol.

It is possible that the inhibitory effects on the infection are due to an accumulation of sphingosine rather than cholesterol. Sphingosine kinase converts sphingosine to sphingosine-1-phosphate (S1P). For intracellular infections with *Neisseria gonorrhoeae*, increasing sphingosine levels was toxic and prevented the formation of progeny (Solger et al., 2020). Also, sphingosine is known to accumulate in NPC1 deficient cells (Newton et al., 2020). Therefore, inhibition of NPC1 or SphK1 would increase cellular sphingosine levels, which could be toxic for the chlamydial infection. However, because we show that cholesterol addition under H89 conditions improved inclusion growth and rescued RB-to-EB conversion, sphingosine toxicity may not be the case.

An interesting question is why would an abundance of cholesterol not benefit the infection? Although H89, NPC1 inhibitors, and PF543 cause lysosomal cholesterol

accumulation, they prevent cholesterol trafficking out of the lysosome, which may limit the accessibility of cholesterol that can be acquired by the infection. Perhaps chlamydiae can only use cholesterol once it has been exported out of the lysosome. H89, like PF543 and NPC1 inhibitors, blocks cholesterol export and so chlamydiae would be less likely to intercept cholesterol that is in transit to other cellular membranes.

Inclusion growth may require a certain cholesterol concentration to maintain a stable vacuole and limiting cholesterol could slow growth and/or cause early inclusion lysis. We observed an earlier onset of inclusion lysis with H89+cholesterol and control+cholesterol conditions. However, with H89 treatment alone, there was a 12-hour delay in lysis, which suggests that cholesterol acquisition is likely impaired rather than blocked (Fig. 5.5C). Also, perhaps RBs need the right balance of cholesterol in their membranes before conversion into an EB and an insufficient amount of cholesterol stalls conversion. In future studies, we can address these questions by isolating the inclusions and chlamydiae for lipid analyses to determine changes in cholesterol levels as well as changes in the incorporation of other lipids.

In our studies, we evaluated the mechanism by which H89 inhibits the chlamydial infection. We report a new phenotype with H89 treatment, which is lysosomal cholesterol accumulation. We also found that H89 inhibits sphingosine kinase activity, which is known to cause decreased lysosomal acidity and induce cholesterol accumulation. These data suggest that the block in cholesterol trafficking caused by H89 may be partly because of SphK1 inhibition. Under *C. trachomatis* infection, H89-treatment and inhibition of cholesterol transport with inhibitors (U18666A, Itraconazole,

Astemizole, and PF543) correlate with defects in inclusion growth and RB-to-EB conversion. Thus, H89 with its newly described lysosomal accumulation of cholesterol can be used as a tool for understanding the cholesterol requirements of the chlamydial infection.

CHAPTER 6: CONCLUSIONS AND FUTURE DIRECTIONS

"Science, for me, gives a partial explanation for life. In so far as it goes, it is based on fact, experience and experiment." - Rosalind Franklin, Ph.D. in Physical Chemistry

6.1 Proposing a standardized approach for studying manipulations of the chlamydial infection

Although there has been great progress in studying the *Chlamydia* infection, the fundamental mechanisms that promote inclusion growth, RB replication, and RB-to-EB conversion are still unclear. Manipulations of the chlamydial infection through temperature shifts, genetic modifications, siRNA knockdown, and inhibitor treatments have all been effective tools for understanding the host and bacterial pathways that are necessary for *Chlamydia* infection. For example, Brothwell *et al*. screened for temperature sensitive (TS) mutants of *Chlamydia* and showed that four of the TS alleles corresponded to genes that were essential for processes in other bacteria, such as DNA replication (*dnaE*) and translation (*rpsH*) (Brothwell et al., 2016). Another example is how type III secretion (T3SS) inhibitors such as C1 have been shown to cause defects in inclusion growth and progeny production (refer to Table 1.2). In addition to testing the effects of C1 when added from the start of the infection, C1 was also added at different times during the infection to corresponded with different parts of chlamydial development. This approach revealed that C1 caused a block in RB-to-EB conversion, however, we still do not know how the T3SS system promotes EB production (Wolf et al., 2006).

There are several assays used by the field to measure the effects of different conditions on inclusion growth, RB replication, and RB-to-EB conversion, but a major challenge is that there is no standard method to assess and compare these effects during the 48–72-hour chlamydial developmental cycle. The studies presented in Chapter 3 of this dissertation seek to redefine the way the *Chlamydia* field assesses manipulations of *Chlamydia* infection to more accurately describe the developmental steps that are affected. We focus on the use of inhibitors because they are the most widely reported method of altering chlamydial infection conditions (>700 publications). We highlight the limitations of the current methods used by the field and pose several questions: 1. When should the effects of an inhibitor on the intracellular infection be measured? 2. How accurately do analyses at one or two time points reflect the overall effects on the infection? 3. How do you compare the effects of inhibitors if they alter the temporal course of the developmental cycle? 4. Which assays are most suitable to determine the effects on the infection? and 5. How can the effects of different inhibitors be compared? Applying a standard method to understand how these conditions affect specific steps in chlamydial development is essential to understand *Chlamydia* biology and to develop anti-chlamydial therapies.

6.2 Limitations in using small molecule inhibitors to study *Chlamydia* infection

We found it challenging to compare our inhibitor studies with published chlamydial inhibitors because there is no standard method of monitoring inhibitor treatment during *Chlamydia* infection. Most publications conduct one or two analyses

such as inclusion size quantifications and progeny assays and evaluate the infection at one or two time points. We showed in Chapter 3 that one of the issues with this system is that small molecule inhibitors can have temporal effects on the intracellular infection. For example, we showed that BFA causes a progeny production defect when measured at late times during the infection, but the *Chlamydia* field reports that BFA does not cause any defects on progeny number. This is based on research from the mid 1990's, which has been cited over 300 times (Hackstadt et al., 1996). These BFA studies are particularly important because they have shaped how other *Chlamydia* labs investigate the mechanisms of their inhibitor studies. In one case, Rotterlin-treatment of the *Chlamydia* infection caused defects in ceramide transport to the inclusion, which correlated with progeny defects (Shivshankar et al., 2008). However, because BFA was previously reported to inhibit ceramide transport and cause no defects on progeny, ceramide trafficking was ruled out as the cause of the Rotterlin-induced progeny defects (Shivshankar et al., 2008). Shivshankar *et al.* did not actually test whether blocking ceramide trafficking contributes to progeny defects. This means that many potential targets and mechanisms of chlamydial inhibitors may be overlooked based on publications of previous inhibitors.

We also showed that when measuring inclusion growth, it is possible to distinguish between a block and a delay with measurements at multiple time points. KSK120 samples were smaller than controls up to 36 hpi but were similar in size to controls after this time. Unlike BFA, which showed a defect in progeny at later times in the infection, KSK120 showed an inclusion defect only at early times. BFA and KSK120

both caused time-dependent phenotypes, highlighting the dynamic nature of the infection. Thus, to address the first two questions, we suggest it is best to measure the effects of an inhibitor on the intracellular infection at multiple time points.

A second issue we found with inhibitor studies is that defects in progeny were often reported at a single time point in the infection and did not consider changes in the length of the developmental cycle with the inhibitor. *C. trachomatis* infections typically lyse between 48-72 hpi, but we showed that inhibitors such as BFA can cause an earlier onset of inclusion lysis. Therefore, one should first determine whether an inhibitor alters the length of the developmental cycle by monitoring the time point of inclusion lysis. From this terminal time point, one can then make decisions about what additional time points would be useful for further analyses. Although we used immunofluorescence microscopy to detect inclusion lysis, one could also use simpler methods such as brightfield microscopy.

A factor that complicates determining the length of the developmental cycle is inclusion extrusion. Rather than inclusion lysis at the end of the infection, inclusions can also be extruded out of the host and remain intact in the extracellular space. Studies by Hybiske *et al.* demonstrated by live imaging that about 50% of inclusions will undergo extrusion (Hybiske & Stephens, 2007), however these intact inclusions are rarely observed or reported. If an inhibitor promotes inclusion extrusion and one chooses to monitor lysis by brightfield, one may wrongly assume that the infection is prolonged because no lysis is observed. Additionally, if infection studies are conducted *in vivo*, a treatment that promotes extrusion may not cause the same signs of damage from a

Chlamydia infection because host cell and inclusion lysis is reduced. The best way to measure extrusion would be by live imaging, however, this is not a standard practice in the *Chlamydia* field.

Another issue we came across was that a defect in one developmental process such as inclusion growth does not necessarily coincide with a defect in another developmental process like RB-to-EB conversion. With inhibitors KSK120 and MK2206, we showed that despite normal inclusion growth, there were significantly fewer infectious progeny compared to controls. These data mean that inhibitors can cause discordant effects on specific steps of chlamydial development.

Additionally, progeny assays are widely used in the *Chlamydia* field as a measure for defects in RB-to-EB conversion; however, there are other explanations for why certain conditions result in decreased progeny. Firstly, if an inhibitor prevents or limits inclusion formation, only a fraction of the infectious progeny will be produced compared to controls (Fig. 6.1). This is not because there was an RB-to-EB conversion defect, but because there were fewer infectious EBs that were successful in initiating an infection in the first place. In our studies, we monitored inclusion formation by immunofluorescence microscopy to ensure that a similar number of cells were infected for the control and treatment conditions. Secondly, if the initial EB is unable to convert to the replicative RB form, then there can be no chlamydial replication and subsequently no infectious EBs (Fig. 6.1). Thirdly, if an inhibitor causes defects in chlamydial replication, there will be fewer chlamydiae that can undergo RB-to-EB conversion (Fig. 6.1). Many papers do not quantify replication (Table 1.1-1.2) and they assume that there

is decreased replication based on the progeny data, which we have shown can lead to inaccurate conclusions (Shivshankar et al., 2008). For this reason, in our studies we conducted analyses that measured the number of chlamydial genomes as an indicator of chlamydial replication and measured the number of infectious progeny to indicate RB-to-EB conversion. Fourthly, if a particular condition induces chlamydial persistence, a dormant, non-infectious state of the infection, no infectious EBs will be detected by progeny assay. We used electron microscopy (EM) in our studies to rule out persistence as a factor in blocking RB-to-EB conversion (Fig. 6.1). Fifthly, a defect in RB-to-EB conversion directly affects the formation of infectious chlamydiae, which can be measured by EM and progeny assay (Fig. 6.1). Lastly, another explanation for decreased progeny is that the EBs can still form, but do not mature, as was the case with KSK213 inhibitor treatment (Fig. 6.1) (Table 1.2) (Núñez-Otero et al., 2021b). Therefore, if there are fewer infectious progeny by progeny assay and EBs are still visible by EM, it is possible that the EBs are not fully developed and are non-infectious.

To address our fourth question about how many assays should be conducted, our data show the importance of conducting multiple assays at each time point. For one, inhibitors can either independently alter specific steps of chlamydial development like inclusion growth or RB-to-EB conversion. Secondly, inhibitors may cause a defect in inclusion growth, EB-to-RB conversion, replication, RB-to-EB conversion, EB maturation, or induce persistence, which can all cause indirect consequences on infectious progeny production.

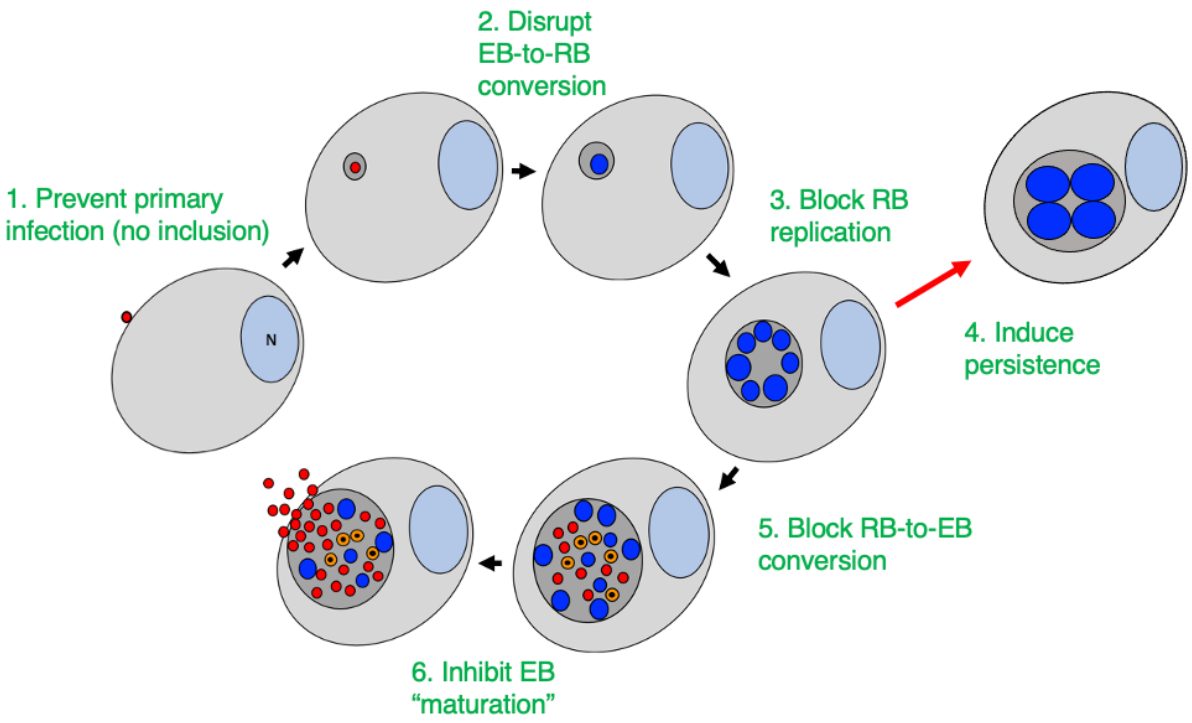

Figure 6.1 The many ways to prevent the production of infectious EBs.
There are many steps in the *Chlamydia* developmental cycle that can be targeted by different infection conditions and result in decreased infectious progeny. 1) The treatment may prevent the primary chlamydial infection, which will result in no inclusion formation and subsequently no infectious EBs. 2) A disruption in the initial EB-to-RB conversion will halt the remaining steps of the infection. 3) If RB replication is blocked, there will be a smaller pool of RBs that can convert into infectious EBs. 4) If the condition induces persistence, aberrant bodies will form, but no infectious EBs are made during this time. 5) If RB-to-EB conversion is blocked, no infectious progeny can be produced. 6) Lastly, even if EBs are produced, the treatment condition may cause an inhibition in EB maturation, which results in non-infectious EBs and no secondary chlamydial infection.

Lastly, in Chapter 3, we proposed a new quantification called $Progeny_{max}$ to facilitate the comparison of different inhibitors on the *Chlamydia* infection. $Progeny_{max}$ identifies the maximum number of progeny produced by a given condition and is independent of any changes to the length of the developmental cycle. Of note, $Progeny_{max}$ should only be used once the inhibitor has been shown to have no effects on inclusion formation and does not induce persistence. To address our fifth and final

question of how to compare effects across inhibitors, one should examine the overall defects at the end of the infection. For the first time, the *Chlamydia* field will have a standardized method of comparing the effects of inhibitors. Also, because the time point of $Progeny_{max}$ corresponds to the time point just prior to lysis, the slight differences in the length of the chlamydial infection that vary from lab to lab are accounted for.

6.3 Advantages of small molecule inhibitors

Of the readily available tools to manipulate the chlamydial infection, inhibitors provide many advantages. Eukaryotic inhibitors are most often commercially available. For example, of the inhibitors listed in Table 1.1, about 86% of them are available through credible scientific vendors. They are also affordable because the inhibitors are offered in small amounts for as little as $50, which is beneficial for initial testing purposes. In comparison, siRNAs from Dharmacon can cost up to a few hundred dollars to test the knockdown of a single gene. Another advantage of inhibitors is that they are less time consuming because they do not require plasmid design for gene deletions or testing multiple siRNAs to have sufficient knockdown.

Also, inhibitors can be used to enhance or diminish functions of proteins directly, which is not always the case with siRNAs. With siRNAs there needs to first be effective knockdown of a gene of interest, which can then decrease expression of the protein encoded by that gene. In some cases, you need to perform multiple knockdowns to achieve sufficient knockdown, which is time consuming and cumbersome. Also, even if a gene is effectively targeted by siRNAs, it still takes time for the host cell to break down

the protein encoded by that gene, which was present prior to the knockdown.

There are also cases where knockdown of a gene causes the cell to increase expression of other genes to compensate for lost function. For example, when I tested siRNAs against NPC1, I detected an increase in NPC2 expression by western blot (data not shown). **I hypothesize** that NPC2 expression increased to overcome the loss of NPC1. Even with NPC1 knockdown, this increase in NPC2 expression did not allow me to successfully achieve the cholesterol accumulation phenotype. Another possibility is that despite the 70% reduction in NPC1 expression by western blot, the residual 30% was sufficient for maintaining cholesterol trafficking.

Another benefit of inhibitors is that inhibitors can be used at any time during the experiment. For experiments that occur over longer time periods, such as the 48-72-hour chlamydial infection, inhibitors can be easily replenished in the media to sustain inhibition. The activity of the inhibitor targets can be monitored by kinase assay or western blot over time to determine whether the inhibitor is still effective at later times and if drug re-addition is necessary. Also, for our *Chlamydia* studies, inhibitors can be added at different times during the infection to test whether the inhibitor is more effective at blocking a certain stage of chlamydial development. Inhibitors can even be incubated with the EBs directly prior to the infection to test if they inhibit inclusion formation, as is the case with inhibitor C1 (Claywell et al., 2018; Wolf et al., 2006). Lastly, if using a reversible inhibitor, the drug can be washed out at any time to affirm that the observed effects are caused by the treatment and not some other factor. The flexibility of inhibitors was a major reason why we chose to pursue them for our studies.

6.4 Disadvantages of small molecule inhibitors

Despite the convenience of inhibitors, there are also several disadvantages. A major disadvantage is that one inhibitor may have multiple targets. As we have seen with the small molecule inhibitor H89, in addition to its known kinase target, protein kinase A (PKA), there are reports of H89 targeting other kinases such as ROCK-II, MSK1, S6K1, and AMPK. H89 is a serine/threonine kinase inhibitor and there are approximately 125 serine/threonine kinases in eukaryotic cells (Capra et al., 2006), making it challenging to pinpoint which ones are targeted under our infection conditions. Also, it is possible that H89 targets a combination of kinases to produce the observed phenotypes of cholesterol accumulation and an inhibition of the chlamydial infection. Thus, the lower the specificity of a drug, the greater the likelihood that the inhibitor affects multiple targets.

Another drawback of inhibitors is that many are tested for efficacy through controlled biochemical analyses *in vitro*, but few are validated for use in tissue culture and *in vivo* studies. Although a drug may be potent *in vitro*, it may not be as effective in cells or *in vivo* models. There are other competing factors in the cellular environments such as variable ATP levels and different expression patterns of a drug target that cannot be ignored. Thus, inhibitor effects *in vitro* cannot assumed to be true *in vivo*.

It is also important to ensure that the inhibitor is not toxic to the host cell by conducting viability assays because cell free assays do not have this issue. Performing an MTT assay takes into consideration changes in metabolic activity under different treatment conditions. A simpler approach to measuring cell viability is to quantify the

number of cells in a certain area of the plate, either by immunofluorescent staining for DAPI or by counting live cells on a hemocytometer, which will provide an idea of whether a treatment causes cell death. This is important because one can wrongly conclude that an inhibitor causes a defect, when in reality the phenotype is a consequence of a dying host cell.

When trying to identify effective inhibitors, a major question is whether it is membrane permeable. In some cases, to target an intracellular kinase, the drug must either have the capacity to diffuse across the cell membrane or be taken up endocytically. For inhibitors to block the function of an intracellular bacterium, this is even a greater challenge. For example, for a drug to inhibit *Chlamydia* directly, it needs to be able to traverse three membrane layers including the host cell membrane, inclusion membrane, and chlamydial membrane. Thus, a majority of the effective inhibitors used to study the chlamydial infection target host cell functions and pathways because there are fewer physical barriers (Tables 1.1-1.2).

6.5 H89 is a novel small molecule inhibitor of the chlamydial infection

Through my comprehensive understanding of inhibitors and how to study them, I identified a novel inhibitor of the chlamydial infection, H89. In chapter 4, we showed that there was a delay in inclusion growth and a block in progeny production at the step of RB-to-EB conversion. None of the published pathways and targets of H89 were affected under our infection conditions (Table 5.1). We then investigated alternative mechanisms that could be affected based on known phenotypes caused by published inhibitors of

the *Chlamydia* infection. Our challenge with comparing H89 to other chlamydial inhibitors was that studies conduct minimal analyses (Tables 1.1-1.2), supporting the need for more standard and thorough experimentation.

Interestingly, H89 phenocopied the cholesterol trafficking defect of the NPC1 inhibitor U18666A, which has previously been reported to cause smaller inclusions and a defect in progeny production (Beatty, 2006, 2008). We pursued this phenotype because cholesterol has been found within the inclusion and chlamydial membranes (Carabeo et al., 2003), meaning it may be important for chlamydial development. In support of our findings, we showed that two additional NPC1 inhibitors, Itraconazole and Astemizole, also caused cholesterol accumulation and were associated with smaller inclusions and a defect in RB-to-EB conversion. It is challenging to justify that H89 blocks NPC1 function because H89 is a kinase inhibitor and NPC1 is not a kinase (Bain et al., 2007; Lochner & Moolman, 2006; Murray, 2008). However, it was previously reported that defects in NPC1-mediated cholesterol trafficking are associated with decreased sphingosine kinase function (SphK1) (Newton et al., 2020). Thus, **I hypothesized** that H89 inhibits cholesterol trafficking through inhibition of SphK1 activity. Our comprehensive approach to studying chlamydial inhibitors was critical for implicating H89 cholesterol trafficking defects in limiting the chlamydial infection and SphK1 as a possible H89 target.

6.6 The importance of cholesterol during intracellular infections

In contrast to facultative intracellular bacteria or extracellular pathogens, obligate

intracellular pathogens face a unique set of challenges and rely heavily on their eukaryotic host to provide nutrients for a successful infection. Cholesterol appears to be an important nutrient for many intracellular infections, as it is one of the resources that *Coxiella, Anaplasma, Ehrlichia, Rickettsia,* and *Chlamydia* steal to help establish their intracellular niche (Samanta et al., 2017). One of the reasons why cholesterol may be targeted is that it strongly influences membrane structure, fluidity, and function. To start, the pathogen must bind to and recognize its eukaryotic host cell target and induce endocytosis. For *Rickettsia*, *Coxiella, Anaplasma,* and *Ehrlichia*, attachment and entry into the host cell is mediated through cholesterol-rich lipid rafts. Next, depending on the pathogen, they need to either replicate within the phagosome or escape the phagosome to replicate in the cytosol. The pathogens residing within vacuoles do not readily have access to host cell nutrients. Therefore, they must alter host metabolism and redirect host cell trafficking pathways to sustain the intracellular compartment. Cholesterol is found on the vacuole membranes of *Chlamydia, Coxiella, Anaplasma, Ehrlichia,* and *Eimeria bovis* (Hamid et al., 2015; Samanta et al., 2017). Even intracellular pathogens that temporarily reside within a vacuole, like *Rickettsia,* and *Orientia*, still require cholesterol from their eukaryotic host to support their pathogenesis (Samanta et al., 2017; Silva et al., 2022). These data suggest a general requirement of cholesterol during intracellular bacterial infections, which provides strong evidence for the role of cholesterol in promoting the chlamydial infection.

One approach these pathogens use to acquire cholesterol is by manipulating the expression of genes required for cholesterol uptake, efflux, and storage. *Coxiella,*

Anaplasma, and *Chlamydia* upregulated expression of LDL receptors to increase intracellular cholesterol levels (Howe & Heinzen, 2006; Kalayoglu & Byrne, 1998; Xiong & Rikihisa, 2012). *Chlamydia* also downregulated the expression of ABC transporter A1 (ABCA1), which promotes cholesterol efflux out of the lysosome (Dong et al., 2014). *Chlamydia, Coxiella, Rickettsia,* and *Anaplasma* all increased expression of lipid droplet proteins (Samanta et al., 2017). This process may not only be to increase cholesterol levels, but also serve as a method of regulating an overproduction of cholesterol by promoting cholesterol storage in lipid droplets.

Enhancing cholesterol uptake and reducing cholesterol efflux likely increases the pool of available cholesterol that can be acquired by the bacteria. **I hypothesize** that the bacteria delicately regulate these intracellular cholesterol levels because having too much cholesterol could also negatively affect membrane structures. More specifically, cholesterol-rich microdomains on the vacuole membranes of *Chlamydia* promoted microtubule-dependent trafficking of the inclusion (Carabeo et al., 2003; Mital et al., 2010). As cholesterol is known to regulate interactions between endosomal trafficking and fusion, these microdomains may recruit other nutrients from endosomes to support the developing infection. These pathogens also likely require cholesterol to ensure the membrane integrity of the bacteria themselves, although the structural role of cholesterol for these intracellular bacterial membranes has not been tested.

In summary, bacteria-host cholesterol interactions can be observed at various stages of the intracellular infection from binding and internalization, establishment of the phagosome niche, and bacterial replication. It is not known whether the bacteria use the

host cholesterol directly or modify the cholesterol prior to incorporating it in their membranes. Additional studies to address the mechanisms facilitating these interactions would be beneficial to understand the role of cholesterol for these intracellular pathogens.

6.7 Cholesterol and the chlamydial infection

The block in cholesterol trafficking and the defects in the infection that I describe in my studies are purely correlative. Thus, we asked: 1. Is cholesterol important for the chlamydial infection? and 2. Does H89 mediate its inhibitory effects on inclusion growth and RB-to-EB conversion by disrupting cholesterol trafficking?

The importance of cholesterol during the chlamydial infection has been debated. A MEF cell line encoding a mutation in DHCR24, which synthesizes the final step of cholesterol synthesis by converting desmosterol to cholesterol, showed no defects in progeny production (Gilk et al., 2013). From these results, they concluded that cholesterol was not necessary or the chlamydial infection (Gilk et al., 2013). However, desmosterol alone may be sufficient for the infection. Desmosterol can be incorporated in membranes as a substitute for cholesterol to support cell survival and proliferation in J774 mouse macrophages (Rodríguez-Acebes et al., 2009). This is not surprising because the structures of cholesterol and desmosterol are nearly identical, with the only difference being a double bond at C24 (Esfahani et al., 1984). From these results, I speculate that cholesterol or it's nearly identical precursor, desmosterol, can be used interchangeably by the chlamydial infection.

Other studies have provided evidence to suggest that cholesterol is a nutrient required for the chlamydial infection. Carabeo *et al.* isolated chlamydiae to assess their lipid content. They found that approximately 6% of the total cellular cholesterol was associated with EBs (Carabeo et al., 2003). Additionally, they showed that cholesterol localized to the chlamydial inclusion and chlamydiae by immunofluorescence (Carabeo et al., 2003). Blocking cholesterol biosynthesis with the inhibitor mevastatin caused the *C. trachomatis* infection in hepatocytes to produce smaller inclusions and fewer chlamydiae (Bashmakov et al., 2010). Beatty *et al*. showed that blocking endolysosomal cholesterol trafficking with an NPC1 inhibitor caused smaller inclusions and defects in RB-to-EB conversion (Beatty, 2006, 2008). Together, this evidence supports that *Chlamydia* acquires cholesterol from its eukaryotic host and that cholesterol trafficking promotes the chlamydial infection.

The evidence from our cholesterol studies supports the work of Beatty *et al.* and Carabeo *et al.* Interestingly, we found that exogenous cholesterol addition partially rescued progeny production under H89-treatment conditions. This result was unexpected because we hypothesized that any additional cholesterol would also end up in the lysosome and would not aid the infection. However, NPC1-deficient cells, which also have lysosomal accumulation of cholesterol, can still traffic cholesterol from late endosomes to the Golgi and ER using Rab9 (Urano et al., 2008). Thus, transport of cholesterol through the alternative Rab9-mediated vesicular trafficking could explain why even under H89 conditions, exogenous cholesterol partially rescued progeny production. These data show that cholesterol supports RB-to-EB conversion.

It is possible that the infection prioritizes cholesterol incorporation into the chlamydiae themselves rather than the inclusion membrane. For example, we showed in Chapter 3 that even though BFA causes smaller inclusions, the number of chlamydial genomes was unaffected. **I hypothesize** that under BFA-treatment conditions, although sphingolipid and cholesterol transport is affected, chlamydial replication does not change because these lipids are preferentially used up by chlamydiae, which increases the likelihood of generating infectious EBs for a productive infection. To test this hypothesis, one could monitor the lipid contents of the chlamydial and inclusion membranes throughout the infection and determine whether cholesterol incorporation occurs more quickly in one membrane versus the other.

In Chapter 3, we also described 2 novel chlamydial inhibitors, MK2206 and Compound C (CompC), which disrupt cholesterol transport and metabolism, respectively. MK2206 blocks Akt activity, which promotes cholesterol trafficking through the Golgi (Capmany et al., 2019). Inhibiting Akt significantly decreased RB-to-EB conversion supporting the role of cholesterol in EB production. CompC blocks AMPK activity, which is a kinase that inhibits cholesterol synthesis (Capmany & Damiani, 2010). By blocking AMPK activity, CompC increases intracellular cholesterol levels. **I hypothesize** that CompC treatment increased chlamydial numbers because there was more cholesterol available for chlamydiae to use for replication. This means that cholesterol availability could be a limiting factor during chlamydial development, where less intracellular or extracellular cholesterol means less chlamydial replication. Our data

and published data support that *Chlamydia* subverts several different host trafficking pathways to acquire lipids such as cholesterol to promote chlamydial development.

Furthermore, our immunofluorescence microscopy analysis in Chapter 5 showed that H89 and NPC1 inhibitor-treatment caused lysosomal accumulation of cholesterol. Initially, our approach was to determine whether H89 caused cholesterol accumulation by blocking NPC1 function. We tested whether the H89-mediated defects on the infection would still be present after siRNA knockdown of NPC1. Unfortunately, we were unable to achieve sufficient NPC1 knockdown to achieve the cholesterol accumulation defect. Another challenge was in measuring whether NPC1 function was altered by H89 when H89 is a kinase inhibitor and NPC1 is not a kinase (Lochner & Moolman, 2006; Murray, 2008). We decided to identify possible kinase targets that are also associated with cholesterol transport.

Decreased sphingosine kinase (SphK1) activity is commonly associated with the Niemann-Pick lysosomal cholesterol storage disease caused by mutations in NPC1 or NPC2 (Newton et al., 2020), which prompted us to investigate whether H89 affected sphingosine kinase activity. Sphingosine kinases are highly conserved enzymes that catalyze the conversion of sphingosine to sphingosine-1-phosphate (S1P) (Cannavo et al., 2017). SphK activation promotes various cell functions including motility, proliferation, growth, cytoskeletal organization, survival, and stress response (Cannavo et al., 2017). We demonstrated that H89 decreased sphingosine kinase activity by an *in vitro* kinase assay and by measuring protein levels of M6PR, which is negatively regulated by sphingosine kinase(Newton et al., 2020). We then used the SphK1

inhibitor PF543 to test whether SphK1 was necessary for the chlamydial infection. Again, based on our comprehensive inhibitor analyses, PF543 phenocopied the H89-mediated defects including decreased inclusion size and a defect in progeny at the step of RB-to-EB conversion all without affecting host cell viability or inclusion formation. Although we identified SphK1 as a potential kinase target of H89, we wanted to further investigate why cholesterol accumulated in the lysosome.

SphK1 also promotes endocytic membrane trafficking and proper lysosomal acidification (Young et al., 2016). Not only did we show that PF543-treatment caused defects in lysosome acidification like known lysosomal acidification inhibitors, bafilomycin and chloroquine, but H89 caused this same defect. We propose a mechanism by which H89 inhibits lysosomal acidification by disrupting SphK1 activity and causes cholesterol accumulation. It is likely that because the cholesterol is sequestered within the lysosome, it is not as readily accessible to the chlamydial infection.

We showed in Chapter 5 that H89 and PF543 inhibit SphK1 activity, which correlates with cholesterol accumulation. Newton *et al.* showed that activation of SphK1 rescued cholesterol trafficking defects in NPC1-defficient cells (Newton et al., 2020). For future studies, **I propose** activating SphK1 activity under H89-treatment conditions to restore cholesterol trafficking. If cholesterol trafficking can be restored while treated with H89, and inclusion growth and progeny production are rescued, the data would support that H89 mediates its defects on the chlamydial infection through SphK1.

Unfortunately, the activator used by Newton *et al.* was custom-made and is not commercially available, so I instead suggest activating SphK1 with PMA treatment (Pitson et al., 2003) or by increasing cellular glucose levels (L. Wang et al., 2005). One possible outcome is that there is a rescue in inclusion growth and RB-to-EB conversion with SphK1 activation, which suggests that H89 inhibits the chlamydial infection through SphK1. Another possibility is that there is no rescue with SphK1 activation because H89 targets another kinase(s), which I began investigating with my inhibitor screen in Chapter 5. A partial rescue or no rescue is also possible if there is insufficient activation of SphK1. Immunofluorescence microscopy analyses of cholesterol localization within the cell by filipin staining would serve as an indirect method of testing for sufficient SphK1 activation. Regardless of the outcome, activating sphingosine kinase under H89 conditions would not only test whether H89 mediates the cholesterol accumulation phenotype through SphK1, but also tests whether restoring cholesterol trafficking is necessary for the chlamydial infection.

There could also be other explanations of how having nonfunctional SphK can be detrimental to the chlamydial infection. Perhaps as a consequence of defective SphK1 function, the accumulation of sphingosine becomes toxic for the intracellular infection, as is the case with *Neisseria gonorrhea* (Solger et al., 2020). Another speculation is that these increased sphingosine levels increase sphingomyelin production downstream, which we know is found in chlamydial membranes (Hackstadt et al., 1996; Muñoz et al., 2021). However, too much sphingomyelin may disrupt the membrane integrity of the chlamydiae, causing them to be not as infectious.

On another note, in Chapter 5 we showed that cholesterol transport defects correlated with defects in the chlamydial infection, but we did not measure cholesterol acquisition or acquisition of other lipids by chlamydiae. *Chlamydia* membranes also incorporate other host lipids including phosphatidylcholine and phosphatidylinositol (Hatch & McClarty, 1998). These lipids may also be affected by the inhibitor-induced trafficking defects, which could contribute to the defects in progeny production. To further support that lipids can promote RB-to-EB conversion, Nguyen *et al.* showed that blocking the synthesis of lipooligosaccharides caused "misshapen" IBs and EBs and decreased progeny production (Nguyen et al., 2011). For future experiments, **I suggest** isolating the inclusions and chlamydiae under H89 and PF543-treatment conditions to analyze their lipid content and verify whether cholesterol levels are altered. This membrane lipid analyses for *Chlamydia* infection is feasible because it has been previously optimized (Carabeo et al., 2003; Hatch & McClarty, 1998). By comparing differences in lipid content with these inhibitors, we can also test whether H89 and PF543 result in the same percentages in lipid membrane contents, which would provide further evidence that H89 mediates its inhibitory effects through the inhibition of SphK1.

An alternative hypothesis is that H89 alters cholesterol transport through NPC2. Using three small molecule inhibitors we showed that inhibition of NPC1 produced negative effects on inclusion growth and RB-to-EB conversion, but we have not evaluated the involvement of NPC2. Like NPC1, NPC2 is a cholesterol binding protein, although it is found in the lumen of the endosome rather than the endosomal membrane. Defects in either NPC1 or NPC2 result in lysosomal cholesterol

accumulation; however, defects in NPC1 are more widely studied because 95% of NPC-related disease in humans is caused by mutations in NPC1 (Patterson, 1993).

NPC2 has been shown to facilitate cholesterol transport independently of NPC1. NPC2 can directly interact with phospholipid lysobisphosphatidic acid to improve cholesterol trafficking, even in the absence of NPC1 (McCauliff et al., 2019). Also, the ABC transporter A1 (ABCA1) only depends on functional NPC2 to transport cholesterol out of the lysosome (Boadu et al., 2012) and ABCA1 has been observed at the inclusion membrane (Cox et al., 2012). Defects in NPC2 would decrease ABCA1 activity and promote cholesterol retention within the lysosomes (Yvan-Charvet et al., 2008), regardless of the presence of ABCA1 at the inclusion. If *Chlamydia* can only incorporate cholesterol into their membranes after it has left the lysosome, then **I predict** that NPC2 knockdown or inhibition would also cause defects in inclusion growth and progeny production. Since NPC2 participates in multiple methods of cholesterol transport, NPC2 knockdown might produce even stronger cholesterol trafficking defects than NPC1 mutants and a greater inhibition of the chlamydial infection.

A major question is how cholesterol from the lysosome gets incorporated into chlamydial and inclusion membranes. Early studies indicate that chlamydial infection evades lysosomal degradation, but to this day, the mechanism is not well understood (Escalante-Ochoa et al., 1998; Scidmore et al., 2003). Late endosome/lysosomal markers such as Rab7 and Lamp1/2 are not observed at the inclusion membrane (Heinzen et al., 1996; Rzomp et al., 2003; van Ooij et al., 1997), which is why it is unlikely that infection acquires cholesterol by fusing with lysosomes. Decreased

lysosomal activity could be an explanation for why the inclusion does not get degraded by lysosomes, but lysosomal activity in the eukaryotic host was normal during the chlamydial infection (Todd & Storz, 1975). Rather, **I hypothesize** that nutrients must first be trafficked out of the lysosome before they can be acquired by chlamydiae. My rationale is that other amino acid nutrients are exported out of the lysosomes and used by the chlamydial infection (Ouellette et al., 2011). Once cholesterol has left the lysosome, it is mobilized to the plasma membrane by the GTPase Rab8 (Kanerva et al., 2013) and then migrates to the ER with the help of phosphatidylserine (PS) (Trinh et al., 2020). Rab8 localization to the chlamydial inclusion has not been tested and would support the **hypothesis** that the infection acquires cholesterol that has recently exited the lysosome. Another possibility is that rather than intercepting cholesterol immediately leaving the lysosome, *Chlamydia* blocks the transport of cholesterol from the plasma membrane to the ER. As PS aids in cholesterol transport from the plasma membrane to the ER, and we know that there are close ER-inclusion membrane interactions, **I predict** that PS can be found at the inclusion membrane. To test these hypotheses, I would visualize the localization of Rab8 and PS by immunofluorescence microscopy.

If cholesterol transport from lysosomes promotes the chlamydial infection, **I hypothesize** that restoring cholesterol trafficking will rescue the H89, PF543, and NPC1 inhibitor-mediated defects on inclusion growth and progeny production. Cyclodextrin (CD) has been shown to reverse U18666A-mediated cholesterol accumulation in neurons, although it is unclear how CD accomplishes its beneficial effects (Barthelemy et al., 2021). **I propose** treating the chlamydial infection with and without cyclodextrin in

the presence of the cholesterol accumulation-inducing inhibitors. These experiments will test whether cholesterol transport is necessary for the chlamydial infection. Cholesterol accumulation is also known to decrease TRPML1 ion channel function, which drives lysosomal biogenesis, acidification, trafficking, degradation, and lipid handling (Krogsaeter et al., 2022). Evidence suggests that TRPML1 promotes lysosomal acidification by exchanging luminal cations (Na+, Ca2+) for protons, which enhances the v-type ATPase lysosomal proton pump (Krogsaeter et al., 2022). Another option to test our hypothesis would be to activate TRPML1 with the synthetic ligand molecule, temsirolimus, under our inhibitor conditions (Gan et al., 2022). A benefit of studying lysosomal cholesterol trafficking is that there are many approaches to block or promote transport, which can be studied in the context of a *Chlamydia* infection.

6.8 Significance of our inhibitor studies

For the first time, we provide a standard method of evaluating the effects of inhibitors on the infection that circumvents the current challenges of analyses. Additionally, I summarized an extensive comparison of the effects of chlamydial inhibitors for targets in eukaryotes and chlamydiae in Tables 1.1 and 1.2, which had not been done previously. I generated the comprehensive tables organized by targets, and sub-categorized based on the inhibitor function. My goal is that this will aid others in identifying common and effective anti-chlamydial targets and provide an accurate description of the step(s) in the developmental cycle that are affected.

Through our methodologies, we identified novel chlamydial inhibitors, H89, MK2206, Compound C, and PF543, which all suggest the role of cholesterol in promoting the chlamydial infection. The experiments were all conducted *in vitro*, but we provide strong evidence for the role of cholesterol in the chlamydial infection, which can now be addressed in *in vivo* models of infection. There are also other *in vivo* considerations based on our studies such as what does the progression of a chlamydial infection look like in patients with a cholesterol storage disease. For example, **I predict** that Niemann-Pick patients with pre-disposed cholesterol trafficking defects may have a milder chlamydial infection because of limited cholesterol availability. Overall, these studies can aid in our understanding of the pathways that support the chlamydial infection and our hope is that they can help lead to new antibiotic approaches or aid in *Chlamydia* vaccine development.

REFERENCES

Abdelsayed, S., Ha Duong, N. T., Hai, J., Hémadi, M., El Hage Chahine, J. M., Verbeke, P., & Serradji, N. (2014). Design and synthesis of 3-isoxazolidone derivatives as new Chlamydia trachomatis inhibitors. *Bioorganic & Medicinal Chemistry Letters*, *24*(16), 3854–3860. https://doi.org/10.1016/j.bmcl.2014.06.056

Ahmadi, M. H., Mirsalehian, A., Sadighi Gilani, M. A., Bahador, A., & Afraz, K. (2018). Association of asymptomatic Chlamydia trachomatis infection with male infertility and the effect of antibiotic therapy in improvement of semen quality in infected infertile men. *Andrologia*. https://doi.org/10.1111/and.12944

Al-Younes, H. M., Rudel, T., Brinkmann, V., Szczepek, A. J., & Meyer, T. F. (2001). Low iron availability modulates the course of Chlamydia pneumoniae infection. *Cellular Microbiology*, *3*(6), 427–437. https://doi.org/10.1046/j.1462-5822.2001.00125.x

Aridor, M., & Balch, W. E. (2000). Kinase Signaling Initiates Coat Complex II (COPII) Recruitment and Export from the Mammalian Endoplasmic Reticulum. *Journal of Biological Chemistry*, *275*(46), 35673–35676. https://doi.org/10.1074/jbc.C000449200

Ashfaq, U. A., Javed, T., Rehman, S., Nawaz, Z., & Riazuddin, S. (2011). Lysosomotropic agents as HCV entry inhibitors. *Virology Journal*, *8*(1), 163. https://doi.org/10.1186/1743-422X-8-163

Bae, Y.-U., Kim, B.-K., Park, J.-W., Seu, Y.-B., & Doh, K.-O. (2012). Endocytic Pathway and Resistance to Cholesterol Depletion of Cholesterol Derived Cationic Lipids

for Gene Delivery. *Molecular Pharmaceutics*, *9*(12), 3579–3585. https://doi.org/10.1021/mp300458h

Bailey, L., Gylfe, Å., Sundin, C., Muschiol, S., Elofsson, M., Nordström, P., Henriques-Normark, B., Lugert, R., Waldenström, A., Wolf-Watz, H., & Bergström, S. (2007). Small molecule inhibitors of type III secretion in Yersinia block the Chlamydia pneumoniae infection cycle. *FEBS Letters*, *581*(4), 587–595. https://doi.org/10.1016/j.febslet.2007.01.013

Bain, J., Plater, L., Elliott, M., Shpiro, N., Hastie, C. J., Mclauchlan, H., Klevernic, I., Arthur, J. S. C., Alessi, D. R., & Cohen, P. (2007). The selectivity of protein kinase inhibitors: A further update. *Biochemical Journal*, *408*(3), 297–315. https://doi.org/10.1042/BJ20070797

Banerjee, A., & Nelson, D. E. (2021). The growing repertoire of genetic tools for dissecting chlamydial pathogenesis. *Pathogens and Disease*, *79*(5), ftab025. https://doi.org/10.1093/femspd/ftab025

Bao, X., Gylfe, Å., Sturdevant, G. L., Gong, Z., Xu, S., Caldwell, H. D., Elofsson, M., & Fan, H. (2014). Benzylidene Acylhydrazides Inhibit Chlamydial Growth in a Type III Secretion- and Iron Chelation-Independent Manner. *Journal of Bacteriology*. https://doi.org/10.1128/JB.01677-14

Barthelemy, A., Demais, V., Stancu, I.-C., Vasile, E., Houben, T., Reber, M., Pallottini, V., Perraut, M., Reibel, S., & Pfrieger, F. W. (2021). Glial contribution to cyclodextrin-mediated reversal of cholesterol accumulation in murine NPC1-

deficient neurons in vivo. *Neurobiology of Disease*, *158*, 105469. https://doi.org/10.1016/j.nbd.2021.105469

Bashmakov, Y. K., Zigangirova, N. A., Pashko, Y. P., Kapotina, L. N., & Petyaev, I. M. (2010). Chlamydia trachomatis growth inhibition and restoration of LDL-receptor level in HepG2 cells treated with mevastatin. *Comparative Hepatology*, *9*, 3. https://doi.org/10.1186/1476-5926-9-3

Bastidas, R. J., & Valdivia, R. H. (2016). Emancipating Chlamydia: Advances in the Genetic Manipulation of a Recalcitrant Intracellular Pathogen. *Microbiology and Molecular Biology Reviews : MMBR*, *80*(2), 411–427. https://doi.org/10.1128/MMBR.00071-15

Beatty, W. L. (2006). Trafficking from CD63-positive late endocytic multivesicular bodies is essential for intracellular development of Chlamydia trachomatis. *Journal of Cell Science*, *119*(2), 350–359. https://doi.org/10.1242/jcs.02733

Beatty, W. L. (2008). Late Endocytic Multivesicular Bodies Intersect the Chlamydial Inclusion in the Absence of CD63. *Infection and Immunity*, *76*(7), 2872–2881. https://doi.org/10.1128/IAI.00129-08

Beatty, W. L., Morrison, R. P., & Byrne, G. I. (1994). Persistent chlamydiae: From cell culture to a paradigm for chlamydial pathogenesis. *Microbiological Reviews*, *58*(4), 686–699. https://doi.org/10.1128/mr.58.4.686-699.1994

Becker, Y. (1996). Chlamydia. In S. Baron (Ed.), *Medical Microbiology* (4th ed.). University of Texas Medical Branch at Galveston. http://www.ncbi.nlm.nih.gov/books/NBK8091/

Belland, R. J., Zhong, G., Crane, D. D., Hogan, D., Sturdevant, D., Sharma, J., Beatty, W. L., & Caldwell, H. D. (2003). Genomic transcriptional profiling of the developmental cycle of Chlamydia trachomatis. *Proceedings of the National Academy of Sciences of the United States of America*, *100*(14), 8478–8483. https://doi.org/10.1073/pnas.1331135100

Black, C. M., Tharpe, J. A., & Russell, H. (1992). Distinguishing Chlamydia species by restriction analysis of the major outer membrane protein gene. *Molecular and Cellular Probes*, *6*(5), 395–400. https://doi.org/10.1016/0890-8508(92)90033-t

Boadu, E., Nelson, R. C., & Francis, G. A. (2012). ABCA1-dependent mobilization of lysosomal cholesterol requires functional Niemann–Pick C2 but not Niemann–Pick C1 protein. *Biochimica et Biophysica Acta (BBA) - Molecular and Cell Biology of Lipids*, *1821*(3), 396–404. https://doi.org/10.1016/j.bbalip.2011.11.013

Brothwell, J. A., Brockett, M., Banerjee, A., Stein, B. D., Nelson, D. E., & Liechti, G. W. (2021). Genome Copy Number Regulates Inclusion Expansion, Septation, and Infectious Developmental Form Conversion in Chlamydia trachomatis. *Journal of Bacteriology*, *203*(6), e00630-20. https://doi.org/10.1128/JB.00630-20

Brothwell, J. A., Muramatsu, M. K., Toh, E., Rockey, D. D., Putman, T. E., Barta, M. L., Hefty, P. S., Suchland, R. J., & Nelson, D. E. (2016). Interrogating Genes That Mediate Chlamydia trachomatis Survival in Cell Culture Using Conditional Mutants and Recombination. *Journal of Bacteriology*, *198*(15), 2131–2139. https://doi.org/10.1128/JB.00161-16

Brown, A. J., & Sharpe, L. J. (2016). Chapter 11—Cholesterol Synthesis. In N. D. Ridgway & R. S. McLeod (Eds.), *Biochemistry of Lipids, Lipoproteins and Membranes (Sixth Edition)* (pp. 327–358). Elsevier. https://doi.org/10.1016/B978-0-444-63438-2.00011-0

Brumell, J. H., & Scidmore, M. A. (2007). Manipulation of Rab GTPase Function by Intracellular Bacterial Pathogens. *Microbiology and Molecular Biology Reviews : MMBR*, *71*(4), 636–652. https://doi.org/10.1128/MMBR.00023-07

Bugalhão, J. N., & Mota, L. J. (2019). The multiple functions of the numerous Chlamydia trachomatis secreted proteins: The tip of the iceberg. *Microbial Cell*, *6*(9), 414–449. https://doi.org/10.15698/mic2019.09.691

Cannavo, A., Liccardo, D., Komici, K., Corbi, G., de Lucia, C., Femminella, G. D., Elia, A., Bencivenga, L., Ferrara, N., Koch, W. J., Paolocci, N., & Rengo, G. (2017). Sphingosine Kinases and Sphingosine 1-Phosphate Receptors: Signaling and Actions in the Cardiovascular System. *Frontiers in Pharmacology*, *8*. https://www.frontiersin.org/article/10.3389/fphar.2017.00556

Capmany, A., & Damiani, M. T. (2010). Chlamydia trachomatis Intercepts Golgi-Derived Sphingolipids through a Rab14-Mediated Transport Required for Bacterial Development and Replication. *PLoS ONE*, *5*(11), e14084. https://doi.org/10.1371/journal.pone.0014084

Capmany, A., Gambarte Tudela, J., Alonso Bivou, M., & Damiani, M. T. (2019). Akt/AS160 Signaling Pathway Inhibition Impairs Infection by Decreasing Rab14-

Controlled Sphingolipids Delivery to Chlamydial Inclusions. *Frontiers in Microbiology*, *10*. https://doi.org/10.3389/fmicb.2019.00666

Capra, M., Nuciforo, P. G., Confalonieri, S., Quarto, M., Bianchi, M., Nebuloni, M., Boldorini, R., Pallotti, F., Viale, G., Gishizky, M. L., Draetta, G. F., & Di Fiore, P. P. (2006). Frequent alterations in the expression of serine/threonine kinases in human cancers. *Cancer Research*, *66*(16), 8147–8154. https://doi.org/10.1158/0008-5472.CAN-05-3489

Carabeo, R. A., Grieshaber, S. S., Fischer, E., & Hackstadt, T. (2002). Chlamydia trachomatis induces remodeling of the actin cytoskeleton during attachment and entry into HeLa cells. *Infection and Immunity*, *70*(7), 3793–3803. https://doi.org/10.1128/iai.70.7.3793-3803.2002

Carabeo, R. A., Mead, D. J., & Hackstadt, T. (2003). Golgi-dependent transport of cholesterol to the Chlamydia trachomatis inclusion. *Proceedings of the National Academy of Sciences*, *100*(11), 6771–6776. https://doi.org/10.1073/pnas.1131289100

CDC – Chlamydia Treatment. (2021, June 30). https://www.cdc.gov/std/chlamydia/treatment.htm

Center for Disease Control and Prevention. (2021, November 5). *Hygiene-related Diseases | Hygiene-related Diseases | Hygiene | Healthy Water | CDC*. https://www.cdc.gov/healthywater/hygiene/disease/trachoma.html

Centers for Disease Control and Prevention. (2019). Annual Tables of Infectious Disease Data. *National Notifiable Diseases Surveillance System, 2019 Annual*

Tables of Infectious Disease Data. Atlanta, GA. CDC Division of Health Informatics and Surveillance, 2021., https://www.cdc.gov/nndss/data-statistics/infectious-tables/index.html.

Centers for Disease Control and Prevention CDC – Chlamydia Statistics. (2019, October 3). https://www.cdc.gov/std/chlamydia/stats.htm

Chiarelli, T. J., Grieshaber, N. A., Omsland, A., Remien, C. H., & Grieshaber, S. S. (2020). Single-Inclusion Kinetics of Chlamydia trachomatis Development. *MSystems*. https://doi.org/10.1128/mSystems.00689-20

Chijiwa, T., Mishima, A., Hagiwara, M., Sano, M., Hayashi, K., Inoue, T., Naito, K., Toshioka, T., & Hidaka, H. (1990). Inhibition of forskolin-induced neurite outgrowth and protein phosphorylation by a newly synthesized selective inhibitor of cyclic AMP-dependent protein kinase, N-[2-(p-bromocinnamylamino)ethyl]-5-isoquinolinesulfonamide (H-89), of PC12D pheochromocytoma cells. *The Journal of Biological Chemistry*, *265*(9), 5267–5272.

Cingolani, G., McCauley, M., Lobley, A., Bryer, A. J., Wesolowski, J., Greco, D. L., Lokareddy, R. K., Ronzone, E., Perilla, J. R., & Paumet, F. (2019). Structural basis for the homotypic fusion of chlamydial inclusions by the SNARE-like protein IncA. *Nature Communications*, *10*(1), 2747. https://doi.org/10.1038/s41467-019-10806-9

Claywell, J. E., Matschke, L. M., & Fisher, D. J. (2016). The Impact of Protein Phosphorylation on Chlamydial Physiology. *Frontiers in Cellular and Infection Microbiology*, *6*. https://doi.org/10.3389/fcimb.2016.00197

Claywell, J. E., Matschke, L. M., Plunkett, K. N., & Fisher, D. J. (2018). Inhibition of the Protein Phosphatase CppA Alters Development of Chlamydia trachomatis. *Journal of Bacteriology*, *200*(19). https://doi.org/10.1128/JB.00419-18

Cocchiaro, J. L., Kumar, Y., Fischer, E. R., Hackstadt, T., & Valdivia, R. H. (2008). Cytoplasmic lipid droplets are translocated into the lumen of the Chlamydia trachomatis parasitophorous vacuole. *Proceedings of the National Academy of Sciences of the United States of America*, *105*(27), 9379–9384. https://doi.org/10.1073/pnas.0712241105

Cockburn, C. L., Green, R. S., Damle, S. R., Martin, R. K., Ghahrai, N. N., Colonne, P. M., Fullerton, M. S., Conrad, D. H., Chalfant, C. E., Voth, D. E., Rucks, E. A., Gilk, S. D., & Carlyon, J. A. (2019). Functional inhibition of acid sphingomyelinase disrupts infection by intracellular bacterial pathogens. *Life Science Alliance*, *2*(2). https://doi.org/10.26508/lsa.201800292

Cortes, C., Rzomp, K. A., Tvinnereim, A., Scidmore, M. A., & Wizel, B. (2007). Chlamydia pneumoniae Inclusion Membrane Protein Cpn0585 Interacts with Multiple Rab GTPases. *Infection and Immunity*, *75*(12), 5586–5596. https://doi.org/10.1128/IAI.01020-07

Cortina, M. E., Ende, R. J., Bishop, R. C., Bayne, C., & Derré, I. (2019). Chlamydia trachomatis and Chlamydia muridarum spectinomycin resistant vectors and a transcriptional fluorescent reporter to monitor conversion from replicative to infectious bacteria. *PloS One*, *14*(6), e0217753. https://doi.org/10.1371/journal.pone.0217753

Cotlin, L. F., Siddiqui, M. A., Simpson, F., & Collawn, J. F. (1999). Casein Kinase II Activity Is Required for Transferrin Receptor Endocytosis*. *Journal of Biological Chemistry*, *274*(43), 30550–30556. https://doi.org/10.1074/jbc.274.43.30550

Cox, J. V., Abdelrahman, Y. M., Peters, J., Naher, N., & Belland, R. J. (2016). Chlamydia trachomatis utilizes the mammalian CLA1 lipid transporter to acquire host phosphatidylcholine essential for growth. *Cellular Microbiology*, *18*(3), 305–318. https://doi.org/10.1111/cmi.12523

Cox, J. V., Naher, N., Abdelrahman, Y. M., & Belland, R. J. (2012). Host HDL biogenesis machinery is recruited to the inclusion of Chlamydia trachomatis-infected cells and regulates chlamydial growth. *Cellular Microbiology*, *14*(10), 1497–1512. https://doi.org/10.1111/j.1462-5822.2012.01823.x

Davies, S. P., Reddy, H., Caivano, M., & Cohen, P. (2000). Specificity and mechanism of action of some commonly used protein kinase inhibitors. *Biochemical Journal*, *351*(1), 95–105. https://doi.org/10.1042/bj3510095

De Clercq, E., Kalmar, I., & Vanrompay, D. (2013). Animal Models for Studying Female Genital Tract Infection with Chlamydia trachomatis. *Infection and Immunity*, *81*(9), 3060–3067. https://doi.org/10.1128/IAI.00357-13

Delevoye, C., Nilges, M., Dehoux, P., Paumet, F., Perrinet, S., Dautry-Varsat, A., & Subtil, A. (2008). SNARE Protein Mimicry by an Intracellular Bacterium. *PLOS Pathogens*, *4*(3), e1000022. https://doi.org/10.1371/journal.ppat.1000022

Derré, I. (2015). Chlamydiae interaction with the endoplasmic reticulum: Contact, function and consequences. *Cellular Microbiology*, *17*(7), 959–966. https://doi.org/10.1111/cmi.12455

Derré, I. (2017). Hijacking of Membrane Contact Sites by Intracellular Bacterial Pathogens. *Advances in Experimental Medicine and Biology*, *997*, 211–223. https://doi.org/10.1007/978-981-10-4567-7_16

Derré, I., Pypaert, M., Dautry-Varsat, A., & Agaisse, H. (2007). RNAi Screen in Drosophila Cells Reveals the Involvement of the Tom Complex in Chlamydia Infection. *PLOS Pathogens*, *3*(10), e155. https://doi.org/10.1371/journal.ppat.0030155

Derré, I., Swiss, R., & Agaisse, H. (2011). The Lipid Transfer Protein CERT Interacts with the Chlamydia Inclusion Protein IncD and Participates to ER-Chlamydia Inclusion Membrane Contact Sites. *PLOS Pathogens*, *7*(6), e1002092. https://doi.org/10.1371/journal.ppat.1002092

Dickinson, M. S., Anderson, L. N., Webb-Robertson, B.-J. M., Hansen, J. R., Smith, R. D., Wright, A. T., & Hybiske, K. (2019). Proximity-dependent proteomics of the Chlamydia trachomatis inclusion membrane reveals functional interactions with endoplasmic reticulum exit sites. *PLoS Pathogens*, *15*(4). https://doi.org/10.1371/journal.ppat.1007698

Dietschy, J. M. (1984). Regulation of cholesterol metabolism in man and in other species. *Klinische Wochenschrift*, *62*(8), 338–345. https://doi.org/10.1007/BF01716251

Dong, F., Mo, Z., Eid, W., Courtney, K. C., & Zha, X. (2014). Akt Inhibition Promotes ABCA1-Mediated Cholesterol Efflux to ApoA-I through Suppressing mTORC1. *PLOS ONE*, *9*(11), e113789. https://doi.org/10.1371/journal.pone.0113789

Elwell, C. A., & Engel, J. N. (2012). Lipid Acquisition by Intracellular Chlamydiae. *Cellular Microbiology*, *14*(7), 1010–1018. https://doi.org/10.1111/j.1462-5822.2012.01794.x

Elwell, C. A., Jiang, S., Kim, J. H., Lee, A., Wittmann, T., Hanada, K., Melancon, P., & Engel, J. N. (2011). Chlamydia trachomatis Co-opts GBF1 and CERT to Acquire Host Sphingomyelin for Distinct Roles during Intracellular Development. *PLoS Pathogens*, *7*(9). https://doi.org/10.1371/journal.ppat.1002198

Elwell, C., Mirrashidi, K., & Engel, J. (2016). Chlamydia cell biology and pathogenesis. *Nature Reviews Microbiology*, *14*(6), 385–400. https://doi.org/10.1038/nrmicro.2016.30

Engström, P., Bergström, M., Alfaro, A. C., Syam Krishnan, K., Bahnan, W., Almqvist, F., & Bergström, S. (2015). Expansion of the Chlamydia trachomatis inclusion does not require bacterial replication. *International Journal of Medical Microbiology*, *305*(3), 378–382. https://doi.org/10.1016/j.ijmm.2015.02.007

Engström, P., Krishnan, K. S., Ngyuen, B. D., Chorell, E., Normark, J., Silver, J., Bastidas, R. J., Welch, M. D., Hultgren, S. J., Wolf-Watz, H., Valdivia, R. H., Almqvist, F., & Bergström, S. (2014). A 2-Pyridone-Amide Inhibitor Targets the Glucose Metabolism Pathway of Chlamydia trachomatis. *MBio*, *6*(1). https://doi.org/10.1128/mBio.02304-14

Escalante-Ochoa, C., Ducatelle, R., & Haesebrouck, F. (1998). The intracellular life of Chlamydia psittaci: How do the bacteria interact with the host cell? *FEMS Microbiology Reviews*, *22*(2), 65–78. https://doi.org/10.1111/j.1574-6976.1998.tb00361.x

Esfahani, M., Scerbo, L., & Devlin, T. M. (1984). A requirement for cholesterol and its structural features for a human macrophage-like cell line. *Journal of Cellular Biochemistry*, *25*(2), 87–97. https://doi.org/10.1002/jcb.240250204

Farley, T. A., Cohen, D. A., & Elkins, W. (2003). Asymptomatic sexually transmitted diseases: The case for screening. *Preventive Medicine*, *36*(4), 502–509. https://doi.org/10.1016/s0091-7435(02)00058-0

Fedele, A. O., & Proud, C. G. (2020). Chloroquine and bafilomycin A mimic lysosomal storage disorders and impair mTORC1 signalling. *Bioscience Reports*, *40*(4), BSR20200905. https://doi.org/10.1042/BSR20200905

Gallegos, K. M., Taylor, C. R., Rabulinski, D. J., Del Toro, R., Girgis, D. E., Jourha, D., Tiwari, V., Desai, U. R., & Ramsey, K. H. (2019). A Synthetic, Small, Sulfated Agent Is a Promising Inhibitor of Chlamydia spp. Infection in vivo. *Frontiers in Microbiology*, *9*. https://www.frontiersin.org/article/10.3389/fmicb.2018.03269

Gan, N., Han, Y., Zeng, W., Wang, Y., Xue, J., & Jiang, Y. (2022). Structural mechanism of allosteric activation of TRPML1 by PI(3,5)P2 and rapamycin. *Proceedings of the National Academy of Sciences*, *119*(7), e2120404119. https://doi.org/10.1073/pnas.2120404119

Geisler, W. M., Suchland, R. J., Rockey, D. D., & Stamm, W. E. (2001). Epidemiology and clinical manifestations of unique Chlamydia trachomatis isolates that occupy nonfusogenic inclusions. *The Journal of Infectious Diseases*, *184*(7), 879–884. https://doi.org/10.1086/323340

Gilk, S. D., Cockrell, D. C., Luterbach, C., Hansen, B., Knodler, L. A., Ibarra, J. A., Steele-Mortimer, O., & Heinzen, R. A. (2013). Bacterial Colonization of Host Cells in the Absence of Cholesterol. *PLOS Pathogens*, *9*(1), e1003107. https://doi.org/10.1371/journal.ppat.1003107

Gloeckl, S., Ong, V. A., Patel, P., Tyndall, J. D. A., Timms, P., Beagley, K. W., Allan, J. A., Armitage, C. W., Turnbull, L., Whitchurch, C. B., Merdanovic, M., Ehrmann, M., Powers, J. C., Oleksyszyn, J., Verdoes, M., Bogyo, M., & Huston, W. M. (2013). Identification of a serine protease inhibitor which causes inclusion vacuole reduction and is lethal to Chlamydia trachomatis. *Molecular Microbiology*, *89*(4), 676–689. https://doi.org/10.1111/mmi.12306

Goldstein, J. L., & Brown, M. S. (2015). A Century of Cholesterol and Coronaries: From Plaques to Genes to Statins. *Cell*, *161*(1), 161–172. https://doi.org/10.1016/j.cell.2015.01.036

Gordon, D. E., Bond, L. M., Sahlender, D. A., & Peden, A. A. (2010). A targeted siRNA screen to identify SNAREs required for constitutive secretion in mammalian cells. *Traffic (Copenhagen, Denmark)*, *11*(9), 1191–1204. https://doi.org/10.1111/j.1600-0854.2010.01087.x

Goulart, A. C. X., Farnezi, H. C. M., França, J. P. B. M., Santos, A. D., Ramos, M. G., & Penna, M. L. F. (2020). HIV, HPV and Chlamydia trachomatis: Impacts on male fertility. *JBRA Assisted Reproduction*, *24*(4), 492–497. https://doi.org/10.5935/1518-0557.20200020

Grieshaber, N. A., Sager, J. B., Dooley, C. A., Hayes, S. F., & Hackstadt, T. (2006). Regulation of the Chlamydia trachomatis Histone H1-Like Protein Hc2 Is IspE Dependent and IhtA Independent. *Journal of Bacteriology*, *188*(14), 5289–5292. https://doi.org/10.1128/JB.00526-06

Grishin, A. V., Luyksaar, S. I., Kapotina, L. N., Kirsanov, D. D., Zayakin, E. S., Karyagina, A. S., & Zigangirova, N. A. (2018). Identification of chlamydial T3SS inhibitors through virtual screening against T3SS ATPase. *Chemical Biology & Drug Design*, *91*(3), 717–727. https://doi.org/10.1111/cbdd.13130

Günyeli, İ., Abike, F., Dünder, İ., Aslan, C., Tapısız, Ö. L., Temizkan, O., Payaslı, A., & Erdemoğlu, E. (2011). Chlamydia, Mycoplasma and Ureaplasma infections in infertile couples and effects of these infections on fertility. *Archives of Gynecology and Obstetrics*, *283*(2), 379–385. https://doi.org/10.1007/s00404-010-1726-4

Hackstadt, T., Fischer, E. R., Scidmore, M. A., Rockey, D. D., & Heinzen, R. A. (1997). Origins and functions of the chlamydial inclusion. *Trends in Microbiology*, *5*(7), 288–293. https://doi.org/10.1016/S0966-842X(97)01061-5

Hackstadt, T., Rockey, D. D., Heinzen, R. A., & Scidmore, M. A. (1996). Chlamydia trachomatis interrupts an exocytic pathway to acquire endogenously synthesized

sphingomyelin in transit from the Golgi apparatus to the plasma membrane. *The EMBO Journal*, *15*(5), 964–977.

Hackstadt, T., Scidmore, M. A., & Rockey, D. D. (1995). Lipid metabolism in Chlamydia trachomatis-infected cells: Directed trafficking of Golgi-derived sphingolipids to the chlamydial inclusion. *Proceedings of the National Academy of Sciences of the United States of America*, *92*(11), 4877–4881.

Hamid, P. H., Hirzmann, J., Kerner, K., Gimpl, G., Lochnit, G., Hermosilla, C. R., & Taubert, A. (2015). Eimeria bovis infection modulates endothelial host cell cholesterol metabolism for successful replication. *Veterinary Research*, *46*(1), 100. https://doi.org/10.1186/s13567-015-0230-z

Hanada, K., Kumagai, K., Tomishige, N., & Yamaji, T. (2009). CERT-mediated trafficking of ceramide. *Biochimica Et Biophysica Acta*, *1791*(7), 684–691. https://doi.org/10.1016/j.bbalip.2009.01.006

Hanada, K., Kumagai, K., Yasuda, S., Miura, Y., Kawano, M., Fukasawa, M., & Nishijima, M. (2003). Molecular machinery for non-vesicular trafficking of ceramide. *Nature*, *426*(6968), 803–809. https://doi.org/10.1038/nature02188

Hasegawa, A., Sogo, L. F., Tan, M., & Sütterlin, C. (2009). Host Complement Regulatory Protein CD59 Is Transported to the Chlamydial Inclusion by a Golgi Apparatus-Independent Pathway. *Infection and Immunity*, *77*(4), 1285–1292. https://doi.org/10.1128/IAI.01062-08

Hatch, G. M., & McClarty, G. (1998). Phospholipid Composition of Purified Chlamydia trachomatis Mimics That of the Eucaryotic Host Cell. *Infection and Immunity*, *66*(8), 3727–3735.

Heinzen, R. A., Scidmore, M. A., Rockey, D. D., & Hackstadt, T. (1996). Differential interaction with endocytic and exocytic pathways distinguish parasitophorous vacuoles of Coxiella burnetii and Chlamydia trachomatis. *Infection and Immunity*, *64*(3), 796–809.

Henrichfreise, B., Schiefer, A., Schneider, T., Nzukou, E., Poellinger, C., Hoffmann, T.-J., Johnston, K. L., Moelleken, K., Wiedemann, I., Pfarr, K., Hoerauf, A., & Sahl, H. G. (2009). Functional conservation of the lipid II biosynthesis pathway in the cell wall-less bacteria Chlamydia and Wolbachia: Why is lipid II needed? *Molecular Microbiology*, *73*(5), 913–923. https://doi.org/10.1111/j.1365-2958.2009.06815.x

Heuer, D., Lipinski, A. R., Machuy, N., Karlas, A., Wehrens, A., Siedler, F., Brinkmann, V., & Meyer, T. F. (2009). Chlamydia causes fragmentation of the Golgi compartment to ensure reproduction. *Nature*, *457*(7230), 731–735. https://doi.org/10.1038/nature07578

Hoenderboom, B. M., van Bergen, J. E. A. M., Dukers-Muijrers, N. H. T. M., Götz, H. M., Hoebe, C. J. P. A., de Vries, H. J. C., van den Broek, I. V. F., de Vries, F., Land, J. A., van der Sande, M. A. B., Morré, S. A., & van Benthem, B. H. B. (2020). Pregnancies and Time to Pregnancy in Women With and Without a Previous

Chlamydia trachomatis Infection. *Sexually Transmitted Diseases*, *47*(11), 739–747. https://doi.org/10.1097/OLQ.0000000000001247

Hogan, R. J., Mathews, S. A., Mukhopadhyay, S., Summersgill, J. T., & Timms, P. (2004). Chlamydial Persistence: Beyond the Biphasic Paradigm. *Infection and Immunity*, *72*(4), 1843–1855. https://doi.org/10.1128/IAI.72.4.1843-1855.2004

Homma, Y., Hiragi, S., & Fukuda, M. (2021). Rab family of small GTPases: An updated view on their regulation and functions. *The FEBS Journal*, *288*(1), 36–55. https://doi.org/10.1111/febs.15453

Horn, A., & Jaiswal, J. K. (2019). Structural and signaling role of lipids in plasma membrane repair. *Current Topics in Membranes*, *84*, 67–98. https://doi.org/10.1016/bs.ctm.2019.07.001

Hosseinzadeh, S., Eley, A., & Pacey, A. A. (2004). Semen quality of men with asymptomatic chlamydial infection. *Journal of Andrology*, *25*(1), 104–109. https://doi.org/10.1002/j.1939-4640.2004.tb02764.x

Howe, D., & Heinzen, R. A. (2006). Coxiella burnetii inhabits a cholesterol-rich vacuole and influences cellular cholesterol metabolism. *Cellular Microbiology*, *8*(3), 496–507. https://doi.org/10.1111/j.1462-5822.2005.00641.x

Hua, Z., Frohlich, K. M., Zhang, Y., Feng, X., Zhang, J., & Shen, L. (2015). Andrographolide inhibits intracellular Chlamydia trachomatis multiplication and reduces secretion of proinflammatory mediators produced by human epithelial cells. *Pathogens and Disease*, *73*(1), 1–11. https://doi.org/10.1093/femspd/ftu022

Huitema, K., van den Dikkenberg, J., Brouwers, J. F. H. M., & Holthuis, J. C. M. (2004). Identification of a family of animal sphingomyelin synthases. *The EMBO Journal*, *23*(1), 33–44. https://doi.org/10.1038/sj.emboj.7600034

Hybiske, K., & Stephens, R. S. (2007). Mechanisms of host cell exit by the intracellular bacterium Chlamydia. *Proceedings of the National Academy of Sciences*, *104*(27), 11430–11435. https://doi.org/10.1073/pnas.0703218104

Inman, R. D., & Chiu, B. (2012). Nafamostat mesylate, a serine protease inhibitor, demonstrates novel antimicrobial properties and effectiveness in Chlamydia-induced arthritis. *Arthritis Research & Therapy*, *14*(3), R150. https://doi.org/10.1186/ar3886

Jamora, C., Yamanouye, N., Van Lint, J., Laudenslager, J., Vandenheede, J. R., Faulkner, D. J., & Malhotra, V. (1999). Gβγ-Mediated Regulation of Golgi Organization Is through the Direct Activation of Protein Kinase D. *Cell*, *98*(1), 59–68. https://doi.org/10.1016/S0092-8674(00)80606-6

Johnson, K. A., Lee, J. K., Chen, A. L., Tan, M., & Sütterlin, C. (2015). Induction and inhibition of CPAF activity during analysis of Chlamydia-infected cells. *Pathogens and Disease*, *73*(1), 1–8. https://doi.org/10.1093/femspd/ftv007

Kalayoglu, M. V., & Byrne, G. I. (1998). Induction of macrophage foam cell formation by Chlamydia pneumoniae. *The Journal of Infectious Diseases*, *177*(3), 725–729. https://doi.org/10.1086/514241

Kanerva, K., Uronen, R.-L., Blom, T., Li, S., Bittman, R., Lappalainen, P., Peränen, J., Raposo, G., & Ikonen, E. (2013). LDL cholesterol recycles to the plasma

membrane via a Rab8a-Myosin5b-actin-dependent membrane transport route. *Developmental Cell*, *27*(3), 249–262. https://doi.org/10.1016/j.devcel.2013.09.016

Kokes, M., Dunn, J. D., Granek, J. A., Nguyen, B. D., Barker, J. R., Valdivia, R. H., & Bastidas, R. J. (2015). Integrating chemical mutagenesis and whole-genome sequencing as a platform for forward and reverse genetic analysis of Chlamydia. *Cell Host & Microbe*, *17*(5), 716–725. https://doi.org/10.1016/j.chom.2015.03.014

Krogsaeter, E., Rosato, A. S., & Grimm, C. (2022). TRPMLs and TPCs: Targets for lysosomal storage and neurodegenerative disease therapy? *Cell Calcium*, *103*, 102553. https://doi.org/10.1016/j.ceca.2022.102553

Kuijl, C., Savage, N. D. L., Marsman, M., Tuin, A. W., Janssen, L., Egan, D. A., Ketema, M., van den Nieuwendijk, R., van den Eeden, S. J. F., Geluk, A., Poot, A., van der Marel, G., Beijersbergen, R. L., Overkleeft, H., Ottenhoff, T. H. M., & Neefjes, J. (2007). Intracellular bacterial growth is controlled by a kinase network around PKB/AKT1. *Nature*, *450*(7170), 725–730. https://doi.org/10.1038/nature06345

Kumar, Y., Cocchiaro, J., & Valdivia, R. H. (2006). The Obligate Intracellular Pathogen Chlamydia trachomatis Targets Host Lipid Droplets. *Current Biology*, *16*(16), 1646–1651. https://doi.org/10.1016/j.cub.2006.06.060

Lange, Y., Ye, J., & Steck, T. L. (1998). Circulation of Cholesterol between Lysosomes and the Plasma Membrane *. *Journal of Biological Chemistry*, *273*(30), 18915–18922. https://doi.org/10.1074/jbc.273.30.18915

Lee, J. K., Enciso, G. A., Boassa, D., Chander, C. N., Lou, T. H., Pairawan, S. S., Guo, M. C., Wan, F. Y. M., Ellisman, M. H., Sütterlin, C., & Tan, M. (2018). Replication-dependent size reduction precedes differentiation in Chlamydia trachomatis. *Nature Communications*, *9*(1), 45. https://doi.org/10.1038/s41467-017-02432-0

Lee, T. H., & Linstedt, A. D. (2000). Potential Role for Protein Kinases in Regulation of Bidirectional Endoplasmic Reticulum-to-Golgi Transport Revealed by Protein Kinase Inhibitor H89. *Molecular Biology of the Cell*, *11*(8), 2577–2590.

Li, J. L., Yang, N., Huang, L., Chen, D., Zhao, Y., Tang, M. M., Fan, H., & Bao, X. (2018). Pyocyanin Inhibits Chlamydia Infection by Disabling Infectivity of the Elementary Body and Disrupting Intracellular Growth. *Antimicrobial Agents and Chemotherapy*, *62*(6). https://doi.org/10.1128/AAC.02260-17

Li, Z., Chen, C., Chen, D., Wu, Y., Zhong, Y., & Zhong, G. (2008). Characterization of Fifty Putative Inclusion Membrane Proteins Encoded in the Chlamydia trachomatis Genome. *Infection and Immunity*, *76*(6), 2746–2757. https://doi.org/10.1128/IAI.00010-08

Limbutara, K., Kelleher, A., Yang, C.-R., Raghuram, V., & Knepper, M. A. (2019). Phosphorylation Changes in Response to Kinase Inhibitor H89 in PKA-Null Cells. *Scientific Reports*, *9*(1), 2814. https://doi.org/10.1038/s41598-019-39116-2

Lochner, A., & Moolman, J. A. (2006). The Many Faces of H89: A Review. *Cardiovascular Drug Reviews*, *24*(3–4), 261–274. https://doi.org/10.1111/j.1527-3466.2006.00261.x

Lucas, A. L., Ouellette, S. P., Kabeiseman, E. J., Cichos, K. H., & Rucks, E. A. (2015). The trans-Golgi SNARE syntaxin 10 is required for optimal development of Chlamydia trachomatis. *Frontiers in Cellular and Infection Microbiology*, *5*. https://doi.org/10.3389/fcimb.2015.00068

Luo, J., Jiang, L., Yang, H., & Song, B.-L. (2017). Routes and mechanisms of post-endosomal cholesterol trafficking: A story that never ends. *Traffic*, *18*(4), 209–217. https://doi.org/10.1111/tra.12471

Luo, J., Jiang, L.-Y., Yang, H., & Song, B.-L. (2019). Intracellular Cholesterol Transport by Sterol Transfer Proteins at Membrane Contact Sites. *Trends in Biochemical Sciences*, *44*(3), 273–292. https://doi.org/10.1016/j.tibs.2018.10.001

Lyu, J., Yang, E. J., Head, S. A., Ai, N., Zhang, B., Wu, C., Li, R.-J., Liu, Y., Chakravarty, H., Zhang, S., Tam, K. Y., Dang, Y., Kwon, H. J., Ge, W., Liu, J. O., & Shim, J. S. (2018). Astemizole Inhibits mTOR Signaling and Angiogenesis by Blocking Cholesterol Trafficking. *International Journal of Biological Sciences*, *14*(10), 1175–1185. https://doi.org/10.7150/ijbs.26011

MacDonald, L. J., Graham, J. G., Kurten, R. C., & Voth, D. E. (2014). Coxiella burnetii Exploits Host cAMP-Dependent Protein Kinase Signaling to Promote Macrophage Survival. *Cellular Microbiology*, *16*(1), 146–159. https://doi.org/10.1111/cmi.12213

MacDonald, L. J., Kurten, R. C., & Voth, D. E. (2012). Coxiella burnetii Alters Cyclic AMP-Dependent Protein Kinase Signaling during Growth in Macrophages. *Infection and Immunity*, *80*(6), 1980–1986. https://doi.org/10.1128/IAI.00101-12

Magida, J. A., & Evans, R. M. (2018). Rational application of macrophage-specific LXR agonists avoids the pitfalls of SREBP-induced lipogenesis. *Proceedings of the National Academy of Sciences of the United States of America*, *115*(20), 5051–5053. https://doi.org/10.1073/pnas.1805128115

Marwaha, S., Uvell, H., Salin, O., Lindgren, A. E. G., Silver, J., Elofsson, M., & Gylfe, Å. (2014). N-Acylated Derivatives of Sulfamethoxazole and Sulfafurazole Inhibit Intracellular Growth of Chlamydia trachomatis. *Antimicrobial Agents and Chemotherapy*. https://journals.asm.org/doi/abs/10.1128/AAC.02015-13

Matsumoto, A., & Manire, G. P. (1970). Electron microscopic observations on the effects of penicillin on the morphology of Chlamydia psittaci. *Journal of Bacteriology*, *101*(1), 278–285. https://doi.org/10.1128/jb.101.1.278-285.1970

Maxfield, F. R., & Menon, A. K. (2006). Intracellular sterol transport and distribution. *Current Opinion in Cell Biology*, *18*(4), 379–385. https://doi.org/10.1016/j.ceb.2006.06.012

Maxfield, F. R., & van Meer, G. (2010). Cholesterol, the central lipid of mammalian cells. *Current Opinion in Cell Biology*, *22*(4), 422–429. https://doi.org/10.1016/j.ceb.2010.05.004

McCauliff, L. A., Langan, A., Li, R., Ilnytska, O., Bose, D., Waghalter, M., Lai, K., Kahn, P. C., & Storch, J. (2019). Intracellular cholesterol trafficking is dependent upon NPC2 interaction with lysobisphosphatidic acid. *ELife*, *8*, e50832. https://doi.org/10.7554/eLife.50832

Mital, J., Miller, N. J., Dorward, D. W., Dooley, C. A., & Hackstadt, T. (2013). Role for chlamydial inclusion membrane proteins in inclusion membrane structure and biogenesis. *PloS One*, *8*(5), e63426. https://doi.org/10.1371/journal.pone.0063426

Mital, J., Miller, N. J., Fischer, E. R., & Hackstadt, T. (2010). Specific chlamydial inclusion membrane proteins associate with active Src family kinases in microdomains that interact with the host microtubule network. *Cellular Microbiology*, *12*(9), 1235–1249. https://doi.org/10.1111/j.1462-5822.2010.01465.x

Moore, E. R. (2012). Sphingolipid trafficking and purification in Chlamydia trachomatis-infected cells. *Current Protocols in Microbiology*, *CHAPTER*, Unit11A.2. https://doi.org/10.1002/9780471729259.mc11a02s27

Moore, E. R., Fischer, E. R., Mead, D. J., & Hackstadt, T. (2008). The Chlamydial Inclusion Preferentially Intercepts Basolaterally Directed Sphingomyelin-Containing Exocytic Vacuoles. *Traffic (Copenhagen, Denmark)*, *9*(12), 2130–2140. https://doi.org/10.1111/j.1600-0854.2008.00828.x

Moore, E. R., & Ouellette, S. P. (2014). Reconceptualizing the chlamydial inclusion as a pathogen-specified parasitic organelle: An expanded role for Inc proteins. *Frontiers in Cellular and Infection Microbiology*, *4*. https://doi.org/10.3389/fcimb.2014.00157

Moulder, J. W. (1991). Interaction of chlamydiae and host cells in vitro. *Microbiological Reviews*, *55*(1), 143–190.

Muñiz, M., Martín, M. E., Hidalgo, J., & Velasco, A. (1997). Protein kinase A activity is required for the budding of constitutive transport vesicles from the trans-Golgi network. *Proceedings of the National Academy of Sciences*, *94*(26), 14461–14466. https://doi.org/10.1073/pnas.94.26.14461

Muñoz, K. J., Wang, K., Sheehan, L. M., Tan, M., & Sütterlin, C. (2021). The small molecule H89 inhibits Chlamydia inclusion growth and production of infectious progeny. *Infection and Immunity*. https://doi.org/10.1128/IAI.00729-20

Murray, A. J. (2008). Pharmacological PKA Inhibition: All May Not Be What It Seems. *Sci. Signal.*, *1*(22), re4–re4. https://doi.org/10.1126/scisignal.122re4

Muschiol, S., Bailey, L., Gylfe, Å., Sundin, C., Hultenby, K., Bergström, S., Elofsson, M., Wolf-Watz, H., Normark, S., & Henriques-Normark, B. (2006). A small-molecule inhibitor of type III secretion inhibits different stages of the infectious cycle of Chlamydia trachomatis. *Proceedings of the National Academy of Sciences*, *103*(39), 14566–14571. https://doi.org/10.1073/pnas.0606412103

Muschiol, S., Normark, S., Henriques-Normark, B., & Subtil, A. (2009). Small molecule inhibitors of the Yersinia type III secretion system impair the development of Chlamydia after entry into host cells. *BMC Microbiology*, *9*, 75. https://doi.org/10.1186/1471-2180-9-75

Newton, J., Palladino, E. N. D., Weigel, C., Maceyka, M., Gräler, M. H., Senkal, C. E., Enriz, R. D., Marvanova, P., Jampilek, J., Lima, S., Milstien, S., & Spiegel, S. (2020). Targeting defective sphingosine kinase 1 in Niemann–Pick type C disease with an activator mitigates cholesterol accumulation. *Journal of*

Biological Chemistry, *295*(27), 9121–9133. https://doi.org/10.1074/jbc.RA120.012659

Nguyen, B. D., Cunningham, D., Liang, X., Chen, X., Toone, E. J., Raetz, C. R. H., Zhou, P., & Valdivia, R. H. (2011). Lipooligosaccharide is required for the generation of infectious elementary bodies in Chlamydia trachomatis. *Proceedings of the National Academy of Sciences*, *108*(25), 10284–10289. https://doi.org/10.1073/pnas.1107478108

Njau, F., Wittkop, U., Rohde, M., Haller, H., Klos, A., & Wagner, A. D. (2009). In vitro neutralization of tumor necrosis factor-α during Chlamydia pneumoniae infection impairs dendritic cells maturation/function and increases chlamydial progeny. *FEMS Immunology & Medical Microbiology*, *55*(2), 215–225. https://doi.org/10.1111/j.1574-695X.2008.00512.x

Núñez-Otero, C., Bahnan, W., Vielfort, K., Silver, J., Singh, P., Elbir, H., Almqvist, F., Bergström, S., & Gylfe, Å. (2021a). A 2-Pyridone Amide Inhibitor of Transcriptional Activity in Chlamydia trachomatis. *Antimicrobial Agents and Chemotherapy*. https://doi.org/10.1128/AAC.01826-20

Núñez-Otero, C., Bahnan, W., Vielfort, K., Silver, J., Singh, P., Elbir, H., Almqvist, F., Bergström, S., & Gylfe, Å. (2021b). A 2-pyridone amide inhibitor of transcriptional activity in Chlamydia trachomatis. *Antimicrobial Agents and Chemotherapy*, AAC.01826-20. https://doi.org/10.1128/AAC.01826-20

Ouellette, S. P., Dorsey, F. C., Moshiach, S., Cleveland, J. L., & Carabeo, R. A. (2011). Chlamydia Species-Dependent Differences in the Growth Requirement for

Lysosomes. *PLOS ONE*, *6*(3), e16783. https://doi.org/10.1371/journal.pone.0016783

Pal, S., Peterson, E. M., & de la Maza, L. M. (2005). Vaccination with the Chlamydia trachomatis Major Outer Membrane Protein Can Elicit an Immune Response as Protective as That Resulting from Inoculation with Live Bacteria. *Infection and Immunity*, *73*(12), 8153–8160. https://doi.org/10.1128/IAI.73.12.8153-8160.2005

Panzetta, M. E., Valdivia, R. H., & Saka, H. A. (2018). Chlamydia Persistence: A Survival Strategy to Evade Antimicrobial Effects in-vitro and in-vivo. *Frontiers in Microbiology*, *9*. https://doi.org/10.3389/fmicb.2018.03101

Park, J. S., Helble, J. D., Lazarus, J. E., Yang, G., Blondel, C. J., Doench, J. G., Starnbach, M. N., & Waldor, M. K. (2018). A FACS-Based Genome-wide CRISPR Screen Reveals a Requirement for COPI in Chlamydia trachomatis Invasion. *IScience*, *11*, 71–84. https://doi.org/10.1016/j.isci.2018.12.011

Patel, A. L., Chen, X., Wood, S. T., Stuart, E. S., Arcaro, K. F., Molina, D. P., Petrovic, S., Furdui, C. M., & Tsang, A. W. (2014). Activation of epidermal growth factor receptor is required for Chlamydia trachomatis development. *BMC Microbiology*, *14*, 277. https://doi.org/10.1186/s12866-014-0277-4

Patterson, M. (1993). Niemann-Pick Disease Type C. In M. P. Adam, H. H. Ardinger, R. A. Pagon, S. E. Wallace, L. J. Bean, K. W. Gripp, G. M. Mirzaa, & A. Amemiya (Eds.), *GeneReviews®*. University of Washington, Seattle. http://www.ncbi.nlm.nih.gov/books/NBK1296/

Peng, L., Zhang, H., Hu, Z., Zhao, Y., Liu, S., & Chen, J. (2020). Nafamostat mesylate inhibits chlamydial intracellular growth in cell culture and reduces chlamydial infection in the mouse genital tract. *Microbial Pathogenesis*, *147*, 104413. https://doi.org/10.1016/j.micpath.2020.104413

Peters, J., & Byrne, G. I. (2015). Chlamydia trachomatis growth depends on eukaryotic cholesterol esterification and is affected by Acyl-CoA:cholesterol acyltransferase inhibition. *Pathogens and Disease*, *73*(6). https://doi.org/10.1093/femspd/ftv028

Phillips, S., Quigley, B. L., & Timms, P. (2019). Seventy Years of Chlamydia Vaccine Research – Limitations of the Past and Directions for the Future. *Frontiers in Microbiology*, *10*, 70. https://doi.org/10.3389/fmicb.2019.00070

Piper, R. C., & Katzmann, D. J. (2007). Biogenesis and Function of Multivesicular Bodies. *Annual Review of Cell and Developmental Biology*, *23*, 519–547. https://doi.org/10.1146/annurev.cellbio.23.090506.123319

Pitson, S. M., Moretti, P. A. B., Zebol, J. R., Lynn, H. E., Xia, P., Vadas, M. A., & Wattenberg, B. W. (2003). Activation of sphingosine kinase 1 by ERK1/2-mediated phosphorylation. *The EMBO Journal*, *22*(20), 5491–5500. https://doi.org/10.1093/emboj/cdg540

Qi, M., Gong, S., Lei, L., Liu, Q., & Zhong, G. (2011). A Chlamydia trachomatis OmcB C-Terminal Fragment Is Released into the Host Cell Cytoplasm and Is Immunogenic in Humans ▿. *Infection and Immunity*, *79*(6), 2193–2203. https://doi.org/10.1128/IAI.00003-11

Recuero-Checa, M. A., Sharma, M., Lau, C., Watkins, P. A., Gaydos, C. A., & Dean, D. (2016). Chlamydia trachomatis growth and development requires the activity of host Long-chain Acyl-CoA Synthetases (ACSLs). *Scientific Reports*, *6*(1), 23148. https://doi.org/10.1038/srep23148

Reimer, A., Seufert, F., Weiwad, M., Ebert, J., Bzdyl, N. M., Kahler, C. M., Sarkar-Tyson, M., Holzgrabe, U., Rudel, T., & Kozjak-Pavlovic, V. (2016). Inhibitors of macrophage infectivity potentiator-like PPIases affect neisserial and chlamydial pathogenicity. *International Journal of Antimicrobial Agents*, *48*(4), 401–408. https://doi.org/10.1016/j.ijantimicag.2016.06.020

Rejman Lipinski, A., Heymann, J., Meissner, C., Karlas, A., Brinkmann, V., Meyer, T. F., & Heuer, D. (2009). Rab6 and Rab11 regulate Chlamydia trachomatis development and golgin-84-dependent Golgi fragmentation. *PLoS Pathogens*, *5*(10), e1000615. https://doi.org/10.1371/journal.ppat.1000615

Richards, T. S., Knowlton, A. E., & Grieshaber, S. S. (2013). Chlamydia trachomatis homotypic inclusion fusion is promoted by host microtubule trafficking. *BMC Microbiology*, *13*, 185. https://doi.org/10.1186/1471-2180-13-185

Ripa, K. T., & Mårdh, P. A. (1977). Cultivation of Chlamydia trachomatis in cycloheximide-treated mccoy cells. *Journal of Clinical Microbiology*, *6*(4), 328–331. https://doi.org/10.1128/jcm.6.4.328-331.1977

Robertson, D. K., Gu, L., Rowe, R. K., & Beatty, W. L. (2009). Inclusion Biogenesis and Reactivation of Persistent Chlamydia trachomatis Requires Host Cell

Sphingolipid Biosynthesis. *PLOS Pathogens*, *5*(11), e1000664. https://doi.org/10.1371/journal.ppat.1000664

Rodríguez-Acebes, S., de la Cueva, P., Fernández-Hernando, C., Ferruelo, A. J., Lasunción, M. A., Rawson, R. B., Martínez-Botas, J., & Gómez-Coronado, D. (2009). Desmosterol can replace cholesterol in sustaining cell proliferation and regulating the SREBP pathway in a sterol-Δ24-reductase deficient cell line. *The Biochemical Journal*, *420*(2), 305–315. https://doi.org/10.1042/BJ20081909

Rosario, C. J., & Tan, M. (2020). *"Chapter 10: Chlamydia Gene Regulation," p 219-240. In Chlamydia Biology: From Genome to Disease*. Caister Academic Press.

Rzomp, K. A., Scholtes, L. D., Briggs, B. J., Whittaker, G. R., & Scidmore, M. A. (2003). Rab GTPases Are Recruited to Chlamydial Inclusions in Both a Species-Dependent and Species-Independent Manner. *Infection and Immunity*, *71*(10), 5855–5870. https://doi.org/10.1128/IAI.71.10.5855-5870.2003

Sabet, S. F., Simmons, J., & Caldwell, H. D. (1984). Enhancement of Chlamydia trachomatis infectious progeny by cultivation of HeLa 229 cells treated with DEAE-dextran and cycloheximide. *Journal of Clinical Microbiology*, *20*(2), 217–222.

Sah, P., Nelson, N. H., Shaw, J. H., & Lutter, E. I. (2019). Chlamydia trachomatis recruits Protein Kinase C during infection. *Pathogens and Disease*. https://doi.org/10.1093/femspd/ftz061

Salazar, G., & González, A. (2002). Novel Mechanism for Regulation of Epidermal Growth Factor Receptor Endocytosis Revealed by Protein Kinase A Inhibition.

Molecular Biology of the Cell, *13*(5), 1677–1693. https://doi.org/10.1091/mbc.01-08-0403

Saleeb, M., Mojica, S., Eriksson, A. U., Andersson, C. D., Gylfe, Å., & Elofsson, M. (2018). Natural product inspired library synthesis—Identification of 2,3-diarylbenzofuran and 2,3-dihydrobenzofuran based inhibitors of Chlamydia trachomatis. *European Journal of Medicinal Chemistry*, *143*, 1077–1089. https://doi.org/10.1016/j.ejmech.2017.11.099

Samanta, D., Mulye, M., Clemente, T. M., Justis, A. V., & Gilk, S. D. (2017). Manipulation of Host Cholesterol by Obligate Intracellular Bacteria. *Frontiers in Cellular and Infection Microbiology*, *7*. https://doi.org/10.3389/fcimb.2017.00165

Schettino, C., Bareschino, M. A., Ricci, V., & Ciardiello, F. (2008). Erlotinib: An EGF receptor tyrosine kinase inhibitor in non-small-cell lung cancer treatment. *Expert Review of Respiratory Medicine*, *2*(2), 167–178. https://doi.org/10.1586/17476348.2.2.167

Scidmore, M. A. (2006). Cultivation and Laboratory Maintenance of Chlamydia trachomatis. *Current Protocols in Microbiology*, *00*(1), 11A.1.1-11A.1.25. https://doi.org/10.1002/9780471729259.mc11a01s00

Scidmore, M. A., Fischer, E. R., & Hackstadt, T. (2003). Restricted Fusion of Chlamydia trachomatis Vesicles with Endocytic Compartments during the Initial Stages of Infection. *Infection and Immunity*, *71*(2), 973–984. https://doi.org/10.1128/IAI.71.2.973-984.2003

Seleem, M. A., Rodrigues de Almeida, N., Chhonker, Y. S., Murry, D. J., Guterres, Z. da R., Blocker, A. M., Kuwabara, S., Fisher, D. J., Leal, E. S., Martinefski, M. R., Bollini, M., Monge, M. E., Ouellette, S. P., & Conda-Sheridan, M. (2020). Synthesis and Antichlamydial Activity of Molecules Based on Dysregulators of Cylindrical Proteases. *Journal of Medicinal Chemistry*, *63*(8), 4370–4387. https://doi.org/10.1021/acs.jmedchem.0c00371

Sharma, M., Recuero-Checa, M. A., Fan, F. Y., & Dean, D. (2018). Chlamydia trachomatis regulates growth and development in response to host cell fatty acid availability in the absence of lipid droplets. *Cellular Microbiology*, *20*(2), 10.1111/cmi.12801. https://doi.org/10.1111/cmi.12801

Shaw, E. I., Dooley, C. A., Fischer, E. R., Scidmore, M. A., Fields, K. A., & Hackstadt, T. (2000). Three temporal classes of gene expression during the Chlamydia trachomatis developmental cycle. *Molecular Microbiology*, *37*(4), 913–925. https://doi.org/10.1046/j.1365-2958.2000.02057.x

Shivshankar, P., Lei, L., Wang, J., & Zhong, G. (2008). Rottlerin Inhibits Chlamydial Intracellular Growth and Blocks Chlamydial Acquisition of Sphingolipids from Host Cells. *Applied and Environmental Microbiology*, *74*(4), 1243–1249. https://doi.org/10.1128/AEM.02151-07

Sigalova, O. M., Chaplin, A. V., Bochkareva, O. O., Shelyakin, P. V., Filaretov, V. A., Akkuratov, E. E., Burskaia, V., & Gelfand, M. S. (2019). Chlamydia pan-genomic analysis reveals balance between host adaptation and selective pressure to

genome reduction. *BMC Genomics*, *20*(1), 710. https://doi.org/10.1186/s12864-019-6059-5

Silva, L. M. R., Velásquez, Z. D., López-Osorio, S., Hermosilla, C., & Taubert, A. (2022). Novel Insights Into Sterol Uptake and Intracellular Cholesterol Trafficking During Eimeria bovis Macromeront Formation. *Frontiers in Cellular and Infection Microbiology*, *12*, 809606. https://doi.org/10.3389/fcimb.2022.809606

Skilton, R. J., Cutcliffen, L. T., Barlow, D., Wang, Y., Salim, O., Lambden, P. R., & Clarke, I. N. (2009). Penicillin induced persistence in Chlamydia trachomatis: High quality time lapse video analysis of the developmental cycle. *PloS One*, *4*(11), e7723. https://doi.org/10.1371/journal.pone.0007723

Skilton, R. J., Wang, Y., O'Neill, C., Filardo, S., Marsh, P., Bénard, A., Thomson, N. R., Ramsey, K. H., & Clarke, I. N. (2018). The Chlamydia muridarum plasmid revisited: New insights into growth kinetics. *Wellcome Open Research*, *3*, 25. https://doi.org/10.12688/wellcomeopenres.13905.1

Slepenkin, A., Enquist, P.-A., Hägglund, U., de la Maza, L. M., Elofsson, M., & Peterson, E. M. (2007). Reversal of the Antichlamydial Activity of Putative Type III Secretion Inhibitors by Iron. *Infection and Immunity*, *75*(7), 3478–3489. https://doi.org/10.1128/IAI.00023-07

Snavely, E. A., Kokes, M., Dunn, J. D., Saka, H. A., Nguyen, B. D., Bastidas, R. J., McCafferty, D. G., & Valdivia, R. H. (2014). Reassessing the role of the secreted protease CPAF in Chlamydia trachomatis infection through genetic approaches.

Pathogens and Disease, *71*(3), 336–351. https://doi.org/10.1111/2049-632X.12179

Solger, F., Kunz, T. C., Fink, J., Paprotka, K., Pfister, P., Hagen, F., Schumacher, F., Kleuser, B., Seibel, J., & Rudel, T. (2020). A Role of Sphingosine in the Intracellular Survival of Neisseria gonorrhoeae. *Frontiers in Cellular and Infection Microbiology*, *10*, 215. https://doi.org/10.3389/fcimb.2020.00215

Sonnenberg, P., Clifton, S., Beddows, S., Field, N., Soldan, K., Tanton, C., Mercer, C. H., da Silva, F. C., Alexander, S., Copas, A. J., Phelps, A., Erens, B., Prah, P., Macdowall, W., Wellings, K., Ison, C. A., & Johnson, A. M. (2013). Prevalence, risk factors, and uptake of interventions for sexually transmitted infections in Britain: Findings from the National Surveys of Sexual Attitudes and Lifestyles (Natsal). *Lancet (London, England)*, *382*(9907), 1795–1806. https://doi.org/10.1016/S0140-6736(13)61947-9

Stanhope, R., Flora, E., Bayne, C., & Derré, I. (2017). IncV, a FFAT motif-containing Chlamydia protein, tethers the endoplasmic reticulum to the pathogen-containing vacuole. *Proceedings of the National Academy of Sciences*, *114*(45), 12039–12044. https://doi.org/10.1073/pnas.1709060114

Steinberg, G. R., & Carling, D. (2019). AMP-activated protein kinase: The current landscape for drug development. *Nature Reviews Drug Discovery*, *18*(7), 527–551. https://doi.org/10.1038/s41573-019-0019-2

Stephens, R. S., Kalman, S., Lammel, C., Fan, J., Marathe, R., Aravind, L., Mitchell, W., Olinger, L., Tatusov, R. L., Zhao, Q., Koonin, E. V., & Davis, R. W. (1998).

Genome sequence of an obligate intracellular pathogen of humans: Chlamydia trachomatis. *Science (New York, N.Y.)*, *282*(5389), 754–759. https://doi.org/10.1126/science.282.5389.754

Subramanian, K., & Balch, W. E. (2008). NPC1/NPC2 function as a tag team duo to mobilize cholesterol. *Proceedings of the National Academy of Sciences*, *105*(40), 15223–15224. https://doi.org/10.1073/pnas.0808256105

Tang, W., Mao, J., Li, K. T., Walker, J. S., Chou, R., Fu, R., Chen, W., Darville, T., Klausner, J., & Tucker, J. D. (2020). Pregnancy and fertility-related adverse outcomes associated with Chlamydia trachomatis infection: A global systematic review and meta-analysis. *Sexually Transmitted Infections*, *96*(5), 322–329. https://doi.org/10.1136/sextrans-2019-053999

Theunissen, H. J., Toom, N. A. L., Burggraaf, A., Stolz, E., & Michel, M. F. (1993). Influence of temperature and relative humidity on the survival of Chlamydia pneumoniae in aerosols. *Applied and Environmental Microbiology*. https://doi.org/10.1128/aem.59.8.2589-2593.1993

Tjiam, K. H., van Heijst, B. Y., de Roo, J. C., de Beer, A., van Joost, T., Michel, M. F., & Stolz, E. (1984). Survival of Chlamydia trachomatis in different transport media and at different temperatures: Diagnostic implications. *British Journal of Venereal Diseases*, *60*(2), 92–94.

Todd, W. J., & Storz, J. (1975). Ultrastructural cytochemical evidence for the activation of lysosomes in the cytocidal effect of Chlamydia psittaci. *Infection and Immunity*, *12*(3), 638–646. https://doi.org/10.1128/iai.12.3.638-646.1975

Trinh, M. N., Brown, M. S., Goldstein, J. L., Han, J., Vale, G., McDonald, J. G., Seemann, J., Mendell, J. T., & Lu, F. (2020). Last step in the path of LDL cholesterol from lysosome to plasma membrane to ER is governed by phosphatidylserine. *Proceedings of the National Academy of Sciences*, *117*(31), 18521–18529. https://doi.org/10.1073/pnas.2010682117

United Health Foundation. (2021). *Explore Chlamydia in the United States | 2021 Annual Report*. America's Health Rankings. https://www.americashealthrankings.org/explore/annual/measure/chlamydia/state/ALL

Urano, Y., Watanabe, H., Murphy, S. R., Shibuya, Y., Geng, Y., Peden, A. A., Chang, C. C. Y., & Chang, T. Y. (2008). Transport of LDL-derived cholesterol from the NPC1 compartment to the ER involves the trans-Golgi network and the SNARE protein complex. *Proceedings of the National Academy of Sciences*, *105*(43), 16513–16518. https://doi.org/10.1073/pnas.0807450105

Ur-Rehman, T., Slepenkin, A., Chu, H., Blomgren, A., Dahlgren, M. K., Zetterström, C. E., Peterson, E. M., Elofsson, M., & Gylfe, Å. (2012). Pre-clinical pharmacokinetics and anti-chlamydial activity of salicylidene acylhydrazide inhibitors of bacterial type III secretion. *The Journal of Antibiotics*, *65*(8), 397–404. https://doi.org/10.1038/ja.2012.43

van Ooij, C., Apodaca, G., & Engel, J. (1997). Characterization of the Chlamydia trachomatis vacuole and its interaction with the host endocytic pathway in HeLa

cells. *Infection and Immunity*, *65*(2), 758–766. https://doi.org/10.1128/iai.65.2.758-766.1997

van Ooij, C., Kalman, L., van Ijzendoorn, null, Nishijima, M., Hanada, K., Mostov, K., & Engel, J. N. (2000). Host cell-derived sphingolipids are required for the intracellular growth of Chlamydia trachomatis. *Cellular Microbiology*, *2*(6), 627–637. https://doi.org/10.1046/j.1462-5822.2000.00077.x

Vieira, C. P., Fortmann, S. D., Hossain, M., Longhini, A. L., Hammer, S. S., Asare-Bediako, B., Crossman, D. K., Sielski, M. S., Adu-Agyeiwaah, Y., Dupont, M., Floyd, J. L., Li Calzi, S., Lydic, T., Welner, R. S., Blanchard, G. J., Busik, J. V., & Grant, M. B. (2020). Selective LXR agonist DMHCA corrects retinal and bone marrow dysfunction in type 2 diabetes. *JCI Insight*, *5*(13), e137230. https://doi.org/10.1172/jci.insight.137230

Walenna, N. F., Kurihara, Y., Chou, B., Ishii, K., Soejima, T., & Hiromatsu, K. (2020). Chlamydia pneumoniae infection-induced endoplasmic reticulum stress causes fatty acid-binding protein 4 secretion in murine adipocytes. *The Journal of Biological Chemistry*, *295*(9), 2713–2723. https://doi.org/10.1074/jbc.RA119.010683

Wang, L., Xing, X.-P., Holmes, A., Wadham, C., Gamble, J. R., Vadas, M. A., & Xia, P. (2005). Activation of the Sphingosine Kinase–Signaling Pathway by High Glucose Mediates the Proinflammatory Phenotype of Endothelial Cells. *Circulation Research*, *97*(9), 891–899. https://doi.org/10.1161/01.RES.0000187469.82595.15

Wang, X., Hybiske, K., & Stephens, R. S. (2018). Direct visualization of the expression and localization of chlamydial effector proteins within infected host cells. *Pathogens and Disease*, *76*(2). https://doi.org/10.1093/femspd/fty011

Weber, M. M., Bauler, L. D., Lam, J., & Hackstadt, T. (2015). Expression and Localization of Predicted Inclusion Membrane Proteins in Chlamydia trachomatis. *Infection and Immunity*, *83*(12), 4710–4718. https://doi.org/10.1128/IAI.01075-15

Weber, M. M., Lam, J. L., Dooley, C. A., Noriea, N. F., Hansen, B. T., Hoyt, F. H., Carmody, A. B., Sturdevant, G. L., & Hackstadt, T. (2017). Absence of specific Chlamydia trachomatis inclusion membrane proteins triggers premature inclusion membrane lysis and host cell death. *Cell Reports*, *19*(7), 1406–1417. https://doi.org/10.1016/j.celrep.2017.04.058

Weber, M. M., Noriea, N. F., Bauler, L. D., Lam, J. L., Sager, J., Wesolowski, J., Paumet, F., & Hackstadt, T. (2016). A Functional Core of IncA Is Required for Chlamydia trachomatis Inclusion Fusion. *Journal of Bacteriology*, *198*(8), 1347–1355. https://doi.org/10.1128/JB.00933-15

Wesolowski, J., Weber, M. M., Nawrotek, A., Dooley, C. A., Calderon, M., Croix, C. M. S., Hackstadt, T., Cherfils, J., & Paumet, F. (2017). Chlamydia Hijacks ARF GTPases To Coordinate Microtubule Posttranslational Modifications and Golgi Complex Positioning. *MBio*, *8*(3), e02280-16. https://doi.org/10.1128/mBio.02280-16

Whitford, W., & Manwaring, J. (2022). *Lipids in Cell Culture Media*. 3.

Wolf, K., Betts, H. J., Chellas-Géry, B., Hower, S., Linton, C. N., & Fields, K. A. (2006). Treatment of Chlamydia trachomatis with a small molecule inhibitor of the Yersinia type III secretion system disrupts progression of the chlamydial developmental cycle. *Molecular Microbiology*, *61*(6), 1543–1555. https://doi.org/10.1111/j.1365-2958.2006.05347.x

Wolf, K., Rahnama, M., & Fields, K. A. (2019). Genetic Manipulation of Chlamydia trachomatis: Chromosomal Deletions. *Methods in Molecular Biology (Clifton, N.J.)*, *2042*, 151–164. https://doi.org/10.1007/978-1-4939-9694-0_11

Worboys, M. (2019). Chlamydia: A Disease without a History. In S. Szreter (Ed.), *The Hidden Affliction: Sexually Transmitted Infections and Infertility in History*. University of Rochester Press. http://www.ncbi.nlm.nih.gov/books/NBK547154/

Workowski, K. A. (2021). Sexually Transmitted Infections Treatment Guidelines, 2021. *MMWR. Recommendations and Reports*, *70*. https://doi.org/10.15585/mmwr.rr7004a1

Wylie, J. L., Hatch, G. M., & McClarty, G. (1997). Host cell phospholipids are trafficked to and then modified by Chlamydia trachomatis. *Journal of Bacteriology*, *179*(23), 7233–7242.

Wyrick, P. B. (2010). Chlamydia trachomatis Persistence in Vitro – An Overview. *The Journal of Infectious Diseases*, *201*(Suppl 2), S88–S95. https://doi.org/10.1086/652394

Xiong, Q., & Rikihisa, Y. (2012). Subversion of NPC1 pathway of cholesterol transport by Anaplasma phagocytophilum. *Cellular Microbiology*, *14*(4), 560–576. https://doi.org/10.1111/j.1462-5822.2011.01742.x

Yan, K., Gao, L.-N., Cui, Y.-L., Zhang, Y., & Zhou, X. (2016). The cyclic AMP signaling pathway: Exploring targets for successful drug discovery (Review). *Molecular Medicine Reports*, *13*(5), 3715–3723. https://doi.org/10.3892/mmr.2016.5005

Yao, J., Abdelrahman, Y. M., Robertson, R. M., Cox, J. V., Belland, R. J., White, S. W., & Rock, C. O. (2014). Type II Fatty Acid Synthesis Is Essential for the Replication of Chlamydia trachomatis*. *Journal of Biological Chemistry*, *289*(32), 22365–22376. https://doi.org/10.1074/jbc.M114.584185

Young, M. M., Takahashi, Y., Fox, T. E., Yun, J. K., Kester, M., & Wang, H.-G. (2016). Sphingosine Kinase 1 Cooperates with Autophagy to Maintain Endocytic Membrane Trafficking. *Cell Reports*, *17*(6), 1532–1545. https://doi.org/10.1016/j.celrep.2016.10.019

Yvan-Charvet, L., Welch, C., Pagler, T. A., Ranalletta, M., Lamkanfi, M., Han, S., Ishibashi, M., Li, R., Wang, N., & Tall, A. R. (2008). Increased Inflammatory Gene Expression in ABC Transporter–Deficient Macrophages. *Circulation*, *118*(18), 1837–1847. https://doi.org/10.1161/CIRCULATIONAHA.108.793869

Zhang, X., Wang, K., Zhu, L., & Wang, Q. (2021). Reverse Cholesterol Transport Pathway and Cholesterol Efflux in Diabetic Retinopathy. *Journal of Diabetes Research*, *2021*, e8746114. https://doi.org/10.1155/2021/8746114

Zigangirova, N. A., Kost, E. A., Didenko, L. V., Kapotina, L. N., Zayakin, E. S., Luyksaar, S. I., Morgunova, E. Y., Fedina, E. D., Artyukhova, O. A., Samorodov, A. V., & Kobets, N. V. (2016). A small-molecule compound belonging to a class of 2,4-disubstituted 1,3,4-thiadiazine-5-ones inhibits intracellular growth and persistence of Chlamydia trachomatis. *Journal of Medical Microbiology*, *65*(1), 91–98. https://doi.org/10.1099/jmm.0.000189